

**A GIS- and field-based investigation of
main channel morphological sensitivity to tributary inputs
at the watershed scale in Québec**

Iulia Mazgareanu

A Thesis
in
the Department
of
Geography, Planning and Environment

Presented in Partial Fulfillment of the Requirements
for the Degree of Master of Science (Geography, Urban and Environmental Studies) at
Concordia University
Montreal, Quebec, Canada

August 2019

© Iulia Mazgareanu

CONCORDIA UNIVERSITY

School of Graduate Studies

This is to certify that the thesis prepared

By: Iulia Mazgareanu

Entitled: A GIS- and field-based investigation of main channel morphological sensitivity to tributary inputs at the watershed scale in Québec

and submitted in partial fulfillment of the requirements for the degree of

Master of Science (Geography, Urban and Environmental Studies)

complies with the regulations of the University and meets the accepted standards with respect to originality and quality.

Signed by the final examining committee:

_____ Chair
Dr. Pierre Deslauriers

_____ Examiner
Dr. Leonard Sklar

_____ External Examiner
Dr. Daniel Germain

_____ Thesis Supervisor
Dr. Pascale Biron

_____ Thesis Co-supervisor
Dr. Thomas Buffin-Bélanger

Approved by

_____ Chair of Department or Graduate Program Director

Dean,

Date

ABSTRACT

A GIS- and field-based investigation of main channel morphological sensitivity to tributary inputs at the watershed scale in Québec

Iulia Mazgareanu

Confluences are key nodes of river networks, as a result of the dynamic mixing of water, sediment, wood or ice between tributaries and receiving channels. Geomorphically active tributaries have the potential to disrupt the balance of erosional and depositional processes along main river channels, thereby resetting downstream longitudinal patterns. In turn, main channels respond to or absorb these changes as a function of their spatial and temporal sensitivity, which varies with topography, energy conditions and the system's capacity to recover following major past events. Consequently, confluence zones are areas of increased spatial heterogeneity, with important implications for the resilience of river ecosystems and their management. However, due to their complexity, tributary-main channel interactions represent a relatively understudied component in fluvial geomorphology. The objectives of this study are to 1) improve our understanding of the morphodynamics of active confluences characterized by high sediment load tributaries based on field observations in Gaspésie, Québec and 2) propose a novel semi-automated GIS model that uses a fuzzy approach to integrate multiple key factors (unit stream power, valley confinement and sediment connectivity potential) to assess main channel confluence morphological sensitivity (CMS) to active tributaries at the scale of whole watersheds. The model was tested using digital elevation models (DEM) in Coaticook and Gaspésie watersheds, Québec. Results of the field survey showed that despite all confluences being located in a generally homogeneous geological setting, considerable disparities in the morphological effect of tributaries exist. The fuzzy GIS model was able to identify sensitive locations along the main channel associated to geomorphically active tributaries and has thus the potential to be used as part of watershed geomorphic assessments, particularly when high-resolution (LiDAR) DEMs are available. These findings highlight the spatially contingent distribution of resisting and impelling forces along main channels, including tributary-main channel interactions, in influencing river behaviour.

Acknowledgements

I would like to express my sincere gratitude to my supervisor Dr. Pascale Biron whose patience, diligence and support have created the space in which I could pursue my work without any limitations. Thank you for offering me part of your NSERC Discovery Grant, a financial support which allowed me the luxury of focusing only on my project. I have learned much from your presence and will strive to assiduously continue the work you have done in the service of rivers.

I would also like to thank my co-supervisor Dr. Thomas Buffin-Bélanger for presenting me Gaspésie, as well as for your serenity and your complementing guidance. Thank you for lending me your students, whom I am also grateful, in helping out with the field data collection.

Many thanks to the working bees of the River Management Lab for your inputs and questions, which kept the wheels in my head rolling. In particular, a big thank you to Guéno   Chon   for your masterful work in creating the tools that allowed this work to be carried out, as well as your competence in troubleshooting technical issues.

Lastly, I would like to acknowledge the unrelenting work of my family in demonstrating that there is another way. Thank you for your patience and love. Finally, I wish to thank Berni, my eternal companion, for walking through the fire and building the world with me, as well as for being the best field assistant anyone could ask for.

Contributions of Authors

Chapter 6:

This chapter was written in collaboration with my supervisors Dr. Pascale Biron and Dr. Thomas Buffin-Bélanger.

As first author I was responsible for the development of the methodology, data collection, model creation and validation, presentation of results, statistical analyses and writing of the manuscript.

TABLE OF CONTENTS

LIST OF FIGURES.....	VIII
LIST OF TABLES.....	XII
1. INTRODUCTION.....	1
2. LITERATURE REVIEW.....	2
2.1. Rivers are mobile.....	2
2.2. Confluences: key nodes in the fluvial network.....	2
2.3. The role of tributaries on watershed sediment dynamics	4
2.4. Controls on the impact of tributaries	6
2.5. Detecting more mobile channels near confluences	7
3. RESEARCH OBJECTIVES.....	10
4. METHODOLOGY.....	11
4.1. Study area.....	11
4.2. Field data.....	13
4.3. GIS model	16
5. GEOMORPHOLOGICAL IMPACT OF TRIBUTARIES: FIELD ANALYSIS	18
5.1. Geomorphic characterization of Gaspésie confluences	18
5.1.1. Mont-Saint-Pierre watershed.....	18
5.1.2. Mont Louis watershed	23
5.1.3. Marsoui watershed.....	25
5.1.4. Sainte-Anne-des-Monts watershed	27
5.1.5. Cap Chat watershed.....	30

5.2.	Main channel and tributary characteristics at Gaspésie confluences.....	32
5.2.1.	Bedload grain size	32
5.2.2.	Channel width and number and area of bars	35
5.2.3.	Tributary and main channel slope	37
6.	A FUZZY GIS MODEL TO DETERMINE CONFLUENCE MORPHOLOGICAL SENSITIVITY OF MAIN CHANNELS TO TRIBUTARY INPUTS AT THE WATERSHED SCALE	39
6.1.	Introduction	41
6.2.	Study area	45
6.3.	Methods	46
6.3.1.	Choice of factors	47
6.3.2.	Factor standardization and weighting	48
6.3.3.	Sensitivity analysis and model validation	50
6.4.	Results	54
6.4.1.	Fuzzy GIS Model	54
6.4.2.	LiDAR vs 10-m DEM comparison	58
6.4.3.	Comparison with field observations in Gaspésie (10-m DEM)	61
6.5.	Discussion	64
6.5.1.	Advantages of the proposed approach	64
6.5.2.	Preliminary geomorphic assessment and the choice of the relevant variables	65
6.5.3.	Future avenues for application	68
6.6.	Conclusion	71
7.	CONCLUSION	72
	REFERENCES	74

List of Figures

Figure 2.1: A model of flow-sediment dynamics at confluences. Hydraulic zones are demarcated with numbers, while typically resultant morphologies are listed on the right (modified from Best, 1987: 28).....	3
Figure 4.1: Gaspésie study area comprising five watersheds and nine field study sites (purple stars).	12
Figure 4.2: Sampling zones of bed material for each field study site: pre-confluence (1), confluence (2), post-confluence (3) zones, as well as tributary bars (a) and any other exposed bar in downstream direction (b).	14
Figure 4.3: Summary of steps for the multi-criteria analysis. See Chapter 6 for a more detailed description of each.	17
Figure 5.1: Planform view of study site #1 in the Mont St-Pierre watershed (see Figure 4.1 for its location). Photos illustrate: channel morphology upstream of the confluence (a), at the confluence (b), large woody debris on eroding bank along with a 2m deep pool (c), upstream view into the tributary showing accumulation of sediment (d).....	19
Figure 5.2: Planform view of study site #2 in the Mont St-Pierre watershed (see Figure 4.1 for its location). Photos illustrate: main channel upstream and downstream of the confluence (a), tributary bar (b), tributary mouth jammed by large woody debris (c), upstream in the tributary (d), new (dis)tributary channels forming in the forest (e), former pre-avulsion channel position of the main stream, now vegetated (f).....	21
Figure 5.3: Planform view of study site #3 in the Mont-St-Pierre watershed (see Figure 4.1 for its location). Photos illustrate: the main channel upstream (a) and downstream (b) of the confluence, destabilized hillslope upstream (c), tributary being coupled with the main stream through a culvert (d), upstream in the tributary (e), sediment and wood accumulation zone downstream of the confluence (f).....	22
Figure 5.4: Planform view of study site #4 in the Mont-Louis watershed (see Figure 4.1 for site location). Photos illustrate: the main channel upstream (a), at (b) and downstream (c) of the confluence, hillslope failure, erosion and sediment accumulation upstream in the tributary (d), bank erosion after bedrock controlled river segment (e), bedrock control characteristic of the upstream and downstream reaches of the main river with the exception of the confluence zone (f).....	24

Figure 5.5: Planform view of study site #5 in the Marsoui watershed (see Figure 4.1 for site location). Photos illustrate: the main channel upstream (a), downstream (b) and at the confluence (c), scour pool (d).26

Figure 5.6: Planform view of study site #7 in the Sainte-Anne-des-Monts watershed (see Figure 4.1 for location). Study site #6 is not showed because it contains no tributary-related features and its planform and landform characteristics are homogeneous. Photos illustrate: the Mines Madelaines tributary flowing over and reworking material making up the alluvial fan, which results in the carving of a new channel (a), the now abandoned alluvial fan before reaching the main channel (b), tributary bar and view looking upstream of site #7 (c), view upstream from the end of the sampling zone showing compound bars (d), actively developing channels representing the new confluence (e). Note: the location point and direction of sites d and e are not shown.....28

Figure 5.7: Planform view of site #8 in the Sainte-Anne-des-Monts watershed (see Figure 4.1 for location). The photo illustrates a panoramic view of the upstream (a), confluence (b) and downstream (c) reaches of the main channel.29

Figure 5.8: Planform view of site #9 in the Cap Chat watershed (see Figure 4.1 for location). Photos illustrate: main channel upstream of the confluence (a), upstream in the tributary (b) scour pool at the confluence with bed revetment (c).31

Figure 5.9: Median, interquartile range (IQR=Q75 – Q25), minimum and maximum (squares) of the bedload grain size distribution for the pre-confluence (light gray) and post-confluence (dark grey) zones for all field study sites in Gaspésie. Grain size is given in 0.5 interval phi units (ϕ), calculated as $\log_2 D$, where D is the particle diameter, as well as in mm. Stars indicate statistical significance between the two groups at the 95% level.....33

Figure 5.10: Median and interquartile range (IQR=Q75 – Q25), minimum and maximum (squares, only confluence zone) of the bedload grain size distribution for the pre-confluence (light gray), confluence (grey) and post-confluence (dark grey) zones for all field study sites in Gaspésie. Sites are grouped by the effect of the tributary on the bedload grain size distribution. Grain size is given in 0.5 interval phi units (ϕ). Stars indicate statistical significance between the two groups at the 95% level.34

Figure 5.11: (A) Number of bars and cumulative bar area measured from orthophotos for the same longitudinal distance as the bed sediment sampling. (B) Average bankfull channel width

measured from orthophotos for the same longitudinal distance as the bed sediment sampling.....	36
Figure 5.12: Average water surface slope of the main channel’s pre- and post-confluence zone, along with the tributary slope for all study sites.	38
Figure 6.1: Location of study sites: the Coaticook Watershed (A) and 5 watersheds in Gaspésie (B).	46
Figure 6.2: Methods used to model the geomorphic sensitivity of the main channel to tributary inputs at the watershed scale. (A) The Sediment Connectivity Index has a dotted box to mark that the processing is external to ArcGIS (SedInConnect Tool, see Crema and Cavalli, 2018). (B) Standardization procedure, whereby each factor is transformed using a fuzzy function. Control points were chosen based on thresholds found in the literature (Table 6.1). In case of the SCI, due to values being relative (i.e. the higher the SCI value, the higher the fuzzy score, the higher the likelihood that these are important tributaries and vice versa), the minimum and maximum value of the SCI distribution serve as control points. Each step is described in more detail in the text. Note: If using LiDAR, aggregating first to 5m using the mean, then to 10-m using the minimum is advised (see Biron et al., 2013).....	47
Figure 6.3: (A) An example of an active confluence in Gaspésie (site 7a, see Figure 12 for location) showing tributary effect in the main channel that extends more than 2 km downstream, approximately 14 times the channel width (entire extent not pictured). (B) An example of multiple inactive confluence in the Coaticook watershed.	52
Figure 6.4: Spatial distribution of the 14 active (red triangles, letter i) and randomly selected inactive confluences (black squares, letter n) in the Coaticook watershed.....	53
Figure 6.5: Model output using the basic weight scenario (Table 2) for the Coaticook watershed with LiDAR data. Active confluences, detected from field and remotely-sensed images, are shown with red triangles, while randomly selected, inactive confluences are shown in black squares.....	54
Figure 6.6: Boxplots of the CMS score by confluence type in all weight scenarios considered in the sensitivity analysis (Table 6.3) for the Coaticook watershed using LiDAR data.....	55
Figure 6.7: Number of confluences classified in each CMS class by confluence type.	56
Figure 6.8: CMS scores of active (A) and inactive (B) confluences by their codes (see Figure 6.3) and throughout all scenarios. The numbers within each cell represent the absolute CMS score,	

	while the colour scheme corresponds to the CMS class they belong in. Problematic sites are marked in rectangles.	57
Figure 6.9:	Example of an inactive confluence detected by the model as important (Ruisseau Bissonnette) with a tributary bar of about 580m ² . Not pictured, but present upstream in the tributary, are two additional signs of geomorphic activity: disturbance potentially associated with building of a railroad bridge and increased mobility due to sediment deposition and large wood.	58
Figure 6.10:	Boxplots of the CMS score by confluence type in all weight scenarios for the Coaticook watershed, derived from the 10-m DEM. Contrary to the data extracted from the LiDAR, the model is not able to distinguish between active and inactive confluences in all weight scenarios.....	59
Figure 6.11:	(A) A comparison of the CMS (using the basic weight scenario in the fuzzy model) between the LiDAR and the 10-m DEM. (B) A close-up view of the rectangular area in A) showing cases where the flow accumulation (dashed blue line) does not follow the actual course of the channel (solid blue line), thus explaining the differences between the two DEM results in this area.	60
Figure 6.12:	Overview of model output using the equal weight scenario (Table 6. 2) for Gaspésie with 10-m DEM data. Active confluences, detected from field and remotely-sensed images, are shown with red triangles, while field study sites are marked by an adjacent purple star and labelled according to confluence type (see Figure 6.14 for the label meaning). (A) Cap Chat watershed; (B) Sainte-Anne watershed; (C) Marsoui watershed; (D) Mont-Saint-Pierre watershed; (E) Mont-Louis watershed.....	61
Figure 6.13:	Boxplots of the CMS score by confluence type in all weight scenarios considered in the sensitivity analysis (Table 6.3) for the Gaspésie study area using 10-m DEM data.....	62
Figure 6.14:	CMS score and class of the 9 Gaspésie field study sites. The letters a, i and m stand for active, inactive and modified (anthropogenically) confluence, respectively. For the latter it was hard to distinguish whether the tributaries had an important effect or not, due to their highly modified nature that does not correspond to classic confluence morphologies, such as a tributary bar. Note that the CMS score and class were calculated for each individual watershed so the scores cannot be compared between rows (sites).....	63
Figure 6.16:	Example of a type of tributary-main channel coupling in the Coaticook watershed. Before reaching the main channel, the tributary is dissected by two roads and one railroad. (A)	

and (C) show gullying due to intensive land use, which serves as an additional source of sediment in the tributary. (B) increased mobility associated with increased sediment load. (D) erosion associated with the presence of the road. (E) tributary mouth bar at the junction with the main channel.67

Figure 6.17: Distribution of important confluences (solely along the main river) in the Gaspésie study area and basin shape values for each of the five investigated watersheds. Values closer to 1 indicate more compact basins and small values indicate more rectangular basins.69

List of Tables

Table 4.1: Basin area of study watersheds in Gaspésie.	13
Table 4.2: Tributary and exposed bar sampling zones for the 9 field study sites in Gaspésie (see Figure 4.1). If a feature was present multiple times, the number is indicated within parentheses.	15
Table 4.3.: Statistical tests used to verify whether there is a significant difference between the median bedload grain size between the pre-, confluence and post-confluence zone (Figure 4.2).	16
Table 5.1: Average D95, D84 and D50, Dmax and Dmin values for the entire Gaspésie dataset grouped by sampling zone.	32
Table 6.1: Variables controlling whether a tributary has an effect on the main channel or not. Unit stream power, sediment connectivity and valley confinement (highlighted in grey fill colour) are included in the proposed fuzzy GIS model.....	43
Table 6.2: Basic weight scenario using a pairwise comparison matrix (Saaty, 1980).	50
Table 6.3: The three weight scenarios used in the sensitivity analysis.	51

1. Introduction

We are now living in a time where human activities have modified the Earth to such an extent that a new geologic era has been proposed, that of the Anthropocene (Lewis and Maslin, 2015; Waters et al., 2016). When it comes to rivers, human activities, in terms of direct and indirect modifications of water and sediment regimes (e.g. dams, land use changes, infrastructure development, etc.), have led to less complex, less stable and less functional river ecosystems that are less able to absorb perturbations such as climate change. In light of this, a paradigm shift toward building resilience to change is required (Wohl et al., 2015; Fryirs, 2017). While traditional river management practices have relied on notions of linearity and of equilibrium states, this stands in contradiction to the current scientific understanding of how river systems work, which emphasize instability, change and disturbance regimes. New approaches better adapted at understanding and predicting changes in river systems at various spatial and temporal scales need to be developed.

My research project aims to contribute filling this gap by using field and remotely-sensed methods to better understand interactions between the main river channel and its tributaries. In particular, it will focus on identifying locations along the main channel that are sensitive to increased mobility as a result of tributary inputs of sediment through a fuzzy, multi-criteria model, developed in a Geographic Information System (GIS). This research topic will be applied in mountainous environments of the Gaspé Peninsula and Eastern Townships Region in Québec at the reach-to-watershed scale.

2. Literature review

2.1. Rivers are mobile

It is well established in the field of fluvial geomorphology that rivers are dynamic systems that operate in a state of perpetual adjustment over space and time, as a response to complex interactions between internal and external forcings (Brierley and Fryirs, 2005; Church and Ferguson, 2015). As a consequence, change is an inherent characteristic of river systems and must be taken into account in river management by leaving sufficient space around rivers for fluvial processes to operate.

Change is partly determined by a river's capacity for adjustment, particularly the ease with which the channel is able to adjust its position on the valley floor, i.e. the channel mobility. Channel mobility is particularly obvious in meandering and braided channels, and is closely associated with the presence of bars, such as point bars in meandering streams and mid-channel bars in braided rivers (Knighton, 1988). The overall migration rates are controlled by boundary conditions characteristic of any given location within a watershed and include relief, slope and valley morphology (Brierley and Fryirs, 2005). These set the potential energy of a landscape and how this energy is used, and determine flow and sediment transfer regimes, also governed by the climate setting and, increasingly, human activities (ibid.). Depending on these local variables, the mobility space required around rivers may vary greatly, and in some cases cover most of the floodplain (Piégay et al., 2005; Biron et al., 2014).

2.2. Confluences: key nodes in the fluvial network

Confluences are key nodal points in a drainage network, and major manifestations of the inherent nonlinearity of river systems. While the general downstream trend is for a river's discharge and channel size to increase, and for channel slope and average grain size of sediment to decrease, punctuated inputs of water and sediment delivered to the main channel by tributaries may alter these trends in a significant way, inducing abrupt changes in channel form and process both within the immediate confluence zone and extending some distance up and down the main channel (Richards, 1980; Rhoads, 1987). Despite their importance in terms of geomorphology, hydraulics, sedimentology and ecology, confluences and tributary-main channel interactions have been understudied by the scientific community, partly because of their intricate nature. However, over the last decades, interdisciplinary advances from laboratory tests (Mosley, 1976; Best, 1987; Leite Ribeiro et al., 2012; Guillén-Ludeña

et al., 2015, 2016, 2017a,b), field investigations (Richards, 1980; Biron et al., 1993; De Serres et al., 1999; Parsons et al., 2007; Rhoads et al., 2009; Fryirs and Gore, 2014; Martín-Vide et al., 2015; Lisenby and Fryirs, 2016, 2017) and numerical modelling (Bradbrook et al., 2000a, b, 2001; Benda et al., 2004; Boyer et al., 2006; Ferguson et al., 2006; Roca et al., 2009; Constantinescu et al., 2011; Swanson and Meyer, 2014; Guillén-Ludeña et al., 2017a) have provided valuable information about the structure and function of confluences, as well as interactions between these nodes and their connected links at the scale of the whole watershed. For example, at the scale of the confluence, studies investigating feedbacks among flow, sediment transport and bedform reveal that the most important controls on the dynamics of the confluence are confluence planform, as well as the curvature and varying slope of the incoming channels, junction angle, bed height discordance, discharge and momentum flux ratios, bed material caliber and sediment supply (Mosley, 1976; Best, 1987, 1988; Biron et al., 2002; Best and Rhoads, 2008; Ribeiro et al., 2012). These create six different hydraulic zones at confluences (Best, 1986; Biron et al., 1996; Boyer et al., 2006; Rhoads et al., 2009; Ribeiro et al., 2012), which combined with sediment transport, further help create some principal morphologies (Best, 1987; Figure 2.2.1). This is important, as these zones and elements further influence how different processes operate up- and downstream.

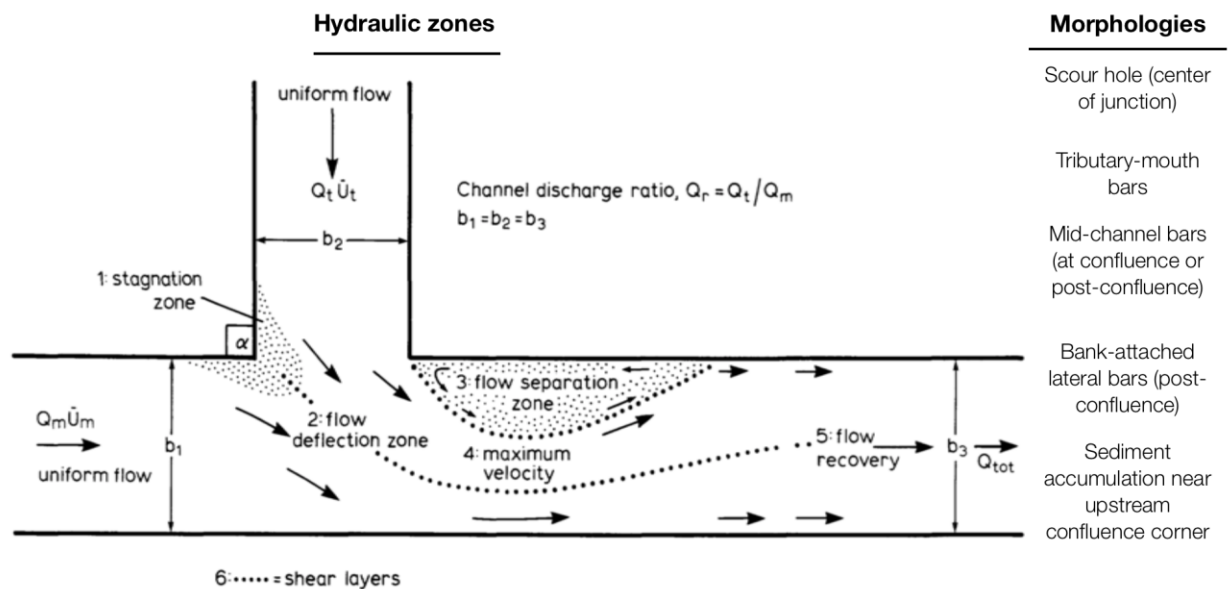


Figure 2.1: A model of flow-sediment dynamics at confluences. Hydraulic zones are demarcated with numbers, while typically resultant morphologies are listed on the right (modified from Best, 1987: 28).

2.3. The role of tributaries on watershed sediment dynamics

The effects of tributaries are not only limited to confluences but extend well into the main channel; it is through the confluence of tributaries with main rivers that flow, sediments, solutes and organic matter are provided to the fluvial system, which further reflects the variability of fluvial transport at the network scale. Discontinuities induced by considerable tributary input of water and sediment have been shown to alter the dimensions (width), slope and/or bed grain-size distribution of the main channel (Richards, 1980; Rhoads, 1987). This is especially prominent where a substantially coarser or finer sediment load than that of the main channel is added (Ferguson and Hoey, 2008). For example, Richards (1980) showed that streams in an upland environment in the UK have constant widths along distinct network links, except for reaches downstream of confluences, which increased in proportion to the 0.6 power of link magnitude. Harvey (1997) found that inputs from gullies and tributaries in a small upland stream in northwestern England lead to instabilities, which are reflected in channel widths increases of 3 to 5 meters up to 2 kilometers downstream of these supply points. Similarly, Duncan et al. (2009) examined the effects of shallow alluvium-dominated confluences, i.e. shoals, on channel morphology in southeastern United States and found that shoals located below large confluences were wider and had higher proportions of gravel and cobble bed sediments. Rhoads et al. (2009) studied changes in bed morphology as a result of variable hydrological conditions at a small, human-impacted confluence in the United States and observed widening of the outer bank of the downstream channel as much as 2 meters over 15 years that occurred due to an asynchronous hydrological response between the tributary and the recipient channel, the former having persistent faster runoff-response times. Conversely, Rhoads (1987), in a review of confluence studies, found that width remains constant or even decreases.

Disruption of main channel gradient and bed material calibre is also common. Sternberg's (1875) work on bed material grain size revealed that grain size decreases with distance downstream. Field investigations revealed that grain size decline was interrupted at confluences (Church and Kellerhals, 1978) and fan contacts (Bradley et al. 1972). Rice and Church (1998) call the pattern of increasing median grain size at the confluence due to significant sediment inputs followed by downstream grain size decline as "sedimentary links". Slope behaves identically: it declines along the sedimentary link and then increases abruptly at the beginning of the next link (Rice and Church, 2001). Rice (1998) found that tributaries that are able to maintain sedimentary links and elicit slope and bed calibre adjustments in the recipient channel are larger and steeper. They also transport coarser sediment

(Knighton, 1980). In a review of 14 case studies across the western US and Canada, Benda et al. (2004) observed that the most common effects were disruptions in grain size and a change in slope below the confluence of larger tributaries relative to the main channel. However, Rengers and Wohl (2007) studied steep tributaries of a tropical mountain river in Panama and did not find any consistent trends in grain size between tributaries, which they attribute to stream width variations that act as a local control on grain size, in that coarse grains are associated with narrow channel reaches, which may be better able to effectively convey the coarse load input from a tributary without a gradient increase, thus masking the effect of sedimentary links.

Tributaries that deliver voluminous and coarse sediment lead to various changes in the morphology of the main channel. Typically, alluvial and debris fans impinge on channels, displacing them across the valley floor (Brierley and Fryirs, 1999; Harvey, 1997, 2001; Florsheim et al, 2001, 2004; Fryirs et al., 2007b; Al Farraj and Harvey, 2010; Fryirs and Gore, 2014). The deposition of material forces a steepening of the gradient and a coarsening of the bed downstream, accompanied by shallowing of the gradient and fining of the bed upstream of the disruption, thus highlighting the role of local factors that override downstream trends (Benda et al., 2004; Al Farraj and Harvey, 2010; Hanks and Webb, 2006; Swanson and Meyer, 2014; Rice, 2017), as well as the role of the confluence zone as an important site of sediment storage. The concept of storage is very strongly related with notions of connectivity, especially that of sediment connectivity, whereby sediment is transferred from its source to a sink, i.e. a storage location, through processes of particle entrainment, transport and deposition (Bracken et al., 2015), operating within and between different landscape compartments, such as hillslopes, channels, floodplains, tributaries and recipient streams (Harvey, 2002; Fryirs et al. 2007a, b). Transfer between landscape compartments can be coupled or interrupted by various landforms, such as buffers, barriers and blankets (*sensu* Fryirs et al, 2007a). These manifestations of sediment disconnectivity impede the lateral, longitudinal and vertical sediment contribution over various spatial and temporal timescales, and their spatial extent and distribution serves as a useful insight into the proportion of a watershed that is sedimentologically connected to the channel network, as well as the location of geomorphic change along a channel network (Harvey, 2002; Fryirs et al., 2007a; Czuba and Foufoula-Georgiou, 2015). The sediment disconnectivity framework also highlights the two-way interactions between tributaries and main channels. For instance, Cohen and Brierley (2000) studied tributary and main channel response to flood disturbances in a forested watershed and found that lateral adjustment of the main channel to recurrent floods induced lagged and complex responses of profound instability

in the tributary, progressing from incision to channel straightening and widening, lateral adjustment and downstream shifts of the erosional foci and the deposition of bars. Florsheim et al. (2001) investigated the effects of culvert maintenance excavation on the interplay between tributary systems and the floodplain and sediment deposits on the valley floor. They documented that excavation considerably deepened and widened tributaries, inducing a lower base level, which further lead to headward migration and incision into the upstream tributary channels. As a consequence, the sediment storage potential of the fan and floodplain, as well as the storage residence time on these landforms were reduced.

2.4. Controls on the impact of tributaries

From the case studies exemplified above it follows that tributary-main channel confluences can be considered hotspots of fluvial geomorphic change at the network scale (Czuba and Foufoula-Georgiou, 2015), with complex interactions between the tributary and the main channel. However, not all tributaries have an effect: Rice (1998) found that less than 20% out of the approximately 100 tributaries studied had any perceptible effect on the grain size or slope of the mainstream and the analysis of Benda et al. (2004) documented geomorphically insignificant tributaries especially in semi-arid environments, such that the question of why only some tributaries have a considerable impact remains pertinent. In order to identify which tributaries elicit adjustments, and thus determine reaches that are susceptible to geomorphic change, knowledge about the factors controlling the magnitude of impact is needed. To date, only a limited number of studies provide a quantitative basis for predicting the effects of tributaries on the main-channel morphology by taking into account a combination of key parameters (Rice, 1998; Benda et al., 2004; Ferguson et al., 2006; Rice et al. 2006; Lisenby and Fryirs, 2017; Rice et al. 2017), but overall knowledge remains mostly qualitative.

Rice (1998) determined that the best parameters to identify significant tributaries are the product of tributary basin area and tributary slope, and the symmetry ratio, expressed as the ratio between the tributary basin area and the main channel basin area. Benda et al. (2004) confirmed through their analyses that the symmetry ratio is a good predictor of tributary impact. The hypothesis is that the probability of tributary impact increases with increasing symmetry ratio and data indicates that very small tributaries, but also that those tributaries approaching the same basin area as the main channel are insignificant. Benda et al. (2004) went beyond local factors and additionally accounted for catchment-wide controls, such as shape, drainage density and local network geometry reflected in the

size, spacing and angle of confluences. They postulated that long rectangular-shaped basins are geomorphologically more active in their headwaters and the magnitude of their potential impact decreasing with distance downstream. Conversely, heart-shaped basins lead to higher impacts, as larger tributary network are able to form. Furthermore, watersheds that are more dissected have a higher density of tributaries, which should lead to higher frequencies of impacts. Higher confluence angles promote higher magnitudes of confluence effects. Rice (2017) tested these assumptions and confirmed that watersheds with a large basin area and a compact shape have a greater occurrence of significant tributaries and that tributary impact in linear watersheds are concentrated in the headwaters. This highlights the importance of network configuration and watershed shape as key controls of coarse sediment transfer and physical heterogeneity across a fluvial network.

Ferguson et al. (2006) developed a numerical model to simulate interactions between the bed grain size distribution and bed elevation as a result of lateral inputs of water and sediment. They suggest that the response of the main channel to tributary inputs are controlled by the ratio of tributary discharge to that of the main channel (Q_r), the ratio of tributary bedload flux to that of the main channel (F_r) and the relative bed load grain sizes of the two fluxes (D_r). Ultimately, patterns of slope and grain size express the interplay between the amount of sediment delivered from the tributary and the discharge available to transport it. Rice et al. (2006) used the same parameters to investigate physical heterogeneity at confluences and found that the product between F_r and D_r was the key control on such heterogeneity.

Lisenby and Fryirs (2017) adopt an approach that is rooted in the framework of sediment (dis)connectivity to identify important tributaries in terms of their impact on the distribution and proportion of bed load along the main channel in a human-impacted catchment in northern Australia. Their findings suggest that both geomorphic and anthropogenic factors act as major controls on the patterns of sedimentary links along the main channel and that the distribution of buffers and barriers, as well as the effective catchment area, i.e. the area that actively contributes sediment to the fluvial network (Fryirs et al., 2007b) have the potential to identify such sedimentologically significant tributaries.

2.5. Detecting more mobile channels near confluences

From these studies emerges the idea that controls on tributary impacts can vary between watersheds

in different environments and that in order to thoroughly identify and predict tributary impacts multiple factors must be taken into consideration. For instance, the methodology and parameters used by Rice (1998) were suitable for dynamic, highly coupled watersheds carrying coarse sediments, but were not applicable in the study site of Lisenby and Fryirs (2017), which was characterised by a lower topography and finer bedload sediments.

An equally powerful predictor of sensitive reaches prone to geomorphic change, but not yet used explicitly to answer questions pertaining to tributary impacts in general and tributary impacts on channel mobility in particular, is stream power. Total (gross) stream power provides a measure of the energy available to be used in any given valley setting, while unit (specific) stream power reflects how energy is used on the valley floor. The analysis of downstream variations of stream power is a very useful indicator of its interactions with morphological change via sediment distribution along the longitudinal profile of channel networks. For instance, averaged values of stream power over reaches of 3 to 5 kilometers give an indication whether the geomorphic response of a river reach is aggradational (stream power decreases longitudinally) or degradational (stream power increases longitudinally) (Bizzi and Lerner, 2015). Sensitivity thresholds can be derived on the basis of such analyses, representing minimum energy conditions necessary to elicit major geomorphic change (Thorne et al., 2011; Vocal Ferencevic and Ashmore, 2012; Bizzi and Lerner, 2015; Gartner et al., 2015; Lea and Legleiter, 2016; Lisenby and Fryirs, 2016; Yochum et al., 2017). The potential of stream power in predicting reaches susceptible to lateral adjustments due to tributary inputs is all the more attractive given the increasing access to high-resolution remotely-sensed spatial data at the scale of whole watersheds, with broad applications, including geomorphic mapping (Marcus and Fonstad, 2008), catchment-wide hydro-geomorphological assessment (Fonstad and Marcus, 2010; Vocal Ferencevic and Ashmore, 2012; Biron et al., 2013; Yochum et al., 2017), analysis of habitat heterogeneity (Hugue et al., 2016), grain size measurement (Carbonneau et al., 2004, 2005), as well as the planform morphodynamics of large river confluences over decadal timescales (Dixon et al., 2018).

Predictions about the location of expected channel mobility are extremely valuable for informing science-based river management. Confluences are sites susceptible to flooding and bed instability associated with significant tributary inputs and can pose serious hazard to infrastructure, such as roads, bridges or culverts that may extend well beyond the confluence zone. Furthermore, uncertainty associated with climate change, superimposed on equally uncertain outcomes of potential river adjustment highlights the need to shift towards a more comprehensive and sensible river management

(Brierley and Fryirs, 2005). Most of the time, this involves the realization that the river knows best how to “look after itself” and the adoption of a passive approach, where the management action is limited to allowing more space for rivers to migrate, adjust and flood naturally (Kondolf, 2011). The last few years have increasingly seen such approaches, under various names: “room for the river” (Baptist et al. 2004), “erodible corridor” (Piégay et al., 2005), “fluvial territory” (Ollero, 2010), “river corridor” (Kline and Cahoon, 2010) and “freedom space” (Biron et al., 2014), the latter being the most comprehensive, as it integrates the natural river mobility, floodplain areas, as well as riparian wetlands into one single common space.

Despite major advances in our knowledge of confluence dynamics in recent years, two main questions require future research to address. The first is concerned with the use of automated tools for the catchment-wide identification of significant tributaries that trigger channel instability and adjustment not only in the confluence zone, but extending both up and down the main channel, which then allows for prediction of this impact based on the integration of multiple key parameters that control it. The second builds on the first and deals with investigating if, within a freedom space management approach, it is necessary to allow more space near confluences that are likely to increase channel mobility and therefore to possibly threaten infrastructure within (e.g. bridges) or near (e.g. roads, railroads, residential development) the channel.

3. Research objectives

Approaches like the freedom space for rivers require hydrogeomorphological knowledge and expertise which is not always available in practice to river managers. There is therefore a need to develop semi-automated methods to help define these zones. In addition, geomorphic disturbances may be amplified at confluences with a high tributary input of sediment; thus, confluence effects constitute an important element that needs to be better understood and incorporated into such approaches. The research presented herein is thus guided by the following research objectives and research questions:

1. To improve our understanding of the morphodynamics of confluences characterized by high sediment load tributaries in Gaspésie.

Q1.1 Is the post-confluence zone distinct from the pre-confluence zone in terms of bedload sediment, number and area of bar deposits, channel width and water surface slope?

Q1.2 Are important tributaries characterized by a higher water surface slope relative to that of the main channel?

2. To develop a semi-automated GIS model based on fuzzy logic to predict morphologically sensitive confluences at the watershed scale.

Q2.1 At the watershed scale, what are the most important factors that govern the impact of tributaries on main channel mobility (understood as the lateral adjustment on the valley floor) and can these be integrated in a GIS model to determine sensitive zones within the main channel, defined as those being prone to lateral adjustment due to high tributary sediment inputs?

Q2.2 How does the resolution of the digital elevation model (DEM) affect the distribution of morphologically sensitive confluences along the main channel in the GIS model?

4. Methodology

4.1. Study area

The Northern Gaspé Peninsula (Figure 4.1) is located in the most eastern tip of southern Quebec and belongs to the Appalachian Range. This is reflected in the headwater areas of all watersheds that are part of the study area. Before draining into the Saint-Lawrence River, the high relief of the Appalachians gives way to plateaus with deep, U-shaped valleys. The shape of the river network is controlled by two faults, which separate sedimentary rocks in the north from predominantly volcanic rocks in the south (Cap Chat and Sainte-Anne watersheds) (MRNF, 2006). The largest watersheds tend to have a more compact basin (i.e. heart-shaped basin with dendritic network), while smaller ones are usually more elongate (i.e. rectangular basin with trellis network). The hydrologic regime of the temperate Gaspé Peninsula is pluvio-nival, which demarcates itself through two periods with intense flood peaks: one in spring during snowmelt and one in the fall during the precipitation season. The area is additionally prone to intense and short rainy periods during the summer, due to hurricane tails from the Atlantic Ocean. This impacts predominantly smaller watersheds. Forestry is the predominant land use with 93% of the entire surface area (MRNFP, 2004).

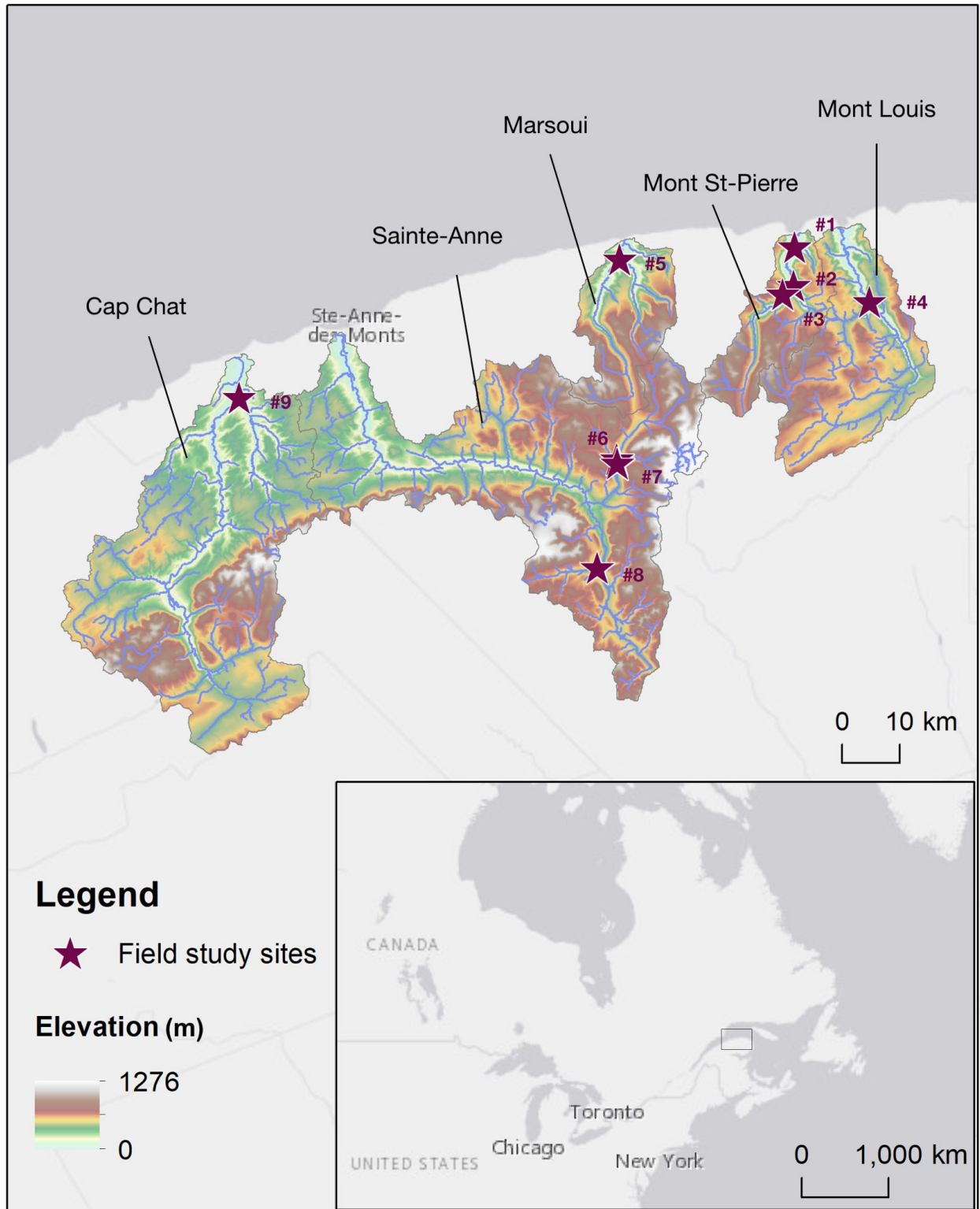


Figure 4.1: Gaspésie study area comprising five watersheds and nine field study sites (purple stars).

The Gaspésie study area is composed out of five watersheds: Cap Chat, Sainte-Anne, Marsoui, Mont-Saint-Pierre and Mont-Louis. Table 4.1.1 presents their watershed area.

Table 4.1: Basin area of study watersheds in Gaspésie.

Watershed	Field study site	Tributary basin area (km²)	Main channel basin area at confluence (km²)	Symmetry ratio (tributary/main channel area)	Total watershed area (km²)
Mont-Saint-Pierre	#1	7.6	125.9	0.06	139
	#2	43.2	67.2	0.64	
	#3	1.8	63.2	0.03	
Mont-Louis	#4	79.5	168.4	0.47	294
Marsoui	#5	50.4	86.3	0.58	156
	#6	24	87.4	0.27	
Sainte-Anne	#7	19	112.5	0.17	822
	#8	32.8	130.2	0.25	
Cap Chat	#9	125	592.9	0.21	740

4.2. Field data

Field data were collected at nine confluences in Gaspésie during summer 2018 (see Figure 4.1, purple stars) in order to address the first research objective (see Chapter 3). Five out of the total nine were already known due to their geomorphologically dynamic nature (from previous research projects carried out in the area by a team from Université du Québec à Rimouski), while the rest were chosen based on digital elevation model (DEM) and orthophoto analysis conducted prior to the field visit. Out of these, two represented inactive confluences, where tributaries appeared to have no effect on the morphology of the main channel. Measurements were carried out in these instances too, in order to see whether there was a contrast between the two confluence types.

To characterize sediment sizes variations in relation to confluences, a random-walk pebble count (Wolman, 1954) was carried out along the main channel. A minimum of 100 samples were taken for each sampling zone and a distance of at least two maximum particle diameters was ensured between sampling points to assure the independence of individual observations (Rice and Church, 1988). Bedload size was determined using a gravelometer at 0.5ϕ intervals ($\phi = \log_2 D$, where D is particle

diameter in mm). For slope measurements, water surface profiles were recorded using a Leica Total Station (TS805L) both along the main river and inside the tributary. The number and area of bars within the sampling zone, as well as the average bankfull channel width, were calculated based on orthophotos in ArcGIS 10.4 (ESRI, 2016).

The distance over which all these variables were sampled was determined based on homogeneous reaches in terms of main channel features and on accessibility. Thus, each study site was divided into three main zones (Figure 4.2): pre-confluence, confluence, post-confluence. The confluence zone extended to the entire length of the tributary mouth or to the downstream end of the tributary bar. When present, bar material was sampled on tributary bars (Figure 4.2, a). Additional exposed bar deposits were also sampled if they were located inside the entire studied river segment, as this is related to longitudinal variations in bed texture (Figure 4.2, b). Table 4.2 illustrates the sites where tributary and exposed bar material was sampled.

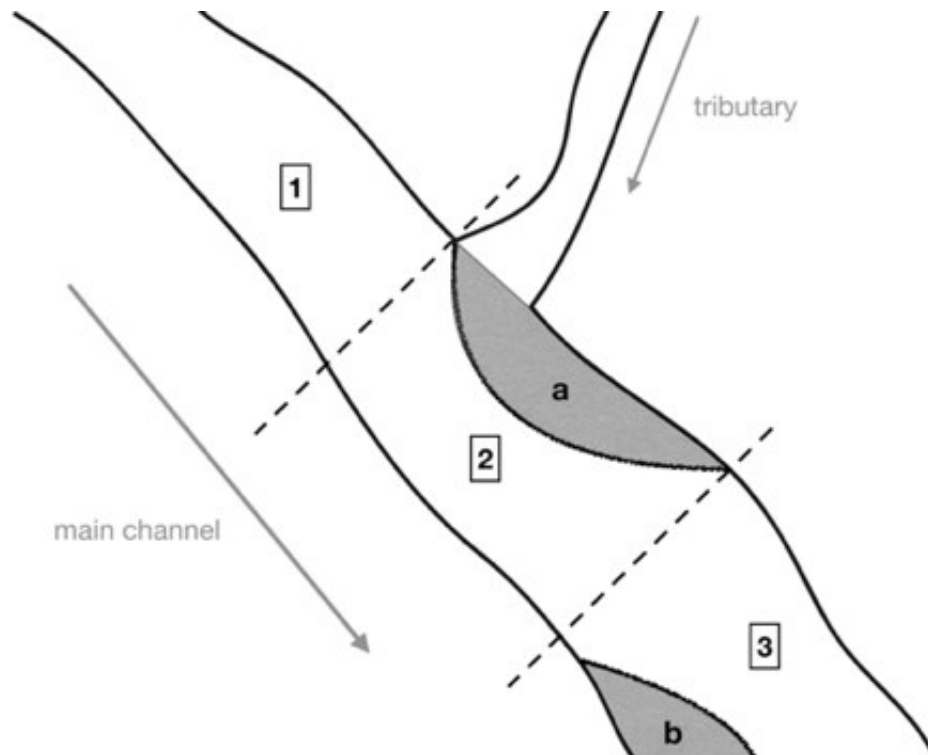


Figure 4.2: Sampling zones of bed material for each field study site: pre-confluence (1), confluence (2), post-confluence (3) zones, as well as tributary bars (a) and any other exposed bar in downstream direction (b).

Table 4.2: Tributary and exposed bar sampling zones for the 9 field study sites in Gaspésie (see Figure 4.1). If a feature was present multiple times, the number is indicated within parentheses.

Sampling zones	Study sites								
	#1	#2	#3	#4	#5	#6	#7	#8	#9
Tributary bar	X	X					X	X	
Exposed bar		X	X	X		X	X (2)		

To verify whether the difference between the pre- and post-confluence zone was significant, statistical tests in the form of analyses of variance were carried out using the RStudio software (RStudio Team, 2016) for each field study site. For cases where the number of samples differed between the individual zones (see Figure 4.2), resampling was used to ensure equal sample size. Data were tested for assumptions of normality of residuals (D’Agostino test due to repeated values and skewed data), homogeneity of variance (Levene’s test due to skewed data) and independence. Generally, ANOVA was used on datasets where all assumptions were respected, whereas Welch’s F or Kruskal Wallis tests were performed when the dataset did not respect the second or none of the assumptions, respectively. However, because ANOVA is fairly robust when the normality assumption is violated (Schmider et al., 2010; Blanca et al., 2017), it was employed also when data was skewed, but respected all other assumptions. Post-hoc tests were conducted when differences in the median were significant, in order to see which groups were different. In order to specify whether the confluence effect was limited to the confluence zone only, the same procedure was applied with three groups (pre-, confluence and post-confluence zone). Table 4.3 presents an overview of the statistical tests employed at each field study site.

Table 4.3: Statistical tests used to verify whether there is a significant difference between the median bedload grain size between the pre-, confluence and post-confluence zone (Figure 4.2).

Statistical test	Study sites								
	#1	#2	#3	#4	#5	#6	#7	#8	#9
ANOVA	X			X		X		X	
Welch's F					X		X		
Kruskal Wallis		X	X						X

4.3. GIS model

A fuzzy approach was decided upon in carrying out the multi-criteria analysis because of the recognition that uncertainty is inevitable when making decisions in real world situations. Uncertainty can be associated with the imprecise nature of the decision environment, the incomplete understanding of the decision problem at hand, as well as with input data and measurement error, all of which should be considered when tackling spatial multi-criteria decision problems (Malczewski and Rinner, 2015).

Fuzzy set theory is multi-valued logic built upon the notion of partial truth, which allows intermediate values to be defined between conventional binary evaluations like true/false (Zadeh, 1965; Malczewski, 1999). Fuzzy set theory allows classes of elements that do not have sharply defined boundaries (fuzzy sets) to be partial members to multiple, overlapping sets (Malczewski, 1999; Malczewski and Rinner, 2015). Such a logic is useful in describing the vagueness inherent in the real world where elements can belong to multiple sets in various degrees. Because of this property, fuzzy logic has found great utility in a broad range of GIS-based multi-criteria decision analysis applications (see Malczewski, 2006 for a review).

Consequently, the identification of river reaches geomorphically sensitive to tributary inputs was carried out by means of a fuzzy multi-criteria analysis in ArcGIS 10.4 (ESRI, 2016) to address the second research objective. This approach is further anchored in (1) the evidence that the impact of tributaries is dependent on multiple factors, (2) the recognition of the role of uncertainty and imprecision in this type of analysis.

Two regions in Quebec were used to test the GIS model: the Gaspésie watersheds described above and the Coaticook watershed, located in southern Québec in the physiographic region of the Appalachian Range, bordering the United States to the south (see chapter 6 for a more detailed description).

The approach is mainly based on DEM analysis. Both a 1m LiDAR (vertical precision +/- 0.15m, aggregated to 10 m) and a governmental 10m DEM data (vertical precision +/- 5m) were used in the Coaticook watershed, whereas only the 10-m governmental DEM was available for the Gaspésie watersheds. Figure 4.3 illustrates the steps employed in the multiple-criteria analysis, which are described in more detail in Chapter 6.

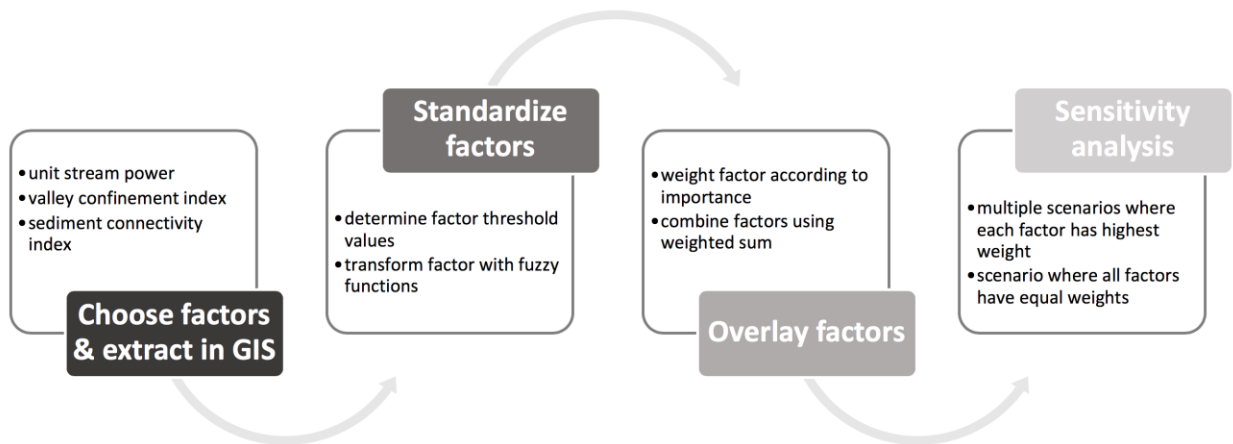


Figure 4.3: Summary of steps for the multi-criteria analysis. See Chapter 6 for a more detailed description of each.

5. Geomorphological impact of tributaries: Field analysis

5.1. Geomorphic characterization of Gaspésie confluences

5.1.1. Mont-Saint-Pierre watershed

Site #1 (Figure 4.1) is the confluence between the Mont-Saint-Pierre River and an intermittent tributary, the Ruisseau de la Youtte (Figure 5.1), located in the lower catchment at about 2.5 km before its outlet into the Saint-Lawrence River. The confluence itself is located in the village municipality of Mont-Saint-Pierre and is thus characterized by additional anthropogenic elements, like roads, road crossings and direct channel intervention. The main channel here flows into a laterally unconfined valley setting and abuts terraces, some forested, some transformed into agricultural land. Upstream from the confluence, channel planform is single-thread, laterally stable and straight with constant width (Figure 5.1a). The bed is made of deep post-glacial alluvial sedimentary rock and particle size is homogeneous. Geomorphic units are limited to pool-riffle sequences.

The tributary flows through mostly colluvial material, with some bedrock and lateral adjustment can be observed from orthophotos before it reaches the valley floor. Once it reaches the flat valley bottom, the tributary flows another 500m before merging with the main channel. Large amounts of woody debris are deposited at the curvature between the tributary and the main valley. At the time of the field visit, the tributary channel was a net aggradational zone, which acted as a buffer to lateral connectivity between the merging channel (Figure 5.1d).

At the confluence, the tributary deposited its relative coarser load so that a tributary bar was formed, displacing the main channel (Figure 5.1b). This triggered lateral adjustment in the main channel, as documented by increased erosion and deposition processes relative to upstream reaches. Structural heterogeneity increases as a result, visible through an abundance of geomorphic units and structural elements that redefine the channel planform: confluence-forced pool just upstream of the confluence, multiple bank-attached bars, a scroll bar, secondary channels on the main bank-attached bar at the confluence, riffle-pool sequences, large woody debris, as well as a 2m deep pool, which could be a scour hole formed as a result of mixing of the two flows (Figure 5.1c). As a result, sinuosity increases downstream, but the channel remains predominantly single-thread, with the exception of some flood channels.

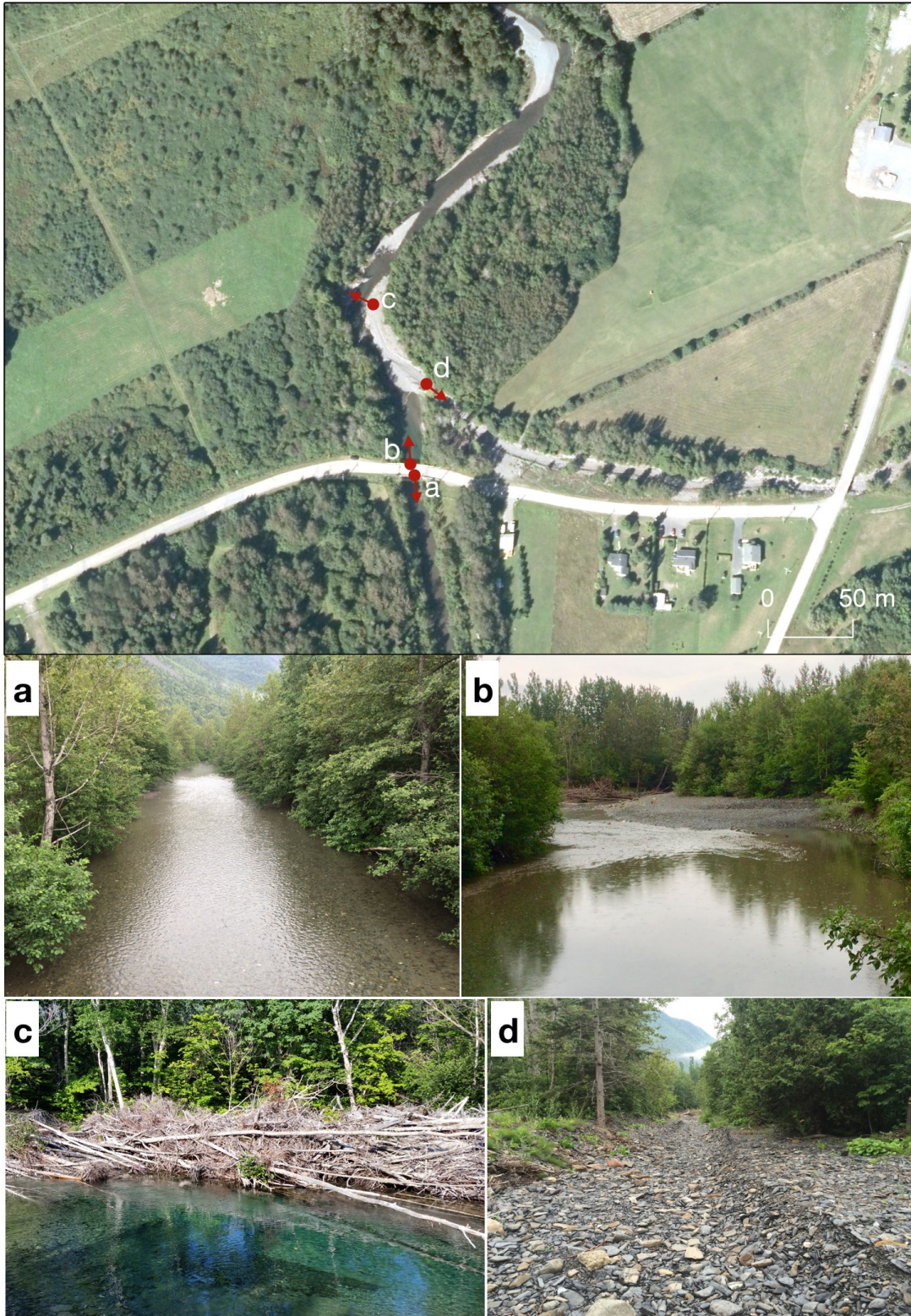


Figure 5.1: Planform view of study site #1 in the Mont-Saint-Pierre watershed (see Figure 4.1 for its location). Photos illustrate: channel morphology upstream of the confluence (a), at the confluence (b), large woody debris on eroding bank along with a 2m deep pool (c), upstream view into the tributary showing accumulation of sediment (d).

Anthropogenic structures like bridge abutments, bank revetments, culverts and roads also control the dynamics of the confluence by locally funneling/blocking sediment carried by the tributary, by disconnecting the channel from its floodplain and by constraining the mobility of the channel.

Site #2 (Figures 4.1; 5.2) is located at the confluence between the Mont-Saint-Pierre River and the Branche de l'Est, the largest tributary of the Mont-Saint-Pierre watershed (43.2 km², drainage area ratio of 0.64 - Table 4.1). Its location coincides with the transition of the valley from a confined setting to partly-confined setting.

Upstream, the channel has low sinuosity and is single thread. However, 200m upstream, mass wasting processes associated with the left valley flank resulted in a substantial depositional zone that forced the channel to avulse, so that the upstream reach is laterally unstable (Figure 5.2f). The new channel was carved within the forest. Bed material is composed out of post-glacial alluvial sediment. Geomorphic units include step-pool sequences, debris and root jams with sandbars trapped behind them.

The tributary flows in a partly-confined to confined valley, is generally single-thread and has low sinuosity. Bed material is similar to the main channel, but generally larger in diameter. The hillslope on the left is characterized by a continuous bench that extends up to the confluence zone and erodes the bank on the opposite side (Figure 5.2d). Other geomorphic units include step-pool sequences. The occurrence of a large wood jam has led to the formation of distributary channels through the forest that are connected to the main channel at high flows (Figure 5.2e).

The confluence is characterized by a tributary bar that pushes the main channel towards the left hillslope, resulting in bank erosion on the opposite bank (Figure 5.2a and b). Another log jam is present at the confluence between the two streams (Figure 5.2c). This obstruction has created a small return channel around it. Further downstream the sinuosity of the main channel increases and multi-thread channels are formed. This marks the beginning of a long aggradational section, with a high occurrence of multiple types of bars (e.g. point bars, mid-channel bars, bar complexes), which stretches about 2km upstream of study site #1.

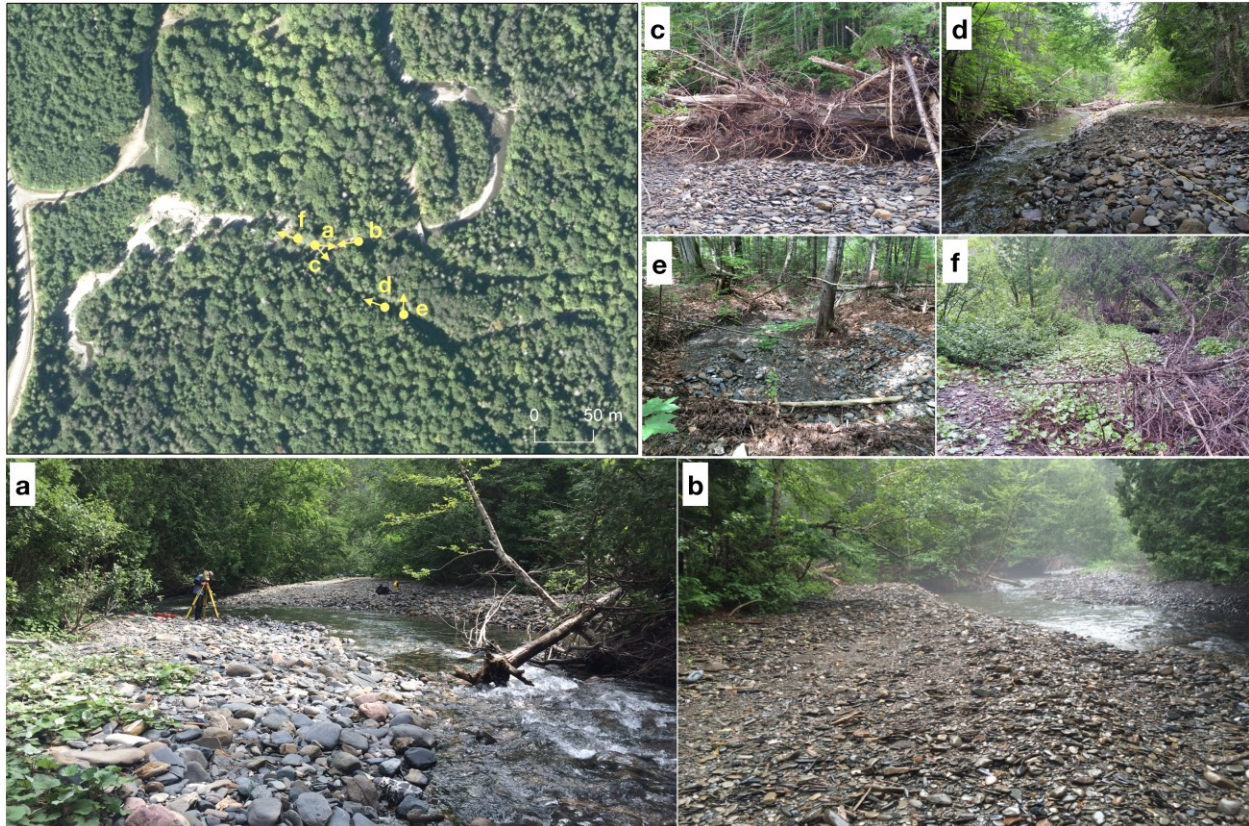


Figure 5.2: Planform view of study site #2 in the Mont-Saint-Pierre watershed (see Figure 4.1 for its location). Photos illustrate: main channel upstream and downstream of the confluence (a), tributary bar (b), tributary mouth jammed by large woody debris (c), upstream in the tributary (d), new (dis)tributary channels forming in the forest (e), former pre-avulsion channel position of the main stream, now vegetated (f).

Study site number #3 is located 2km upstream of site #2 and represents the confluence between the Mont-Saint-Pierre River and a steep, intermittent torrential channel (Figure 5.3). The valley setting is partly-confined with discontinuous floodplain pockets. The channel is sinuous, single-thread and has homogeneous bed material size with the exception of a reach downstream of the confluence, which is characterized by coarser fractions. Lateral stability is relatively low due to inputs from mass wasting processes in the upstream reach (Figure 5.3c), and due to a compound bar that has signs of reworking in the downstream reach (Figure 5.3f). Geomorphic units are an isolated boulder bar, and some steps formed adjacent to the compound bar. The latter pushes the channel towards the exterior left bank, which it erodes. A pool is formed downstream of the compound bar. Presence of large woody debris is widespread on the bar, as well as downstream, but to a lesser degree. Due to the presence of a road next to the channel in this constricted valley segment, the outer bend of the main channel was stabilized with riprap (Figure 5.3a, b). Some material associated with the riprap can be found in the main channel.

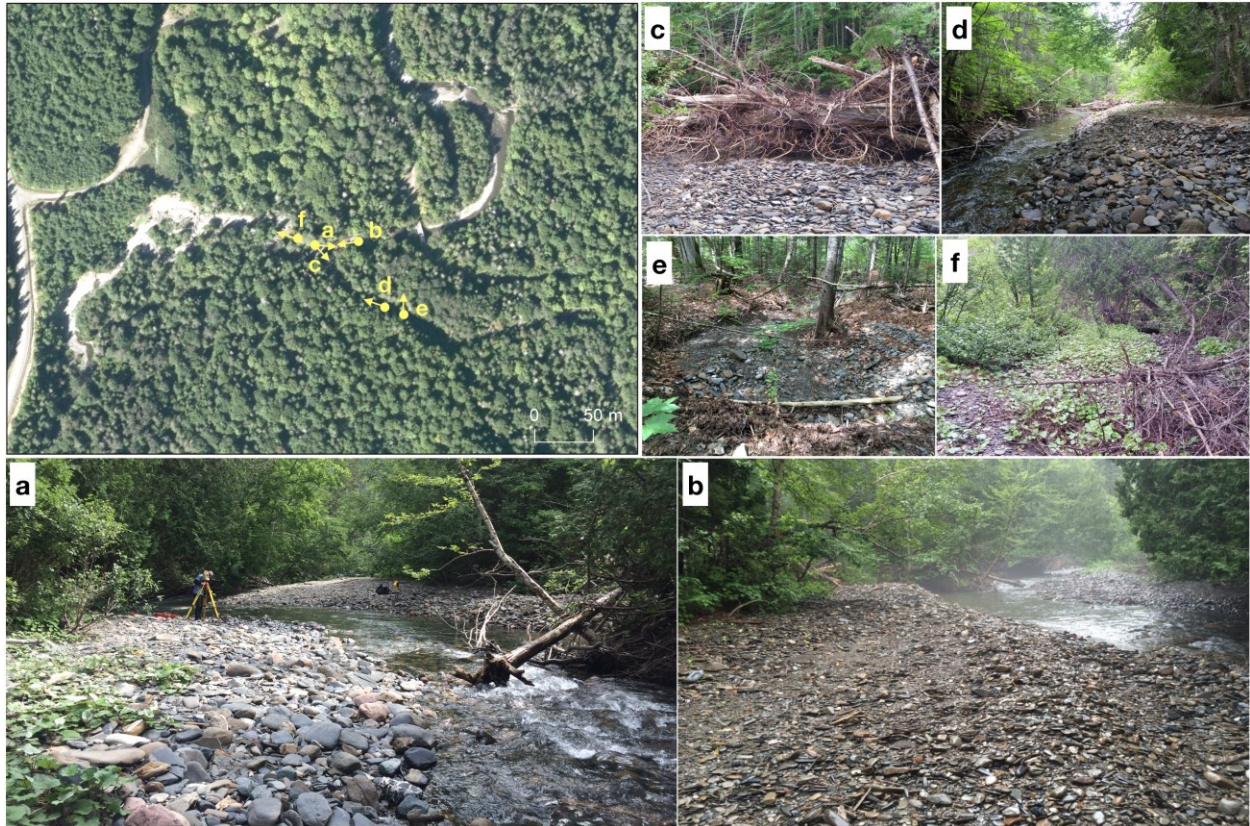


Figure 5.3: Planform view of study site #3 in the Mont-St-Pierre watershed (see Figure 4.1 for its location). Photos illustrate: the main channel upstream (a) and downstream (b) of the confluence, destabilized hillslope upstream (c), tributary being coupled with the main stream through a culvert (d), upstream in the tributary (e), sediment and wood accumulation zone downstream of the confluence (f).

When active, the tributary reworks colluvial and bedrock deposits finer than those found in the main channel, which it transports up to the valley margin. Due to the presence of the road, these deposits have the potential of damaging the infrastructure, as roads generally offer a sloping path with little resistance. The tributary is connected to the main channel by a culvert, which is situated around 3m higher than the bed of the channel (Figure 5.3d). There is some degree of instability in the tributary, especially in proximity to the road and the culvert, which may be related to these features and their position in the valley or to reconfiguration through channel widening (Figure 5.3e).

5.1.2. Mont Louis watershed

Site #4 (Figure 4.1) is located in the mid-catchment of the Mont-Louis watershed at the confluence between the Mont-Louis and Mont-Louis-Ouest Rivers (Figure 5.4). The valley setting is confined and the channel planform is single-thread, straight and stable. Bed material consists of mainly post-glacial alluvial deposits of high caliber with some isolated areas upstream made out of glaciofluvial material, deposited by glacial meltwater. Geomorphic units in the upstream reach of the main channel include step-pool sequences and bedrock ledges and outcrops on the right side (Figure 5.4 a, f). Width remains constant over this segment. Some erosion is present on the right bank directly downstream of the area with bedrock control (Figure 5.4e).

The tributary reworks mainly colluvial material, finer in diameter size than that of the main channel, with some material originating from glacial deposits. Geomorphic units in the tributary are bank-attached bars, potentially forced by large wood deposition, while in-stream forms are step-pools. Before joining the main river, the tributary bends, eroding the left valley flank, contributing to mass-wasting processes there (Figure 5.4d).

At the confluence, a deep pool of over 2m is formed due to the dynamic mixing of flows from the two streams (Figure 5.4b). Width is visibly increased downstream of the confluence. A mid-channel bar is formed at about 25m downstream of the tributary bar (Figure 5.4c). At the time of the field visit (August 2018), the bar extended to the left bank and served as a zone of net sediment accumulation, so that the river flowed only on the left side. Large wood was also present. Lateral migration of the channel towards the right valley wall is controlled by bedrock outcrops and ledges. Further downstream, sequences of step-pools resume in the main channel.

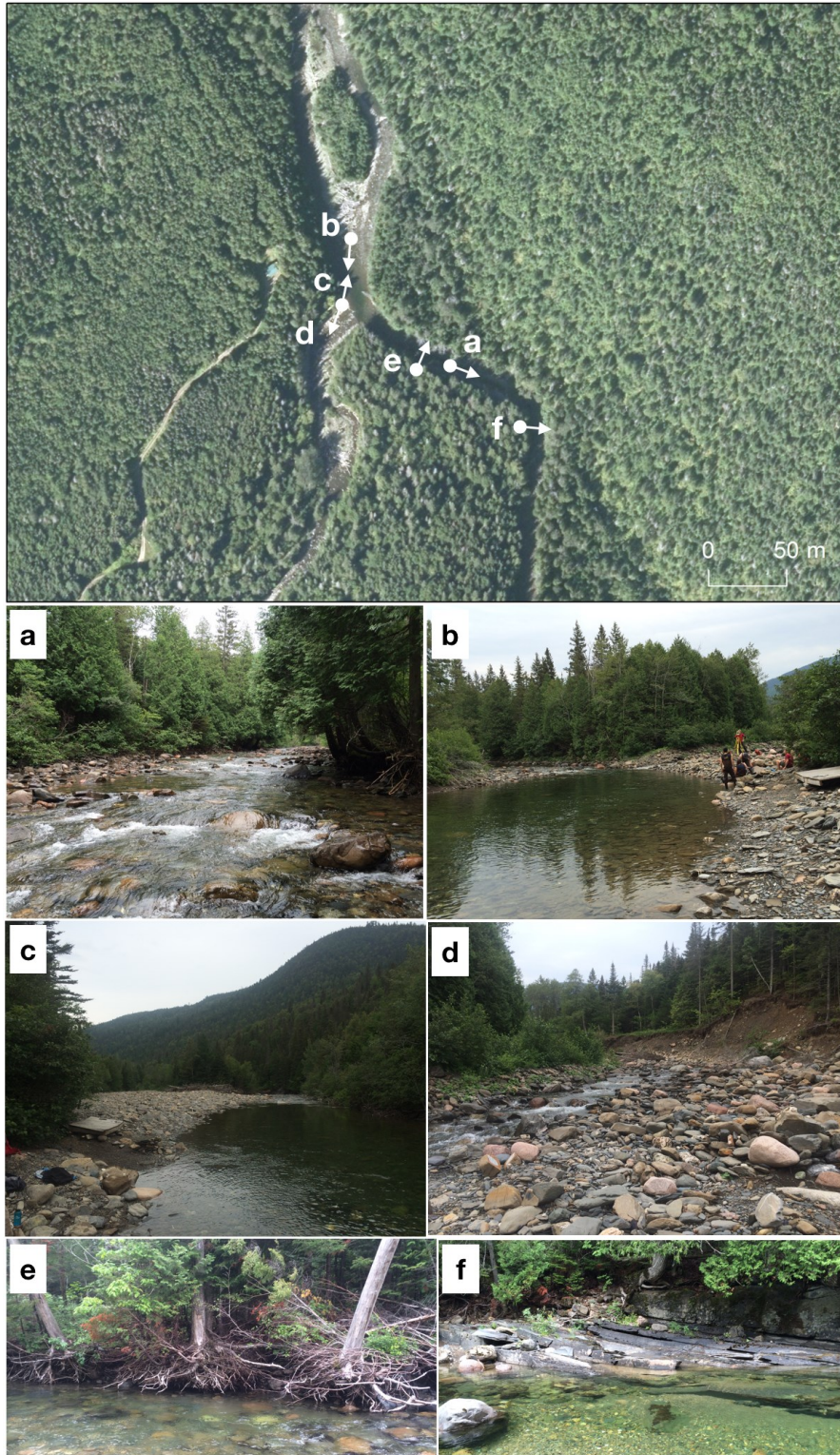


Figure 5.4: Planform view of study site #4 in the Mont-Louis watershed (see Figure 4.1 for site location). Photos illustrate: the main channel upstream (a), at (b) and downstream (c) of the confluence, hillslope failure, erosion and sediment accumulation upstream in the tributary (d), bank erosion after bedrock controlled river segment (e), bedrock control characteristic of the upstream and downstream reaches of the main river with the exception of the confluence zone (f).

5.1.3. Marsoui watershed

Site #5 (see Figure 4.1) is located in the lower catchment of the Marsoui watershed at 2.8 km before it reaches the St. Lawrence River at the confluence between the Marsoui and the Marsoui-Est-Rivers (Figure 5.5). The valley setting is unconfined.

The main channel upstream of the confluence has a meandering planform with a predominantly single-thread channel, although multiple channels can be found locally, so that the lateral stability is low. Bed material is composed out of fluvio-glacial and alluvial deposits. There are many geomorphic units including: riffle-pool sequences, mid-channel, point and alternate bars (Figure 5.5a). This area can be also characterized as a gravel sheet consisting of bedload sheets deposited across the bed. In-stream features are riffles and pools. There is widespread deposition of large woody debris. This area is generally highly sediment-charged. Large amounts of sediment are delivered by a wide-spread mass wasting process of the valley flank, as well as by tributary that carries a high sediment load.

The tributary shares the same characteristics as the main channel but is relatively less sediment-charged. When it reaches the confluence, the tributary slopes down thereby creating a stepped morphology (Figure 5.5c). The confluence itself has a complex morphology due to direct human intervention, which completely altered the natural configuration of the adjoining channels so that they now almost intersect at a 180° angle. The confluence zone is rip-rapped along both banks. A scour pool has formed directly upstream the bridge, which continues for some distance downstream of the bridge (Figure 5.5b and d). Amounts of large woody debris are reduced downstream of the confluence. In-stream geomorphic units include riffle-pool sequences (Figure 5.5b). Downstream of the bridge, the main channel is laterally active on the left bank.

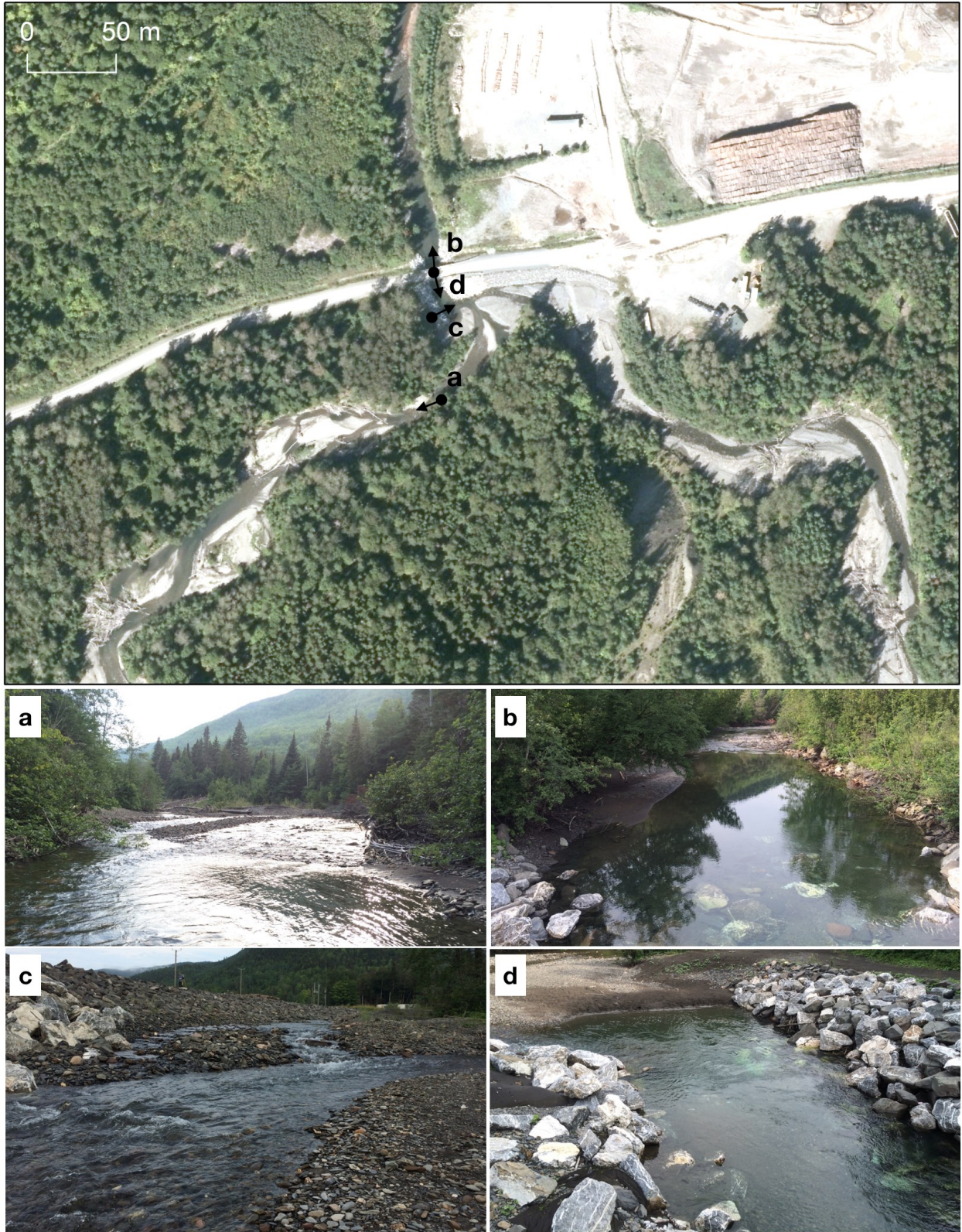


Figure 5.5: Planform view of study site #5 in the Marsouli watershed (see Figure 4.1 for site location). Photos illustrate: the main channel upstream (a), downstream (b) and at the confluence (c), scour pool (d).

5.1.4. Sainte-Anne-des-Monts watershed

Sites #6 and #7 are located in the Sainte-Anne-Nord-Est watershed, a subwatershed of the Sainte-Anne River (Figure 4.1). The first is the confluence between the Porc-Épic and the Saint-Anne-Nord-Est Rivers and is situated 300m upstream of the latter (approx. 15 channel widths). Valley setting is predominantly partly-confined, with localized bedrock-controlled segments. Reaches upstream and downstream of site #6 have the same planform characteristics: stable, single-thread channel, with low sinuosity. Bed material is composed out of fluvio-glacial deposits containing sedimentary and igneous rock of boulder-range caliber. Geomorphic units include occasional boulder mounds, along with occasional bedrock ledges on the right valley margin.

The Mines Madeleines River is a geomorphologically very active tributary joining the main channel at site #7. Its planform is sinuous, mainly single-thread and unstable. Bedload material includes alluvial as well as a large portion of colluvial material of granitic origin. Sediment bars are very frequent. As the channel reaches the main valley, it develops a stepped morphology. The tributary is intersected by a road, with which it has interacted over time, such that former culverts had to be successively replaced until a bridge was built. As the tributary reaches the main valley bottom, it deposits its sediment load, leading to the formation of an alluvial fan. During active periods, the tributary flowed over the road in downstream direction, reaching the main channel through distributary channels over the alluvial fan. This feature is now overfilled with sediment and the channel has carved a new path through the forest, reaching and overflowing a lake, to form multiple, small channels, which adjust to the base level of the main river at various locations.

At the former confluence location, a small tributary bar formed. This reflects the relative high transport capacity of the main channel. However, the sediment fed by the tributary resulted in the development of a gravel sheet stretching over about 14 channel widths (approx. 2.3km) downstream. Channel planform changes to multi-thread, unstable and highly sinuous. There are unvegetated mid-channel bars which reflect the unstable character of the river, as well as localized areas of bank erosion. Another less common geomorphic unit includes ramps of finer material, which slope towards the active channel. Wood recruitment is sparse.

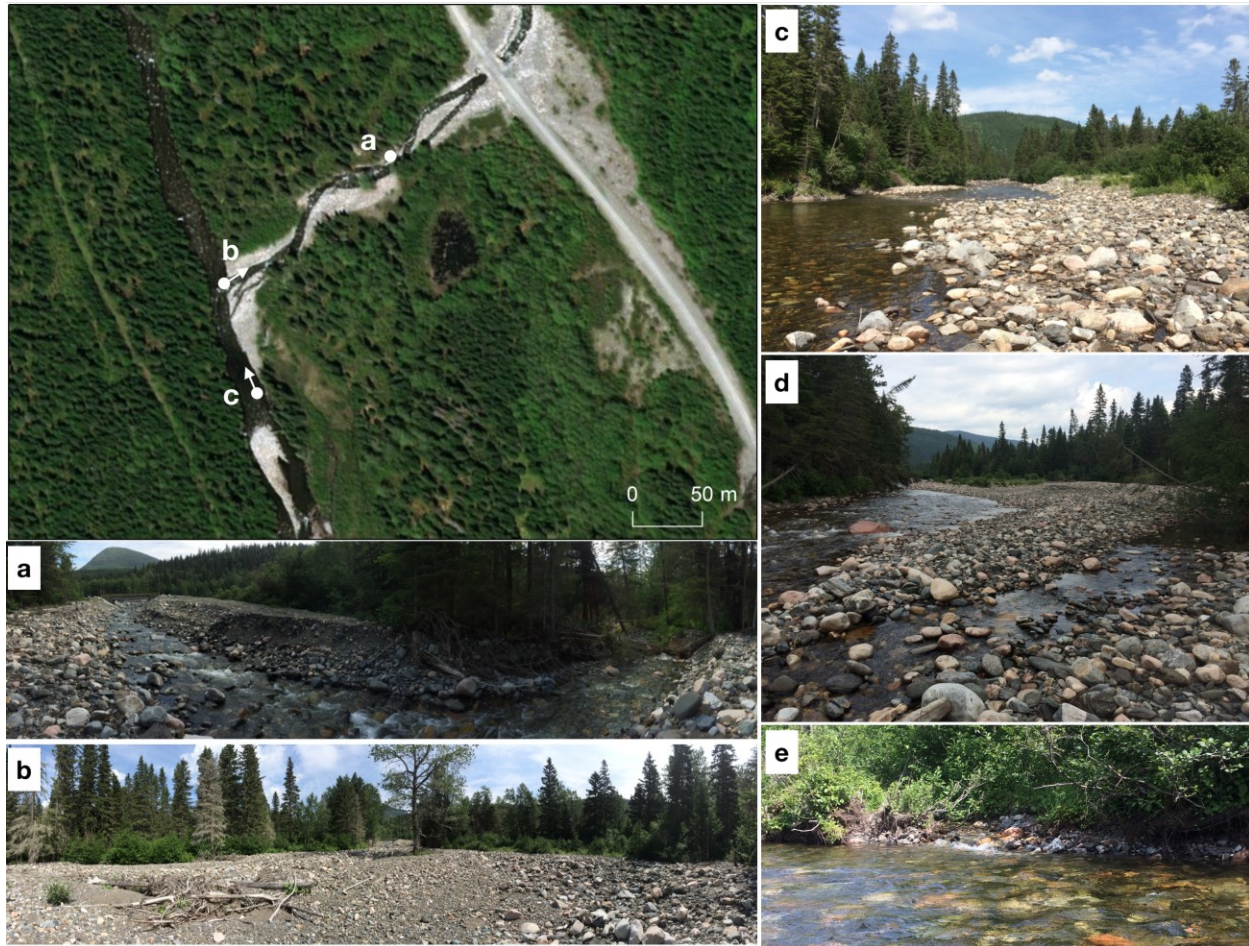


Figure 5.6: Planform view of study site #7 in the Sainte-Anne-des-Monts watershed (see Figure 4.1 for location). Study site #6 is not showed because it contains no tributary-related features and its planform and landform characteristics are homogeneous. Photos illustrate: the Mines Madelaines tributary flowing over and reworking material making up the alluvial fan, which results in the carving of a new channel (a), the now abandoned alluvial fan before reaching the main channel (b), tributary bar and view looking upstream of site #7 (c), view upstream from the end of the sampling zone showing compound bars (d), actively developing channels representing the new confluence (e). Note: the location point and direction of sites d and e are not shown.

Site #8 is located in the upper catchment at the confluence between the Sainte-Anne and Isabelle Rivers (Figure 5.7). The main river flows into a confined valley setting, so that its planform is irregular, single-thread and overall stable. Bed material is made out of alluvial deposits of homogeneous diameter. The underlying geology is the most heterogeneous out of all sites and consists of sheets of basalt, metabasalt, dolomite, granite and mudrock. Geomorphic units are limited to occasional boulder mounds and bedrock ledges on the right valley margin. There is no occurrence of large wood (Figure 5.7a and c).



Figure 5.7: Planform view of site #8 in the Sainte-Anne-des-Monts watershed (see Figure 4.1 for location). The photo illustrates a panoramic view of the upstream (a), confluence (b) and downstream (c) reaches of the main channel.

The tributary is distinct from the main channel in terms of geology, as it drains over mafic and ultramafic rock, like serpentinite. This alters the colour of the tributary to a rusty red (Figure 5.7b). A road crosses the tributary, so that 100m upstream the confluence, the channel is contained by a culvert. Geomorphic units in the tributary are alternate bars and a tributary bar. The channel at the moment of the field visit was flowing to the left of the tributary bar, eroding the outer left bank (ibid.). Some woody debris was present as a result.

5.1.5. Cap Chat watershed

Site #9 is located in the lower Cap Chat catchment at the confluence between the Cap Chat and Petite Cap Chat Rivers (Figure 5.8). The confluence marks the transition of the main valley from a confined to an unconfined setting. Channel planform upstream of the confluence is single-thread, straight and stable (Figure 5.8a). However, further upstream the channel is highly sinuous, often-times multi-thread and unstable. Downstream of the confluence, the channel remains overall single-thread, but sinuosity and instability increase. Bed material is post-glacial alluvial and of sedimentary origin (e.g. sandstone, arkose and greywacke). Geomorphic units include some bank-attached bars both upstream and downstream. Natural processes and form associations have been directly modified by human intervention. Several bridge locations have been changed over time and in order to protect the infrastructure, the channel was riprapped both on the bed and on the banks. Downstream, entire bars have been moved by the municipality in order to protect property damage.

The tributary has similar morphology to the main channel upstream of the confined segment (Figure 5.8b). The highly sediment-charged nature of the tributary lead to the formation of gravel sheets. As the channel reaches the main valley, it is constrained by bank revetments on the left side. A tributary bar is found at the confluence, although its morphology is complicated by the imposed form of the tributary-main-channel connection. At the confluence, a large and deep pool has formed due the mixing of flows from the two channels, as well as due the presence of the bridge piers (Figure 5.8c). Woody debris is sparse.



Figure 5.8: Planform view of site #9 in the Cap Chat watershed (see Figure 4.1 for location). Photos illustrate: main channel upstream of the confluence (a), upstream in the tributary (b) scour pool at the confluence with bed revetment (c).

5.2. Main channel and tributary characteristics at Gaspésie confluences

5.2.1. Bedload grain size

Bed sediment diameter is variable in the study sites in Gaspésie, ranging from sand ($< -1 \phi$; $< 2\text{mm}$) to boulders (-10ϕ ; 1024mm , in the Sainte-Anne watershed). Overall, average D_{95} , D_{84} and D_{50} values for the complete Gaspésie pebble count data show that the post-confluence zone is, on average, 0.5ϕ coarser than the pre-confluence zone and the confluence zone is, on average, 0.16ϕ finer than the pre-confluence zone (Table 5.1). Average particle diameter for the coarsest size fractions is decreasing in the confluence zone and slightly increases downstream, while the average particle size for the smallest fractions only decreases at the confluence (Table 5.1). This suggests that tributaries in Gaspésie feed, on average, relative finer particles to the main channel.

Table 5.1: Average D_{95} , D_{84} and D_{50} , D_{\max} and D_{\min} values for the entire Gaspésie dataset grouped by sampling zone.

	D_{95} (in ϕ)	D_{84} (in ϕ)	D_{50} (in ϕ)	D_{\max}	D_{\min}
Pre-confluence	-7.5	-6.5	-5.5	-9.5	-2
Confluence	-7	-6.5	-5.5	-8.5	-1
Post-confluence	-8	-7	-6	-9	-2

Results of the analysis of variance show great variability in the distribution of bedload grain size (Figure 5.9). Only four out of the total nine study sites have significantly ($p < 0.05$) different median grain sizes between the pre-confluence and post-confluence zones (#1: $F(1)=46.67$; #2: $F(1)= 34$; #6: $F=50.42$; site #7: $F(1)= 20.86$). Out of these, three are characterized by coarser sediment fractions in the post-confluence zone, while one shows the opposite trend. In terms of the remaining, not significant sites, two have finer sediment fractions in the post-confluence zone, two show identical distributions, and only one other has a coarser sediment fraction in the post-confluence zone. Even though not all differences are significant, the results show that, with the exceptions of two cases, the tributary does seem to have an effect on the bedload grain size distribution, skewing it towards coarser or finer fractions, depending on the bed material size of the tributary itself. The largest magnitude of change is in the order of 1ϕ between the median of the pre- and that of the post-confluence zone.

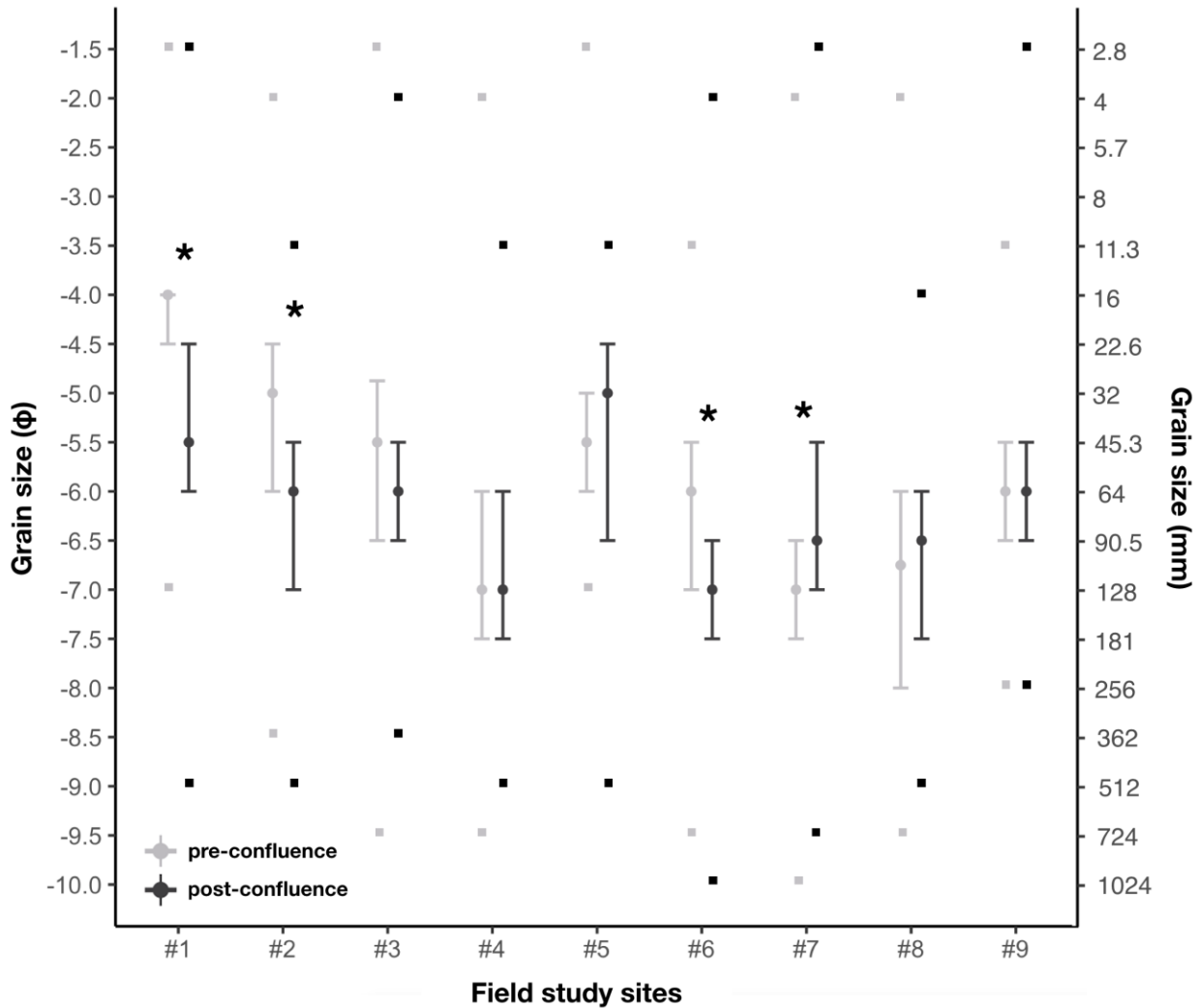


Figure 5.9: Median, interquartile range ($IQR=Q75 - Q25$), minimum and maximum (squares) of the bedload grain size distribution for the pre-confluence (light gray) and post-confluence (dark gray) zones for all field study sites in Gaspésie. Grain size is given in 0.5 interval phi units (ϕ), calculated as $\log_2 D$, where D is the particle diameter, as well as in mm. Stars indicate statistical significance between the two groups at the 95% level.

Interesting patterns emerge for site #2, as well as for sites #6 and #7, which are located successively in downstream direction (Figure 5.9). The first shows that in a distance of 12 channel widths (about 120m) from the tributary mouth, the distribution of bedload grain size is modified towards larger grains in its entirety, so that the tributary has a very clearly disruptive role. The effect of the tributary can be also hinted at in the case of study sites #6 and #7, through a lowering of the grain size in the post-confluence of the former, which constitutes the pre-confluence zone of the latter. Even though the interquartile range of the grain size distribution for the post-confluence zone of site #7 recovers to that of the pre-confluence zone of site #6, the median grain size is lowered from -6ϕ (64mm) to -

6.5 ϕ (90.5mm). This may suggest that the influence of the tributary extends beyond the confluence zone in both upstream and downstream direction.

Out of the non-significant examples (site #4) is most striking, since this was considered to be a geomorphologically active confluence, i.e. marked by active erosional and depositional processes both in the tributary and the main channel (see section 6.3.3). Nonetheless, results show that the tributary does not seem to have any effect on the distribution of the bed material before or after the confluence (median grain size for both is -7 ϕ , 128mm). Introducing the confluence zone into the analysis reveals a more nuanced pattern, i.e. even though it is localized at the confluence, the tributary does have a fining effect on the bedload grain size distribution of the main channel (-6 ϕ , 64mm) (Figure 5.10). Consequently, it follows that the confluence zone itself is not trivial and, when considered, allows for a more accurate classification of tributary effects.

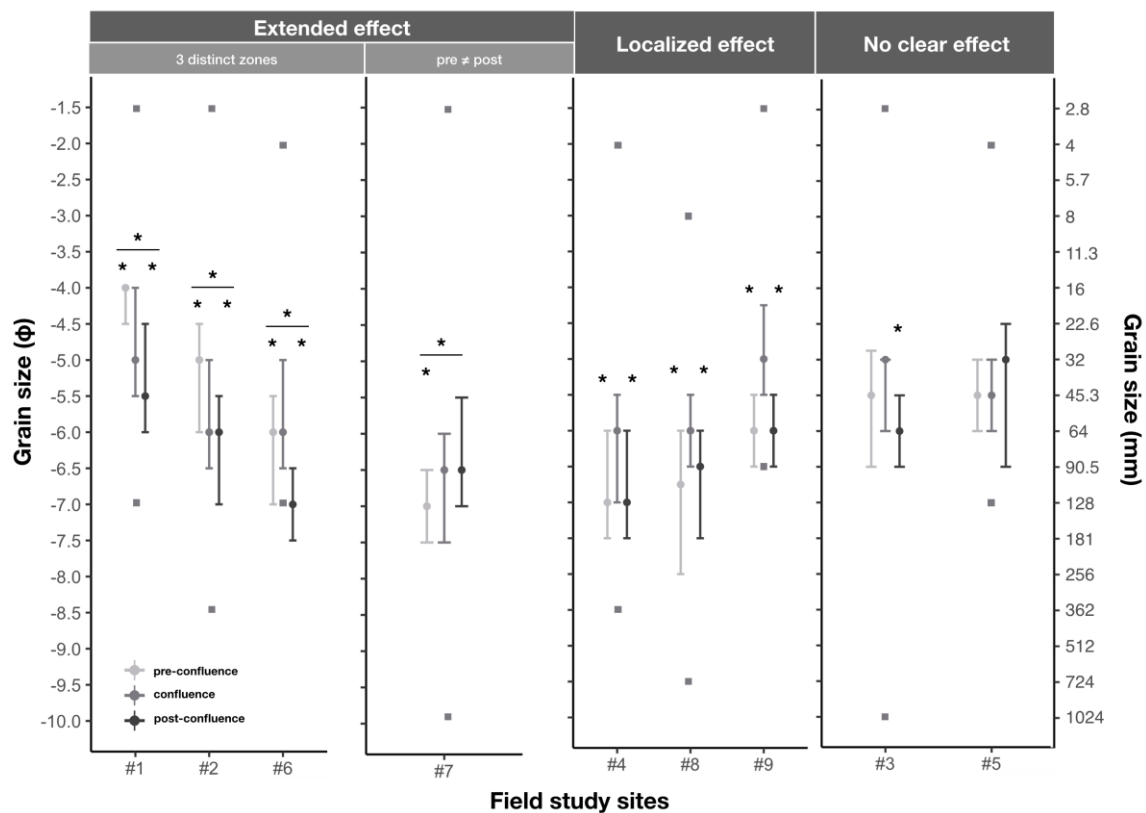


Figure 5.10: Median and interquartile range (IQR=Q75 – Q25), minimum and maximum (squares, only confluence zone) of the bedload grain size distribution for the pre-confluence (light gray), confluence (grey) and post-confluence (dark grey) zones for all field study sites in Gaspésie. Sites are grouped by the effect of the tributary on the bedload grain size distribution. Grain size is given in 0.5 interval phi units (ϕ). Stars indicate statistical significance between the two groups at the 95% level.

In general, a tributary may disrupt downstream fining trends of the main channel by introducing relatively finer or coarser material. The fate of the tributary's sedimentological imprint in that it remains in the confluence zone (localized effect) or it is transported downstream (extended effect), is mainly dependent on the nature of the sediment and the ease with which it can be reworked by the main channel. According to Figure 5.10, both types of confluence effects are characteristic of the examined Gaspésie tributaries. Additionally, a minority of the study sites shows no clear confluence pattern. These are sites with a high degree of anthropogenic influence, where isolation of a tributary effect is rendered difficult: direct reconfiguration of the confluence planform or road protection works resulted in decreased sediment supply at the confluence or alteration to erosional and depositional foci.

Based on the statistical significance of bedload grain size data, the extended effect can be subdivided into those confluences where all three main sampling zones are different and those where only the pre- and post-confluence zones are different. Here again, site #7 is notable. Results show that the post-confluence zone is clearly affected by the tributary input, with both medians coinciding at -6.5ϕ (90.5mm). Although the median between the pre-confluence and confluence zone is significantly different (-6.5ϕ and -7ϕ , respectively), the interquartile range of their distribution are identical in the coarser part of the distribution. This may indicate interference processes (Benda and Dunne, 1997), in which rejuvenated alluvial fans lead to increased sediment storage upstream of a confluence due to reductions in channel slope. This can be viewed also in terms of a disruption of longitudinal connectivity of sediment by the presence of a barrier (i.e. the stored sediment) (Fryirs et al, 2007a). However, according to Benda et al. (2003) in their study of the Boise River in northwestern US, these deposits were finer in size, contrary to site #7, where the material is coarse. A possible explanation for this anomaly may be that the tributary channel avulsed on the alluvial fan in the past and the coarser deposits may be indicative of a former tributary stream position on the alluvial fan. DEM evidence shows that the conical shape of the fan indeed stretches to the beginning of the pre-confluence zone of site #7.

5.2.2. Channel width and number and area of bars

Sediment deposits that are created at tributary mouths can act as a topographic obstruction, which displaces the main channel on the valley floor. Morphological effects include a widening of the pre-

or post-confluence channel, depending on tributary and main channel characteristics. A wider post-confluence channel can be formed when the main channel changes course due to tributary sediment deposits, while backwater effects, coupled with decreased gradients, can widen the pre-confluence zone.

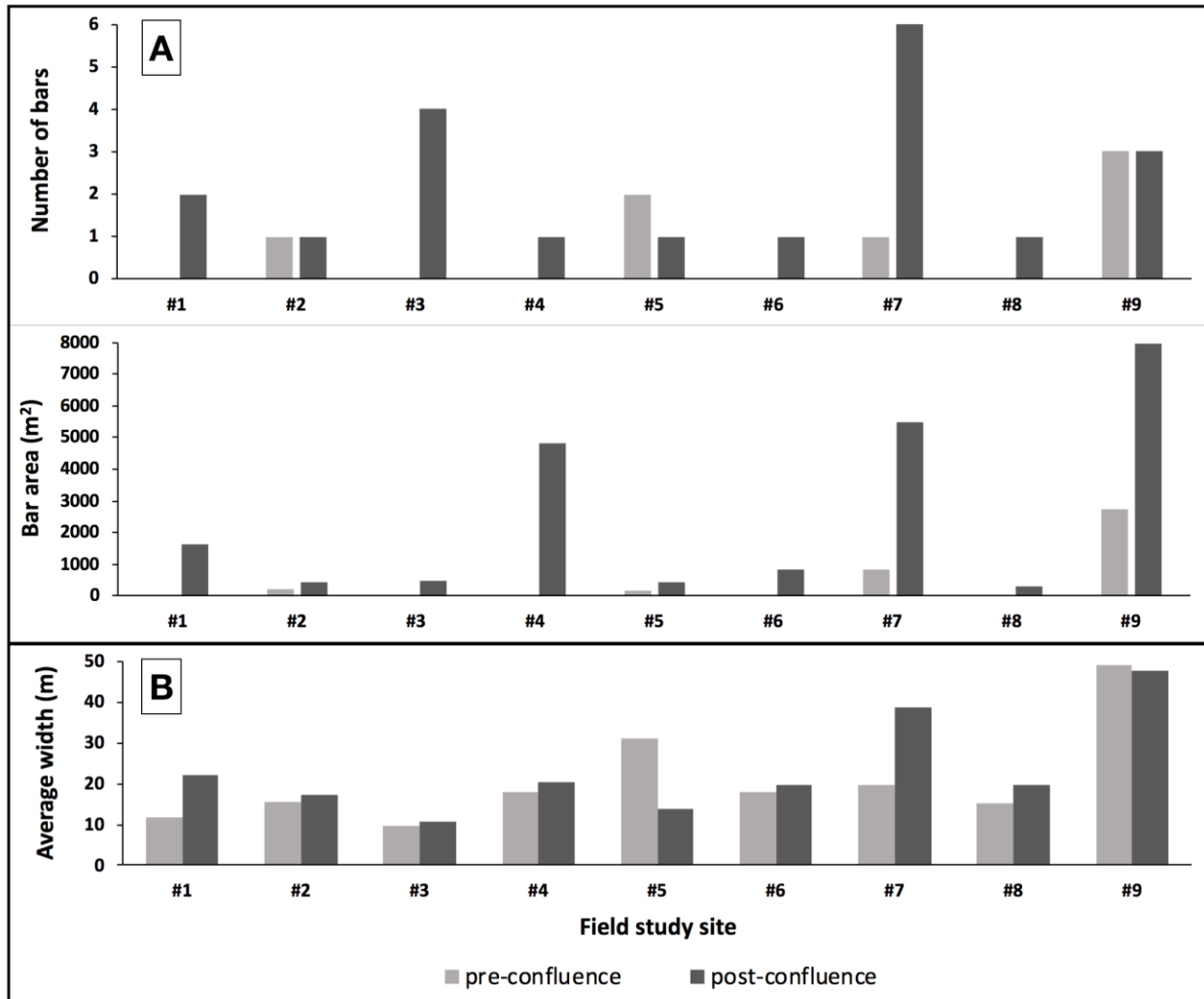


Figure 5.11: (A) Number of bars and cumulative bar area measured from orthophotos for the same longitudinal distance as the bed sediment sampling. (B) Average bankfull channel width measured from orthophotos for the same longitudinal distance as the bed sediment sampling.

Results of the bar data (Figure 5.11A) reveal that post-confluence bar formations are most common for the Gaspésie study sites. The highest number of bars over a distance of 280m downstream (representing approx. 7 channel widths) is 6, with a total area of 5500m² (site #7). Although site #3

has a relatively high number of bars, they are not directly related to the tributary, but to a bar complex located in the post-confluence zone. The highest bar area of about 8000m² is found in the post-confluence zone of site #9, however this does not appear to be confluence-related either, but rather a lateral bar that formed due to altered flow dynamics as a result of direct human intervention. Site #4 has a bar area (4800m²) comparable to that of site #7, despite having only one bar associated with the tributary. Interestingly, site #5 has a larger number of bars in the pre-confluence zone. This could reflect deposition due to backwater effects of the tributary, which with a symmetry ratio of 0.58 (Table 4.1) is quite substantial in terms of flow input. However, this is complicated by a high degree of human intervention to reconfigure the confluence morphology.

In terms of width, sites #1, #5 and #7 are most remarkable, as differences between the two zones are almost or more than double. Whereas for sites #1 and #7 the post-confluence channel widens, the reverse applies to site #5. Despite having a considerable bar area, site #4 shows little changes in channel width in the pre- and post-confluent channel. This could be related to little accommodation space on the valley bottom, as this is a bedrock-constricted river segment. These results suggest that increases in width are associated with geomorphic processes initiated by the deposition of bars, but that sediment accumulation space is constrained by valley morphology.

5.2.3. Tributary and main channel slope

Confluence effects are hypothesized to be more marked when the tributary slope is steeper than that of the main channel, as a higher gradient is more competent of mobilizing greater amounts of sediment. This is true for 7 out of 9 sites in Gaspésie when comparing the pre-confluence slope of the main channel to that of the tributary (Figure 5.12). Sediment inputs delivered by the tributary has the effect of steepening the slope of the post-confluence channel for six sites, while the rest show gentler slopes after the confluence. The highest amplitude of change is found at sites #1 and #2, where the slope of the post-confluence zone is increased almost 6-fold. Interestingly, gradient increase after the confluence is negligible at site #7 (+0.001), which could signify that the sampling zone was smaller than the entire extent of the accumulation zone. In fact, morphological changes resulting from sediment deposition at site #7 extend over the longest longitudinal distance downstream out of all study sites (i.e. about 14 channel widths, approx. 2.5 km).

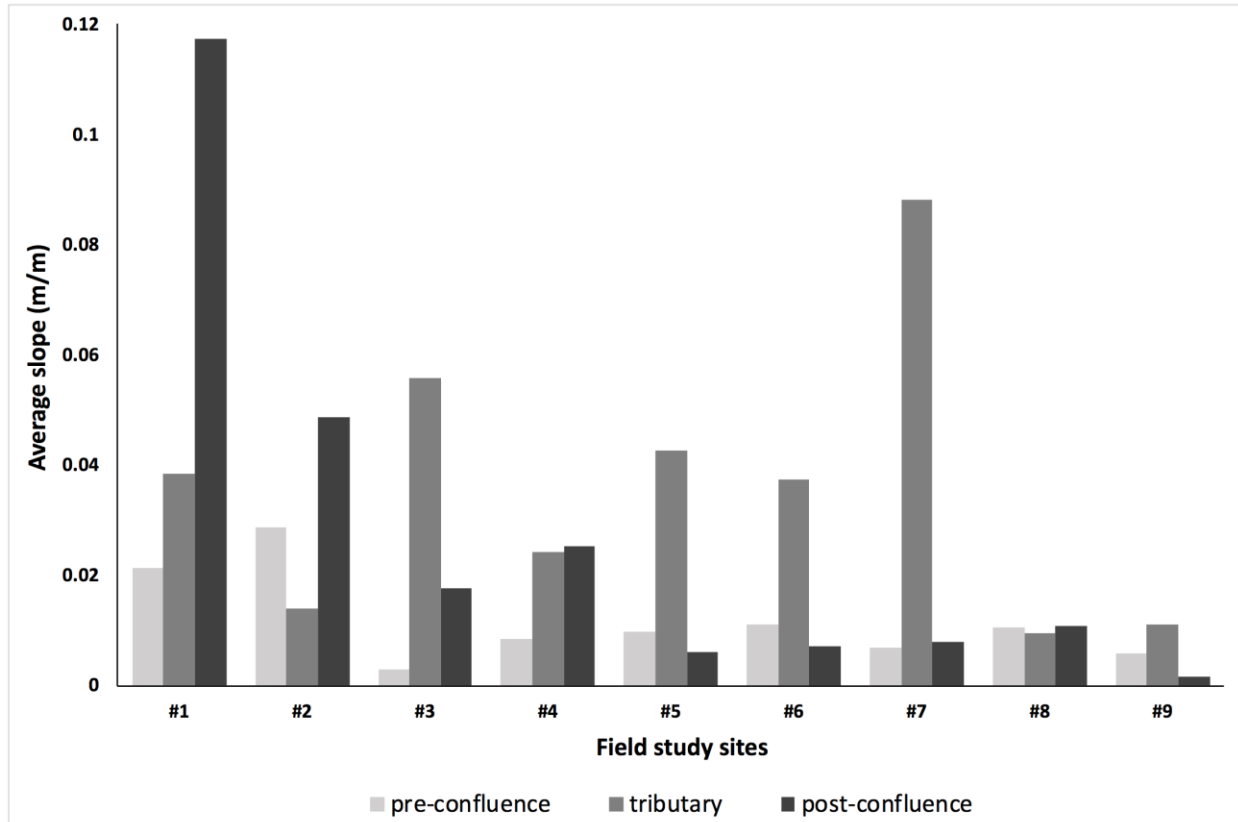


Figure 5.12: Average water surface slope of the main channel's pre- and post-confluence zone, along with the tributary slope for all study sites.

Overall, these results highlight the variability observed between individual confluences in terms of bed sediment size, number and area of bar deposits and the water surface slope between the tributary and the main channel, despite a similar geologic setting. Furthermore, confluences that appear to be morphologically inactive and show no visible morphological effect can be influenced by other, active confluences located in close proximity (site #6). Conversely, effects can be masked or amplified as a result of anthropogenic interventions (site #9). In addition, tributaries deliver finer bedload relative to the main channel, which highlight the quaternary legacy of the study area, as well as related armouring effects that are visible in the coarse sediment size of the main channel. Ultimately, the discrepancy between field sites reflects the intricate nature of tributary-main channel relationships that are contingent on local factors (e.g. variations in valley confinement and lithology, past events, basin-wide sediment connectivity).

6. A fuzzy GIS model to determine confluence morphological sensitivity of main channels to tributary inputs at the watershed scale

This chapter was written in collaboration with my supervisors Dr. Pascale Biron and Dr. Thomas Buffin-Bélanger. The manuscript will be submitted to *Geomorphology* in September 2019.

As first author I was responsible for the development of the methodology, data collection, model creation and validation, presentation of results, statistical analyses and writing of the manuscript.

Author names and affiliations

I. Mazgareanu^a, P.M. Biron^a, T. Buffin-Bélanger^b

^a Department of Geography, Planning and Environment, Concordia University, Montréal, Québec, Canada

^b Département de biologie, chimie et géographie, Université du Québec à Rimouski, Rimouski, Québec, Canada

Corresponding author

Department of Geography, Planning and Environment, Concordia University, 1455 De Maisonneuve Blvd. W., Montréal, Québec, Canada, H3G 1M8 (I. Mazgareanu), julie.mazga@gmail.com

Abstract

River networks consist of links and nodes, through which organic and inorganic fluxes are being transferred. Confluences, key nodes of any river system, have the potential of disrupting downstream longitudinal trends in the main river through inputs of water, sediment, wood or ice delivered from tributaries. From a geomorphological perspective, these confluence zones are particularly active and thus susceptible to increased flooding and bed instability, which, in turn, pose serious threats to infrastructure. However, not all confluences are active. Despite major advances in our knowledge of confluence dynamics, there has been limited progress in the development of low complexity, practical tools that use remotely sensed data to predict the spatial distribution of the main river's sensitivity to tributary inputs. To overcome this issue, we developed a novel semi-automated GIS model that uses a fuzzy approach to integrate multiple key factors (unit stream power, valley confinement and sediment connectivity potential) and produce a map of the distribution of the confluence morphological sensitivity (CMS) index at the watershed scale. The model was tested using LiDAR and digital elevation models in Coaticook and Gaspésie watersheds, Québec. Results indicate that the model is useful for detecting geomorphologically active confluences and the resulting sensitivity of the main channel and has potential to be used in diverse river management applications (e.g. hazard reduction and freedom space mapping).

6.1. Introduction

Confluences are key nodal points in a drainage network, and key manifestations of the inherent nonlinearity of river systems. It is at the confluences that discontinuities of flow, sediments, solutes and organic matter are generated within the fluvial system. Abrupt changes in the downstream longitudinal trends of the morphological characteristics of main channel in terms of width, slope and/or bed grain-size distribution have been largely documented (Richards, 1980; Rhoads, 1987; Rice and Church, 1998). This is especially prominent where a substantially coarser or finer sediment load than that of the main channel is added (Ferguson and Hoey, 2008). Tributaries that deliver voluminous and coarse sediment lead to various changes in the morphology of the main channel. Typically, alluvial and debris fans impinge on channels, displacing them across the valley floor (Brierley and Fryirs, 1999; Harvey, 1997, 2001; Florsheim et al., 2001, 2004; Fryirs et al., 2007b; Al Farraj and Harvey, 2010; Fryirs and Gore, 2014), increasing the chances of avulsions. The deposition of material forces a steepening of the gradient and a coarsening of the bed downstream, accompanied by shallowing of the gradient and fining of the bed upstream, thus highlighting the role of local factors that override downstream trends (Benda et al., 2004; Al Farraj and Harvey, 2010; Hanks and Webb, 2006; Swanson and Meyer, 2014; Rice, 2017), as well as the role of the confluence zone as an important site of sediment storage.

The concept of storage is very strongly related with notions of connectivity, especially that of sediment connectivity, whereby sediment is transferred from its source to a sink, i.e. a storage location, through processes of particle entrainment, transport and deposition (Bracken et al., 2015). These operate within and between different landscape compartments, such as hillslopes, channels, floodplains, tributaries and recipient streams (Harvey, 2002; Fryirs et al. 2007a, b). Transfer between landscape compartments can be coupled or interrupted by various landforms, such as buffers, barriers and blankets (sens. strict. Fryirs et al., 2007a). These manifestations of sediment disconnectivity impede the lateral, longitudinal and vertical sediment contribution over various spatial and temporal timescales, and they provide useful insight into the proportion of a watershed that is sedimentologically connected to the channel network, as well as the location of geomorphic change along a channel network (Harvey, 2002; Fryirs et al., 2007a; Czuba and Foufoula-Georgiou, 2015).

Due to their highly dynamic nature, confluences can be considered “hotspots” of fluvial geomorphic change at the network scale (Czuba and Foufoula-Georgiou, 2015). However, not all tributaries have

an effect on main channel characteristics. Rice (1998) found that less than 20% out of the approximately 100 tributaries studied had any perceptible effect on the grain size or slope of the mainstream in the Canadian Rockies. This was also confirmed by the analysis of Benda et al. (2004) who documented geomorphically insignificant tributaries especially in semi-arid environments, such that the question of why only some tributaries have a considerable impact remains both pertinent and unsolved. In order to identify which tributaries elicit adjustments, and thus determine reaches that are susceptible to geomorphic change, knowledge about the factors controlling the magnitude of impact is needed. To date, only a limited number of studies provide a quantitative basis for predicting the effects of tributaries on the main channel morphology by taking into account a combination of key parameters (Table 1), but overall knowledge remains mostly qualitative. Generally, important controls at the scale of the confluence are tributary size (and related discharge ratio), slope, bedload flux and grain size characteristics relative to those of the main channel (Ferguson et al., 2006). These depend on the overall stream network configuration in terms of watershed shape, drainage density and spacing between confluences, as well as the angle of the confluence (Benda et al., 2004; Benda, 2008). Unfortunately, the field data necessary to obtain such information can be considerably resource-intensive, while many tributaries are located in low accessibility areas.

Stream power is often considered as a key controlling variable for sediment transport and geomorphic changes in rivers. However, to the best of our knowledge, it has not yet been used explicitly to address questions pertaining to tributary-main channel interactions. Total (gross) stream power provides a measure of the energy available to be used in any given valley setting, while unit (specific) stream power reflects how energy is used in the active channel (Brierley and Fryirs, 2005). The analysis of downstream variations of stream power is another useful indicator of morphological change (Graf, 1983; Bizzi and Lerner, 2015; Gartner et al., 2015; Lea and Legleiter, 2016). For instance, Bizzi and Lerner (2015) found that averaged values of stream power over reaches of 3 to 5 km give an indication whether the geomorphic response of a river reach is aggradational (stream power decreases longitudinally) or degradational (stream power increases longitudinally). Sensitivity thresholds can be derived on the basis of such analyses, representing minimum energy conditions necessary to elicit major geomorphic change (Thorne et al., 2011; Vocal Ferencevic and Ashmore, 2012; Bizzi and Lerner, 2015; Gartner et al., 2015; Lea and Legleiter, 2016; Yochum et al., 2017).

The potential of stream power in predicting reaches susceptible to increased geomorphic activity due

to tributary inputs is all the more attractive given the increasing access to high-resolution remotely-sensed spatial data at the scale of watersheds, for example LiDAR (Light Detection and Ranging) digital elevation models (DEMs). Automated GIS tools such as those developed by Vocal Ferencevic and Ashmore (2012) and Biron et al. (2013) can then be used to extract channel slope, width and discharge in order to obtain the spatial distribution of total and unit stream power at all positions along the drainage network. These can combined with other GIS tools to identify key factors for tributary impact (Table 6.1), such as the index of connectivity (IC) (Borselli et al., 2008; Cavalli et al., 2013) and the Valley-Bottom Extraction Tool (V-BET) (Gilbert et al., 2016) to facilitate geomorphic assessment at the watershed scale and thus opening new avenues for various applications.

Table 6.1: Variables controlling whether a tributary has an effect on the main channel or not. Unit stream power, sediment connectivity and valley confinement (highlighted in grey fill colour) are included in the proposed fuzzy GIS model.

	Controlling factors	Useful because	Less useful because	Thresholds	References
	Total stream power	Predictor of channel dimensions, mobility and total transport rate	Does not predict sediment transport	1648 W/m*	Bull, 1979; Graf, 1983; Magilligan, 1992; Lecce, 1997; Lapointe et al., 1998; Willett, 1999; Bizzi and Lerner, 2015
Continuous along a river	Unit stream power	Predictor of channel dynamics, bed sediment entrainment, bedload transport rate; accounts for variations in channel width	Requires high-resolution DEM	Variable, but generally ~ 300 W/m ² ; 86 – 170 W/m ² when induced from deposition**	Magilligan, 1992; Ferguson, 2005; Eaton and Church, 2011; Buraas et al., 2014; Magilligan et al. 2015; Yochum et al., 2017
	Stream power gradient	Allows inference of process, indicator of spatial distribution of erosion and deposition, transport capacity	Reach delineation problematic; relationship with channel response is stronger over long distances	Negative (depositional), positive (erosional)	Bizzi and Lerner, 2015; Lea and Legleiter, 2016
Valley or Watershed scale	Tributary basin area (A) x slope	Surrogate measure of tributary sediment delivery and relative bedload grain size, simple to compute in GIS, no expert knowledge required	Redundant (slope used in stream power)	> 0.63	Rice, 1998

	Basin shape ($B = (A / d)^{0.5}$ where d is basin diameter	Strong control on the spatial distribution of significant tributaries, simple to compute in GIS, no expert knowledge required	Possible confounding variable in complex geology settings or where human disturbances are present	0.70 – 1.00	Rice, 1998; Benda et al., 2004; Rice, 2017
	Sediment connectivity (effective catchment area)	Help identify sedimento- logically significant tributaries and their geomorphic change	Requires expert knowledge, not readily available from a DEM	n.a.	Fryirs et al., 2007a,b; Lisenby and Fryirs, 2017
	Valley confinement	Predictor of channel width increases (in combination with stream power), indicates resistance to geomorphic change	Extraction complex (depends on DEM resolution)	n.a.	Rinaldi et al., 2012; Gilbert et al., 2016; Yochum et al., 2017
	Discharge ratio (QR)	One of the most important predictors of tributary- driven aggradation	Not directly related to bedload transport	Low values of QR	Ferguson et al., 2006; Rice et al., 2006
Ratios (tributary / main channel)	Symmetry (drainage area) ratio	Surrogate measure of tributary sediment delivery and relative bedload grain size, simple to compute in GIS, no required expert knowledge	Redundant with QR and not directly related to bedload)		Ferguson et al., 2006; Rice et al., 2006
	Bedflux (FR)/ bedload size (DR) ratio	One of the most important predictors of tributary- driven aggradation	Watershed-wide calculation problematic	High values of FR; DR > 2	Ferguson et al., 2006; Rice et al., 2006

* *Threshold from Bizzi and Lerner (2015)*

** *According to Yochum et al. (2017)*

Despite major advances made on the topic of confluence dynamics in recent years, to the best of our knowledge, there are no existent tools that take advantage of LiDAR data to model tributary-main channel interactions. To fill this gap, we propose a novel, low complexity GIS model that uses fuzzy logic to determine the geomorphic sensitivity of the main channel to tributary inputs by combining three key factors, i.e. unit stream power, valley confinement index and sediment connectivity index. The approach builds on the work of Biron et al. (2013) and extends it to include the role of tributaries in influencing main channel morphodynamics.

6.2. Study area

The GIS model is tested in the Coaticook watershed as well as in the Gaspé Peninsula in Quebec, Canada. The Coaticook watershed is located in southern Québec in the physiographic region of the Appalachian Range, bordering the United States to the south, which contains one third of its 535 km² area (Figure 6.1A). The 67 km long Coaticook River drains into the Massawippi River, itself a tributary of the Saint-François River, which is a sub-basin of the Saint Lawrence. The predominant land use is agriculture (43%), followed by forestry (41%). The Coaticook River flows for most of its course through unconfined and partly-confined valleys, where it has an alluvial character and has thus more space to move on the valley floor by processes of erosion and deposition. These are divided by three confined valley sections where the river is constrained and controlled by bedrock. Three dams are also located in this zone. The shape of the river network is linear, with many and short adjoining tributaries. Intense summer rain events have the capacity of quickly mobilizing large amounts of material in the tributary basins, which accumulates on tributary bars and alluvial fans upon reaching the main channel. For instance, a torrential rain event in June 2015 caused widespread infrastructure and property damage along valley margins (Demers et al., 2017). Since 1998, the Ministry of Public Security has given financial aids of over one million Canadian dollars to repair damages associated with fluvial processes (COGESAF, 2017).

The Northern Gaspé Peninsula (Figure 1B) is located in the most eastern tip of southern Quebec and, like Coaticook, belongs to the Appalachian Range. This is reflected in the headwater areas of all watersheds that are part of the study area. Before draining into the Saint-Lawrence River, the high relief of the Appalachians gives way to plateaus with deep, U-shaped flat-bottomed valleys. The shape of the river network is controlled by two faults which separate sedimentary rocks in the north from predominantly volcanic rocks in the south (Cap Chat and Sainte-Anne watersheds) (MRNF, 2006). The largest watersheds tend to have a more compact basin (i.e. heart-shaped basin with dendritic network), while smaller ones tend to be more elongate (i.e. rectangular basin with trellis network). Forestry is the predominant land use with 93% of the entire surface area (MRNFP, 2004).

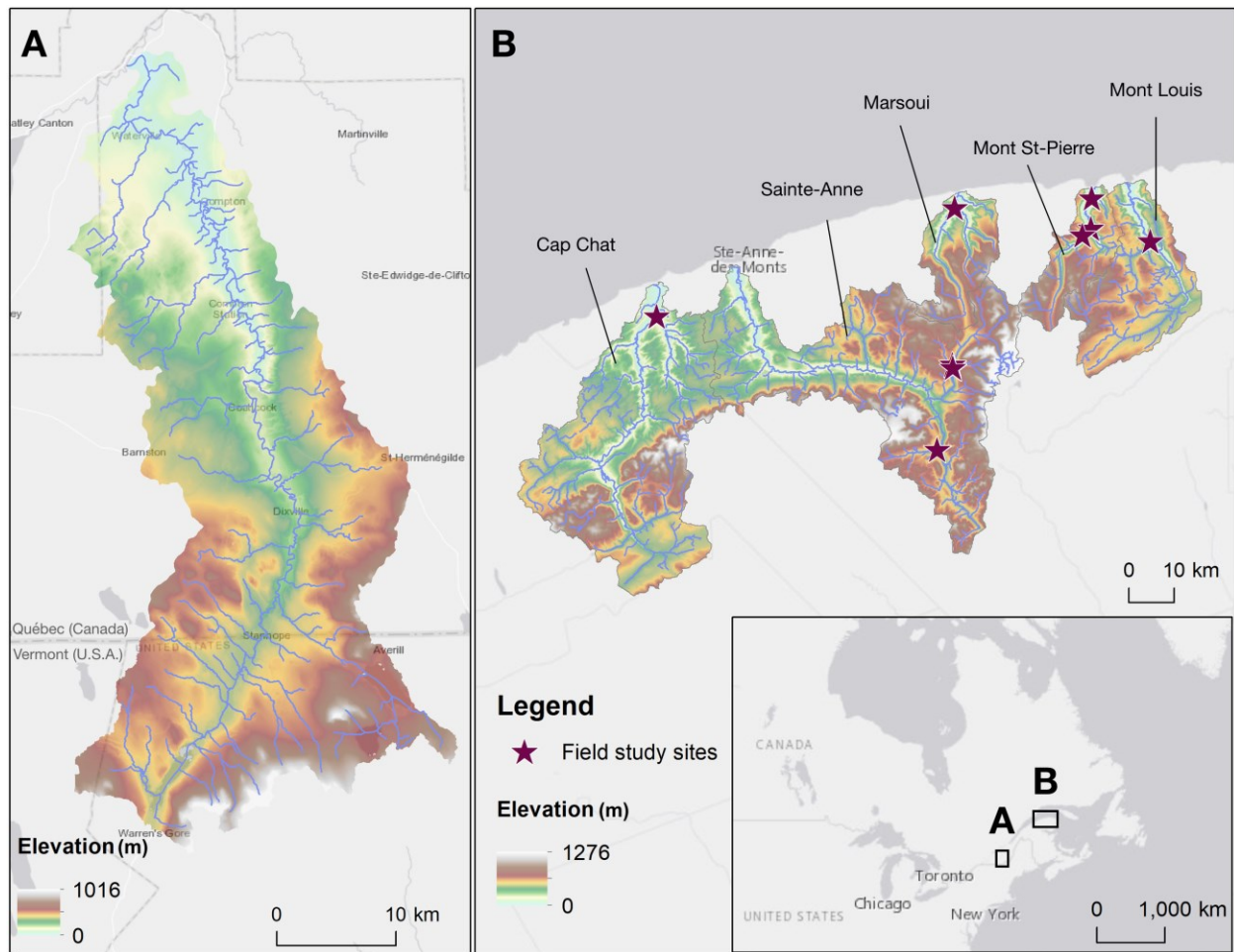


Figure 6.1: Location of study sites: the Coaticook Watershed (A) and 5 watersheds in Gaspésie (B).

6.3. Methods

The identification of river reaches geomorphologically sensitive to tributary inputs was carried out by means of a fuzzy multi-criteria analysis in ArcGIS 10.4 (ESRI, 2016). This approach is based on (1) the evidence that the impact of tributaries is dependent on multiple factors, (2) the recognition of the role of uncertainty and imprecision in this type of analysis. The approach is mainly based on DEM analysis. Both a 1m LiDAR (vertical precision +/- 0.15m, aggregated to 10m) and a governmental 10-m DEM data (vertical precision +/- 5m) were used in the Coaticook watershed, whereas only the 10-m governmental DEM was available for the Gaspésie watersheds.

6.3.1. Choice of factors

Whether a tributary will disrupt the longitudinal trends of the main channel depends on (1) the amount of sediment that the tributary is able to deliver to the confluence, and (2) the capacity of the main channel to effectively transport it. Figure 2A describes the entire processing procedure. For the first category, the sediment connectivity index (SCI) of Cavalli et al. (2013) was chosen to represent the potential sediment delivery from tributary basins to confluence points using the stand-alone application SedInConnect described in Crema and Cavalli (2018). These tools also exist as an add-on Toolbox for ArcGIS. Confluence points (junctions) were taken from the Géobase du réseau hydrographique du Québec (GRHQ, 2016) and buffered to match the average width of the main channel, assessed from orthophotos (resolution of 21 and 30 cm for the Coaticook and Gaspésie watersheds, respectively). The buffered confluence polygons represent the targets that are required as an input to the SedInConnect application, along with the digital elevation model. The resulting raster contains SCI values calculated in respect to the targets on a cell-by-cell basis, except for the target polygons, which contain NoData values. Because SCI values are needed for the entire course of the main river, these NoData areas need to be filled with corresponding SCI values. This is done by assigning an average of nearby cells using the Focal Statistics tool in ArcGIS.

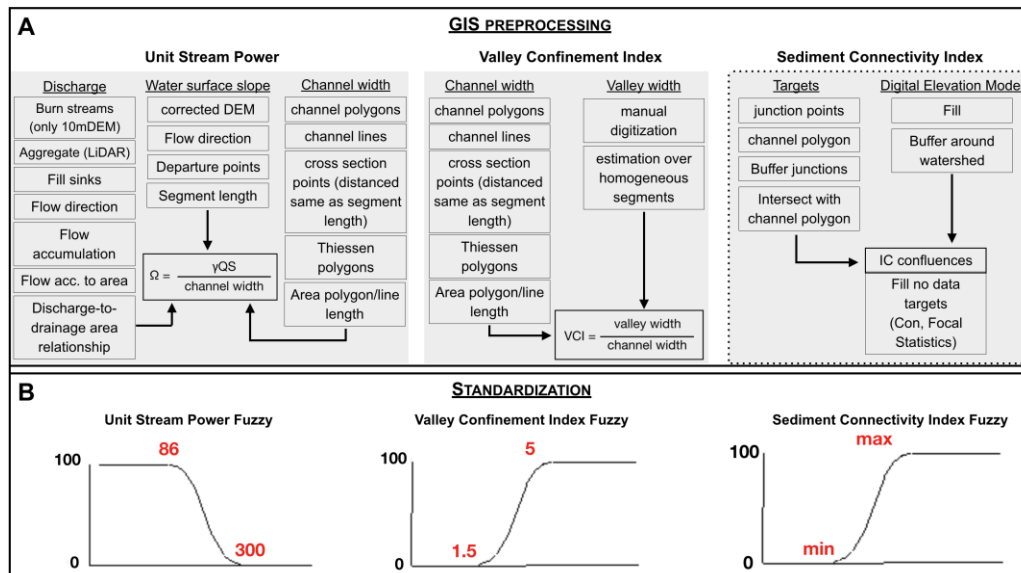


Figure 6.2: Methods used to model the geomorphic sensitivity of the main channel to tributary inputs at the watershed scale. (A) The Sediment Connectivity Index has a dotted box to mark that the processing is external to ArcGIS (SedInConnect Tool, see Crema and Cavalli, 2018). (B) Standardization procedure, whereby each factor is transformed using a fuzzy function. Control points were chosen based on thresholds found in the literature (Table 6.1). In case of the SCI, due to values being relative (i.e. the higher the SCI value, the higher the fuzzy score, the higher the likelihood that these are important tributaries and vice versa), the minimum and maximum value of the SCI distribution serve as control points. Each step is described in more detail in the text. Note: If using LiDAR, aggregating first to 5m using the mean, then to 10-m using the minimum is advised (see Biron et al., 2013).

For the second category, i.e. the capacity of the main channel to effectively transport the delivered sediment, unit stream power (USP) in conjunction with the main valley confinement index (VCI) were chosen, as they exert an influence on the nature and rate of erosional and depositional processes along a river (Magilligan, 1992; Brierley and Fryirs, 2005). The algorithm used to obtain unit stream power is described in detail in Biron et al. (2013). These GIS tools can be applied at multiple scales (reach to watershed, including the entire stream network), but since the focus of this study is the main channel, they have been applied at the watershed scale including only the main channel. For both study sites, unit stream power was calculated over a segment length of 200m, based on Biron et al. (2013) who found that the optimal segment length is roughly 10 times the mean channel width (the average channel width in our study sites is 24m). Segments of 250m were also considered, but statistical tests revealed no significant differences between slopes calculated over 200 and 250m ($F(1)=0.03$, $p\text{-value}=0.863$).

Valley confinement can be expressed by the confinement degree (Brierley and Fryirs, 2005) or the confinement index (Rinaldi et al., 2012). Considering that the confinement degree does not consider channel width and that the tools developed by Biron et al. (2013) can be used to automatically calculate channel widths, the latter index was chosen for this study. Thus, valley width was divided over the channel width, the latter obtained from the GRHQ channel polygons or manually digitized from orthophotos when these polygons were not available. Valley bottom widths were estimated over the same segment length as unit stream power using the hillshade and slope layers obtained through the Spatial Analyst/Surface tools of ArcGIS.

The choice of these factors was also based on data availability and resolution, as well as the possibility and ease of data processing. Because of the nature of fuzzy logic, and because the effect of the tributary may persist for a certain distance downstream, the data had to be continuous.

6.3.2. Factor standardization and weighting

The multi-criteria analysis consists of first choosing key factors that best represent the process being modelled, then standardizing them using fuzzy functions and, lastly, combining them using a weighted sum (Voogd, 1983). Each factor was standardized using a suitable fuzzy membership function that transformed the original values into fuzzy scores ranging from 0 (not morphologically sensitive) to

100 (highly sensitive morphologically) based on a decision rule and thresholds found in the literature (Table 6.1).

In this study, the morphologically significant tributaries are associated with sediment deposition in the main channel that occur as a result of an abrupt gradient decrease between the usually steep hillslopes of the tributary basin and the gentler gradient of the main channel valley. Consequently, if the potential for sediment connectivity between the tributary basin and the confluence is high, there is a high likelihood that sediment will be delivered to and will affect the main channel. However, if the valley configuration is confined, the energy, i.e. stream power, of the main channel will be concentrated in a small zone and the effect of the tributary will likely be “erased”. Conversely, an unconfined valley setting favours energy dissipation, thus allowing the main channel to more freely adjust its planform, i.e. be more mobile. Furthermore, an unconfined valley may also mean that the sediment load carried by the tributary has to travel a greater distance over the valley bottom, increasing the chances that at least part of its load will be deposited before reaching the confluence. In the main channel, high values of unit stream power are associated with erosion, while low stream power values are generally linked to deposition. As a result, the standardization process assigns high fuzzy scores to those conditions of sediment connectivity, valley confinement and unit stream power where deposition is favoured (Figure 6.2B).

The next step involves weighting each factor according to their importance. Weights were defined with a pairwise comparison matrix (Saaty, 1980), wherein two factors were taken at a time and their importance relative to each other were rated on a 9-point continuous scale to form a reciprocal ratio matrix. From this matrix, best-fit weights were derived by calculating the initial weights with each column and then averaging over all columns. To determine the degree of consistency that was used in the development of the weights, a consistency ratio was calculated. This indicates that the matrix ratings were randomly generated, wherein a value greater than 0.1 should be re-evaluated. The consistency ratio (CI) for the base weighting scenario was 0.062. Unit stream power receives the highest weight in the base weight scenario (Table 6.2) due to its well-established importance as a key variable controlling geomorphic change and due to field observations suggesting that, in terms of sediment deposition at the confluence, a tributary effect may be weakened or even erased when the channel has a high capacity to mobilize deposited bed material. The final step of the weighting is to multiply each factor by its weight and sum all factors, i.e.:

$$CMS = \sum w_i x_i$$

where CMS is confluence morphological sensitivity, w_i is weight of factor i and x_i is fuzzy score of factor i .

Table 6.2: Basic weight scenario using a pairwise comparison matrix (Saaty, 1980).

Factor	Weight
Unit stream power (USP)	0.74
Valley confinement index (VCI)	0.20
Sediment connectivity index (SCI)	0.06

The result of this analysis is a map representing the distribution of sensitivity of the main channel to tributary inputs, i.e. the likelihood that the tributary deposits its sediment load in the main channel and induces geomorphic change. In order to be able to compare among different weight scenarios and among different watersheds, which have different CMS distributions, results are displayed using ten quantiles. To improve readability of the map, the ten quantiles were further combined into five classes as follows: very low – 1st quantile; low – 2nd, 3rd, 4th quantile; medium – 5th, 6th quantile; high – 7th, 8th, 9th quantile and very high – 10th quantile. This classification type was determined in order to isolate the most extreme quantiles into the very high and very low categories.

6.3.3. Sensitivity analysis and model validation

Sensitivity analyses were carried out in order to assess how much impact the weights have on the results. Incrementally varying the weights of the most important factor while keeping the ratio of the remaining factors equal resulted in only slight, but insignificant changes to the distribution of the CMS. Consequently, the weights were stretched so that their impact on the results could be observed. Two alternative scenarios were explored, wherein SCI (CI=0.069) and VCI (CI=0.046) factors are each dominant (highest weight), as well as a third scenario where all factors are weighted equally (Table 6.3). The latter scenario was not derived from a pairwise comparison matrix, as the purpose was solely to test whether the model performed better when the factors are weighted equally. The derivation of the VCI dominant scenario was based on some evidence which suggests that stream power is not enough as a sole predictor of geomorphic change and that, valley confinement was the primary variable

explaining geomorphic change (i.e. channel widening), especially in steeper, more confined channels (Surian et al., 2016; Scorpio et al., 2018).

Table 6.3: The three weight scenarios used in the sensitivity analysis.

	Equal	SCI dominant	VCI dominant
USP	0.33	0.1	0.33
VCI	0.33	0.39	0.53
SCI	0.34	0.51	0.14

Model output was validated using field observations and data collected during our summer 2018 field campaign in Gaspésie (described in Mazgareanu, 2019), combined with visual assessment of orthophotos and available field observations and data in the Coaticook watershed (Demers et al., 2017; Massé et al., 2019). To assess the ability of the model to correctly assign high CMS scores to morphologically significant confluences, a distinction was made between active and inactive confluences based on orthophotos and DEM analysis. Morphologically active confluences have high sediment load and are characterized by evidence of sediment reworking in the tributary, by significant sediment deposits at the mouth of the tributary, as well as signs of lateral migration of the main channel downstream from the confluence. A change of fluvial style in the main channel was associated with an active confluence. The inactive confluences are sites which showed no sign of any impact in the main channel and had little to no signs of a geomorphically active tributary. Figure 6.3 provides a characteristic example of each case.



Figure 6.3: (A) An example of an active confluence in Gaspésie (site 7a, see Figure 12 for location) showing tributary effect in the main channel that extends more than 2 km downstream, approximately 14 times the channel width (entire extent not pictured). (B) An example of multiple inactive confluence in the Coaticook watershed.

In the Coaticook watershed, out of a total of 130 confluences, 14 were identified as morphologically active (10.8%). In Gaspésie, out of a total of 294 confluences found in the five study watersheds, 31 were identified as morphologically active (10.5%). The remaining inactive confluences were bootstrapped by taking 14 (Coaticook) and 31 (Gaspésie) subsamples 1000 times to develop a sampling distribution of the median. This was then compared with the distribution of the active confluences at the 95% confidence interval in order to discern whether the model is able to distinguish active from inactive confluences. This was applied for all weight scenarios. Additionally, for a more qualitative insight into the CMS for each weight scenario, another subsample of 14 inactive confluences were randomly selected out of the entire inactive confluence sample for the Coaticook watershed, whereas for the Gaspésie watershed, the field study sites were used for comparison (Figure 6.4).

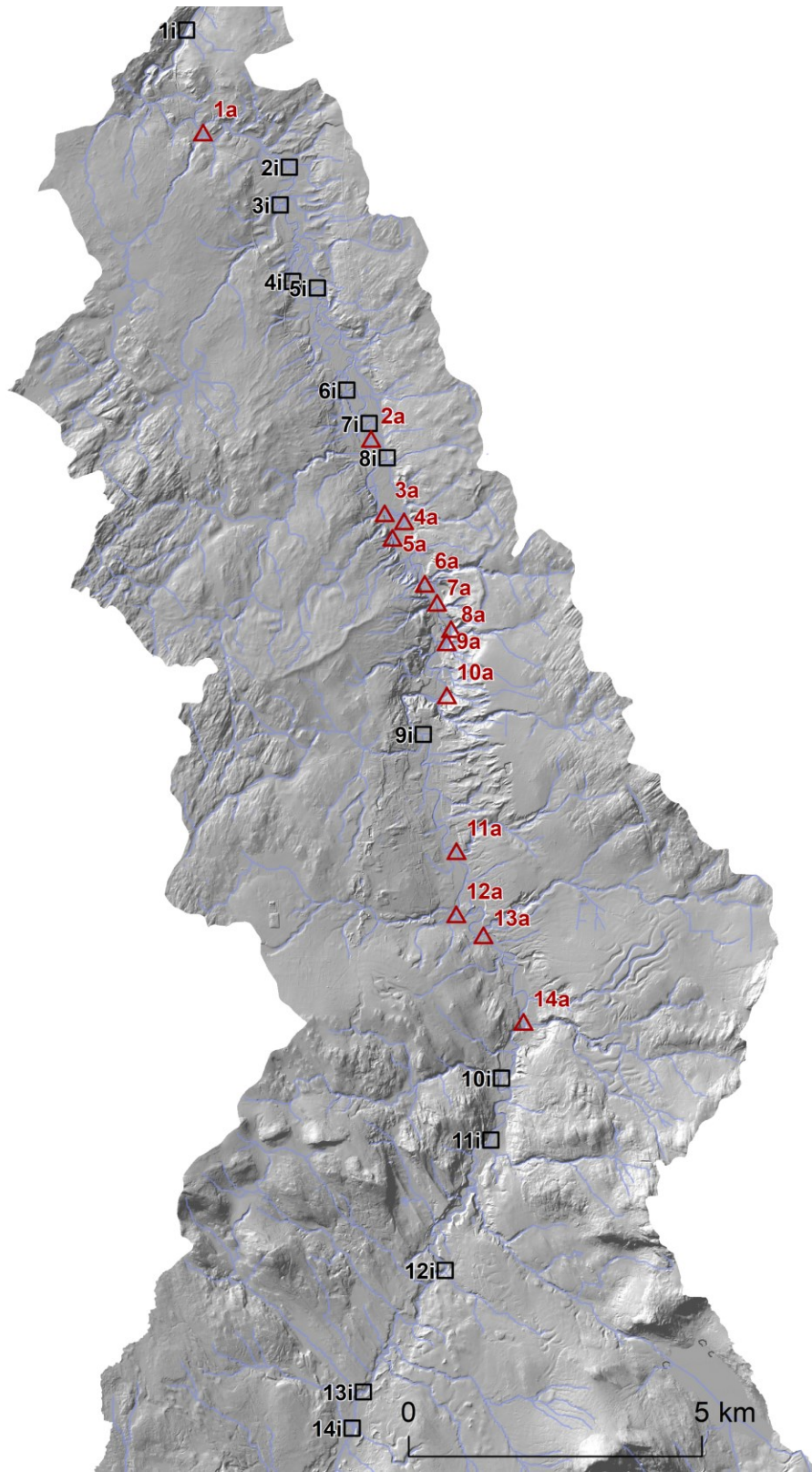


Figure 6.4: Spatial distribution of the 14 active (red triangles, letter a) and randomly selected inactive confluences (black squares, letter i) in the Coaticook watershed.

6.4. Results

6.4.1. Fuzzy GIS Model

The fuzzy GIS model is able to detect most of the active confluences, while also correctly identifying inactive confluences (Figure 6.5).

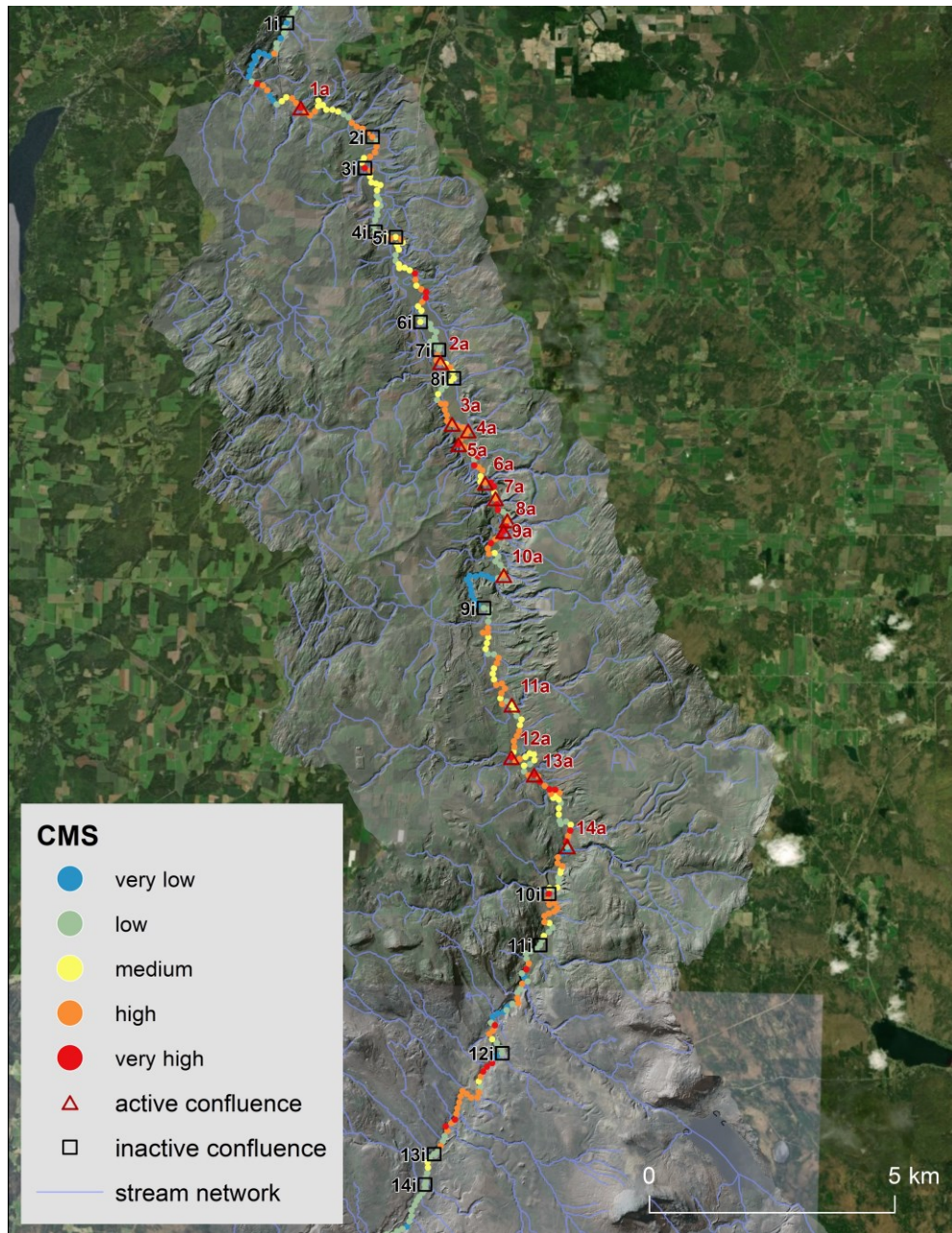


Figure 6.5: Model output using the basic weight scenario (Table 2) for the Coaticook watershed with LiDAR data. Active confluences, detected from field and remotely-sensed images, are shown with red triangles, while randomly selected, inactive confluences are shown in black squares.

Results of the bootstrap show that the model is able to distinguish active from inactive confluences for all weight scenarios (Table 6.3) (Figure 6.6). Medians of the active confluences sample are significantly different from those of the bootstrapped, inactive sample. The greatest differences between the two are in the SCI dominant scenario (5.8), followed by the equal scenario (3.8) and the VCI dominant scenario (1.6). The USP dominant, base weight scenario has the smallest difference between medians (0.98). Consequently, these results seem to suggest that the SCI dominant is the best weighting scenario.

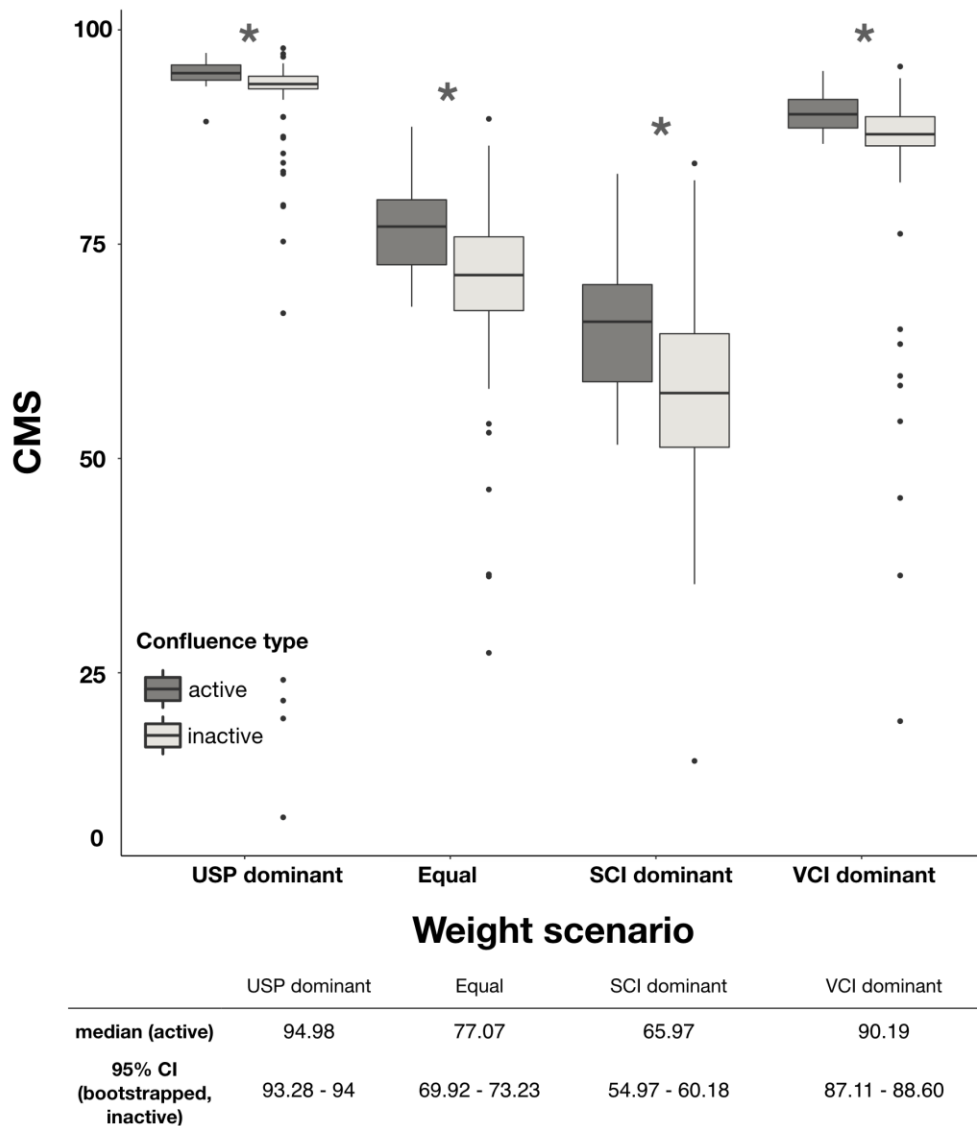


Figure 6.6: Boxplots of the CMS score by confluence type in all weight scenarios considered in the sensitivity analysis (Table 6.3) for the Coaticook watershed using LiDAR data.

Furthermore, when comparing between the 14 active and the 14 randomly selected inactive CMS scores, the model appears to classify active confluences as predominantly having high and very high CMS scores, while inactive ones are mostly classified in the medium and low CMS categories (Figure 6.7).

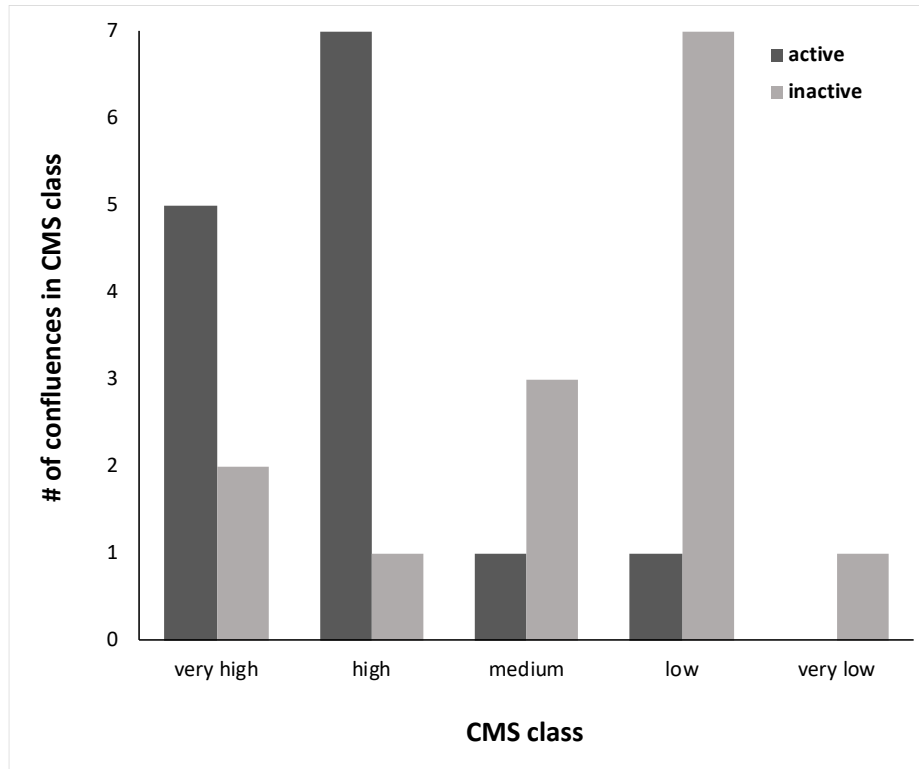


Figure 6.7: Number of confluences classified in each CMS class by confluence type.

The qualitative analysis gives a more nuanced insight to the results. Despite bootstrapping resulting indicating that SCI-dominant and equal-weighting scenarios give the greatest differences between active and inactive confluences in terms of CMS scores, from Figure 6.8 and orthophoto analysis, it becomes apparent that the SCI dominant scenario does not always assign active confluences into higher CMS classes and inactive ones into lower CMS classes. In fact, there are overall 7 points (4 active, 3 inactive) where CMS classes vary according to different weight scenarios. Site 7a is poorly described by the SCI dominant scenario and should belong to a high CMS score due to an active tributary that mobilizes active sediment sources (hillslopes, gully) and a tributary bar deposit of about 550m². Similarly, point 11a is better described by the USP dominant scenario, as a 390m² tributary bar that shows signs of reworking, coupled with an active tributary should belong to a higher CMS class. However, the SCI dominant scenario is best fit in the case of site 14a, as a 4000m² tributary bar, an active tributary and a more mobile main channel should indicate a very high CMS. In terms of the

inactive confluences, two are poorly described by the SCI-dominant weight scenario. Sites 12i and 13i are located in the upper catchment and show no signs of geomorphic activity. Thus, they should receive a low CMS. These results suggest that in some cases the USP and the VCI-dominant scenarios perform better.

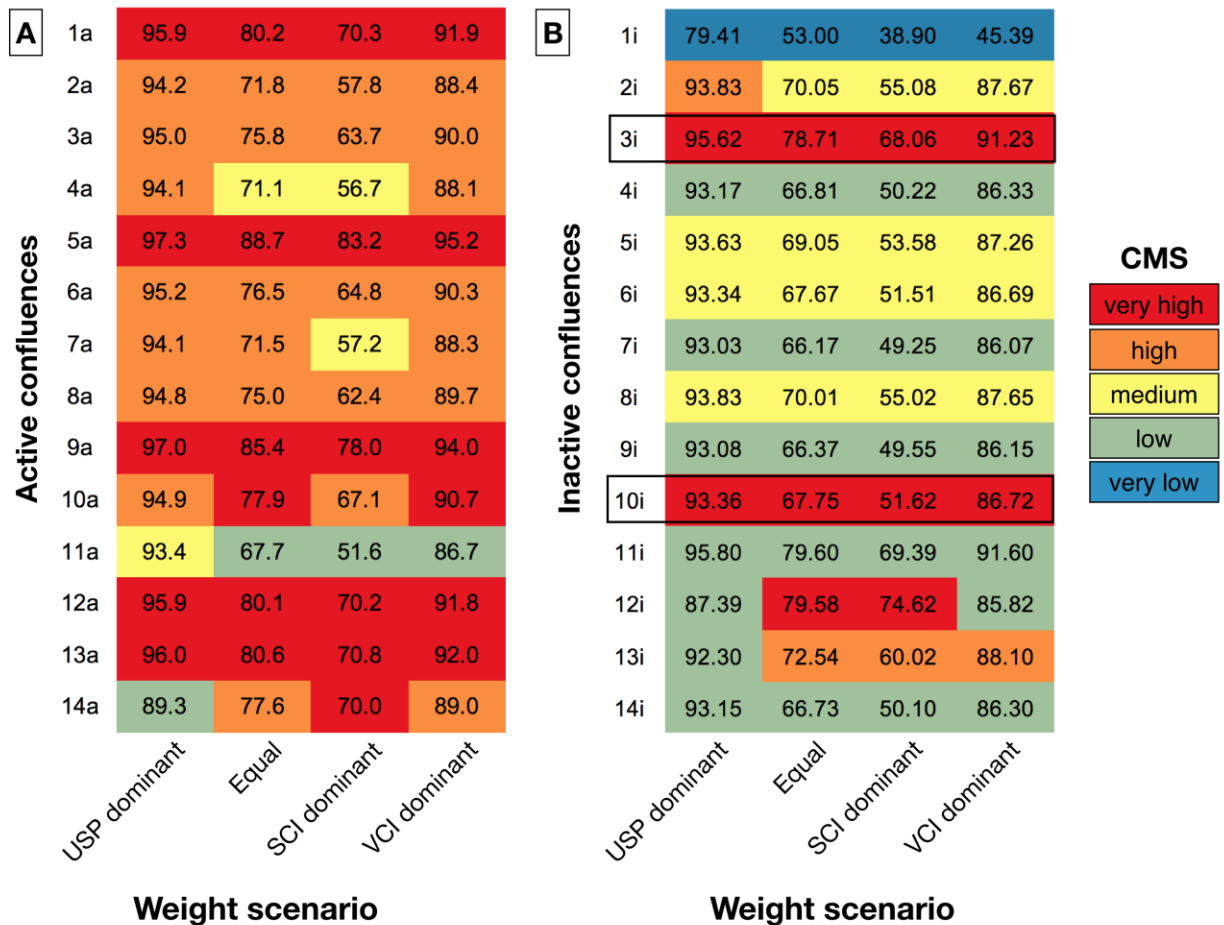


Figure 6.8: CMS scores of active (A) and inactive (B) confluences by their codes (see Figure 6.3) and throughout all scenarios. The numbers within each cell represent the absolute CMS score, while the colour scheme corresponds to the CMS class they belong in. Problematic sites are marked in rectangles.

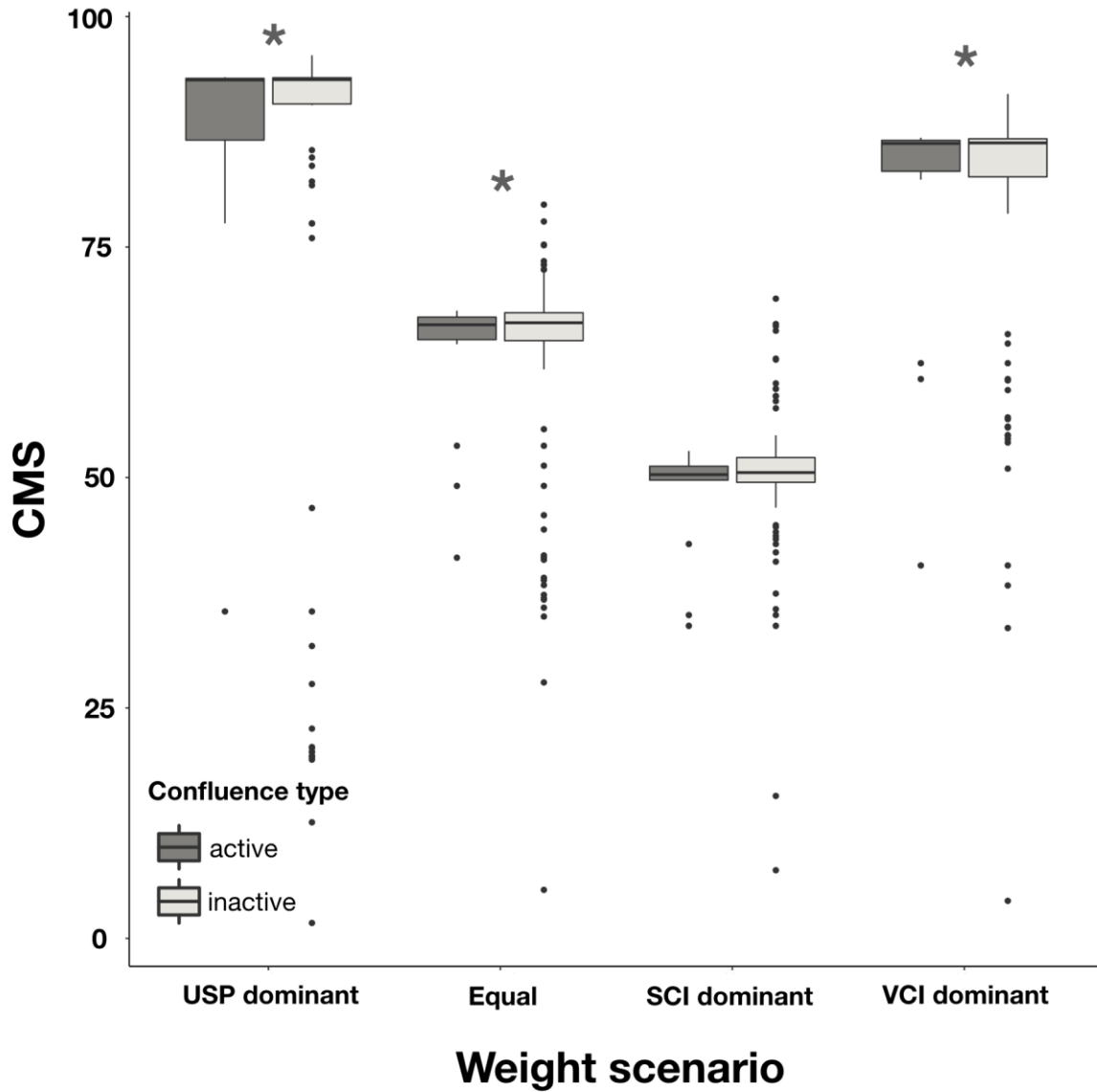
Interestingly, the model was able to detect two confluences that were originally coded as inactive. Figure 6.8B shows that points 3i and 10i are consistently classified by the model as having a very high CMS. These are tributary basins that contributed to past flooding events and are expected to play a role in the future (COGESAF, 2017).



Figure 6.9: Example of an inactive confluence detected by the model as important (Ruisseau Bissonnette) with a tributary bar of about 580m². Not pictured, but present upstream in the tributary, are two additional signs of geomorphic activity: disturbance potentially associated with building of a railroad bridge and increased mobility due to sediment deposition and large wood.

6.4.2. LiDAR vs 10-m DEM comparison

When using the 10-m DEM, there are significant differences between the two confluence types in three of the four weighting scenarios (Figure 6.10). Interestingly, the SCI-dominant scenario cannot distinguish between active and inactive confluences, with the median of the active confluences remaining within the 95% confidence interval of the bootstrapped sample distribution of the inactive confluences. On average, the significant weight scenarios have a difference of 0.08 between medians of the two confluence types.



	USP dominant	Equal	SCI dominant	VCI dominant
median (active)	93.25	67.23	50.58	86.51
95% CI (bootstrapped, inactive)	93.10 - 93.23	66.46 - 67.11	49.96 - 51.04	86.18 - 86.42

Figure 6.10: Boxplots of the CMS score by confluence type in all weight scenarios for the Coaticook watershed, derived from the 10-m DEM. Contrary to the data extracted from the LiDAR, the model is not able to distinguish between active and inactive confluences in all weight scenarios.

The non-significant results of the SCI-dominant case can be attributed to the fact that even after stream burning, the flow accumulation path misses the actual channel because of the low vertical accuracy of this DEM. Thus, several sections of the river channel are in fact located on the floodplain (Figure 6.11). Since the SCI computation uses the flow accumulation procedure, this affects results especially when the tributary has to travel some distance on the valley bottom. Overall, at the scale of the watershed, the two datasets are comparable (Figure 6.11A), with confined areas in particular being recognized in both cases as having very low morphological sensitivity. However, the area in the middle catchment containing most important confluences is, with a few exceptions, entirely missed out by the 10-m DEM (Figure 6.11B).

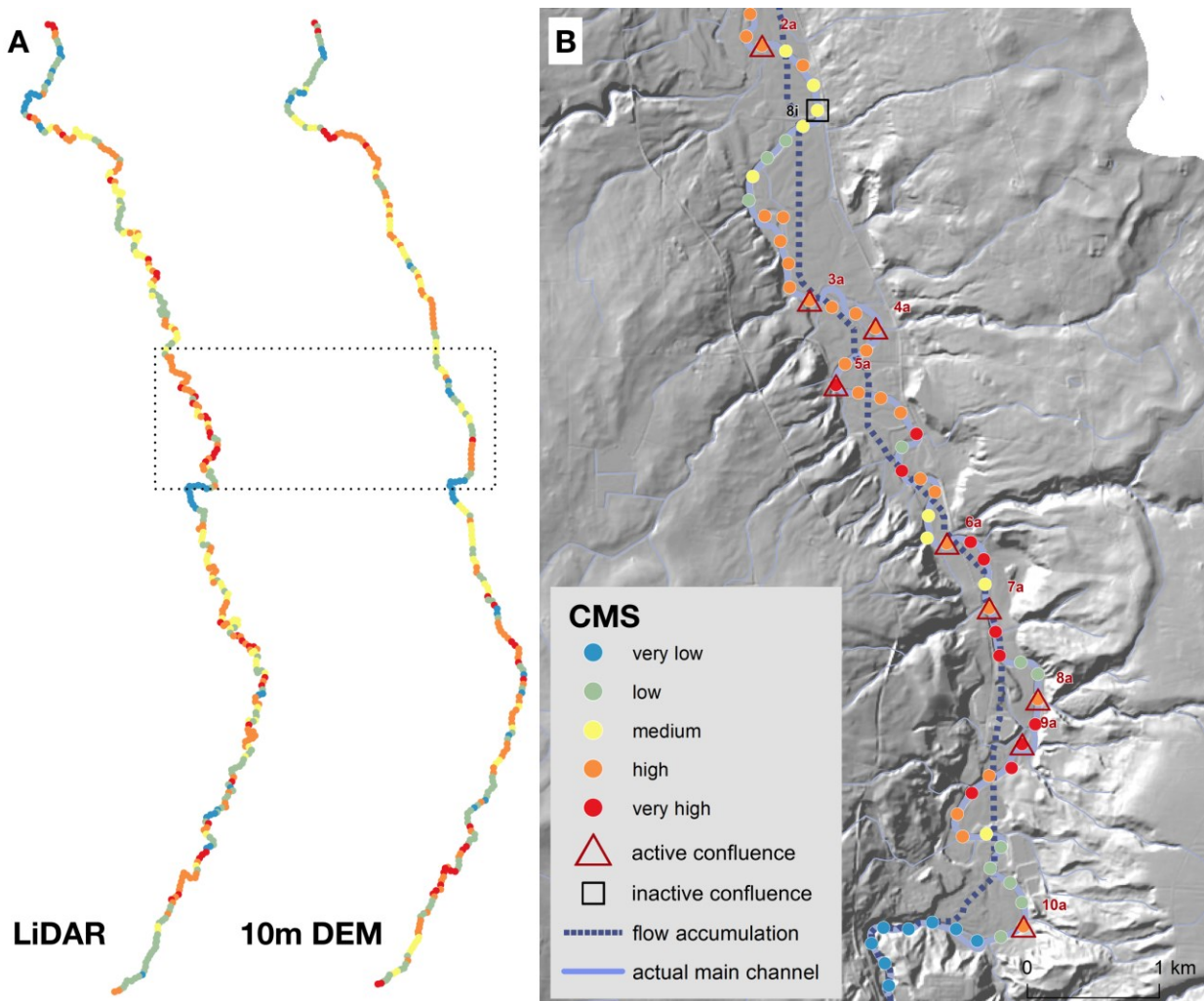


Figure 6.11: (A) A comparison of the CMS (using the basic weight scenario in the fuzzy model) between the LiDAR and the 10-m DEM. (B) A close-up view of the rectangular area in A showing cases where the flow accumulation (dashed blue line) does not follow the actual course of the channel (solid blue line), thus explaining the differences between the two DEM results in this area.

6.4.3. Comparison with field observations in Gaspésie (10-m DEM)

Figure 6.12 presents an overview of the model output for the five study watersheds in Gaspésie. Generally, the average CMS score is 1.2 times higher for sites identified as active than for those identified as inactive. For example, for the VCI dominant weight scenario the difference is highest (18.94), followed by the USP dominant scenario (16.15).

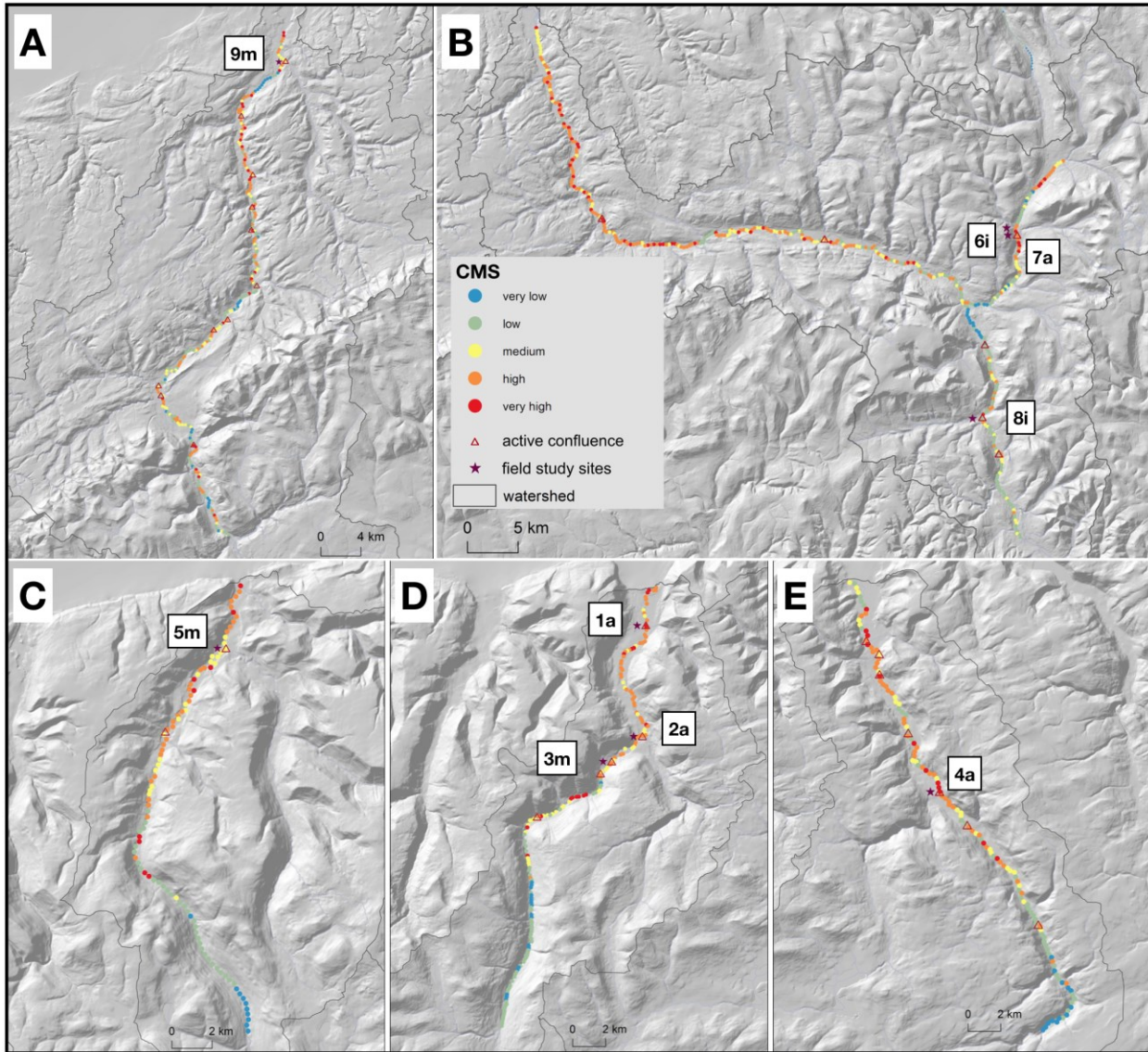
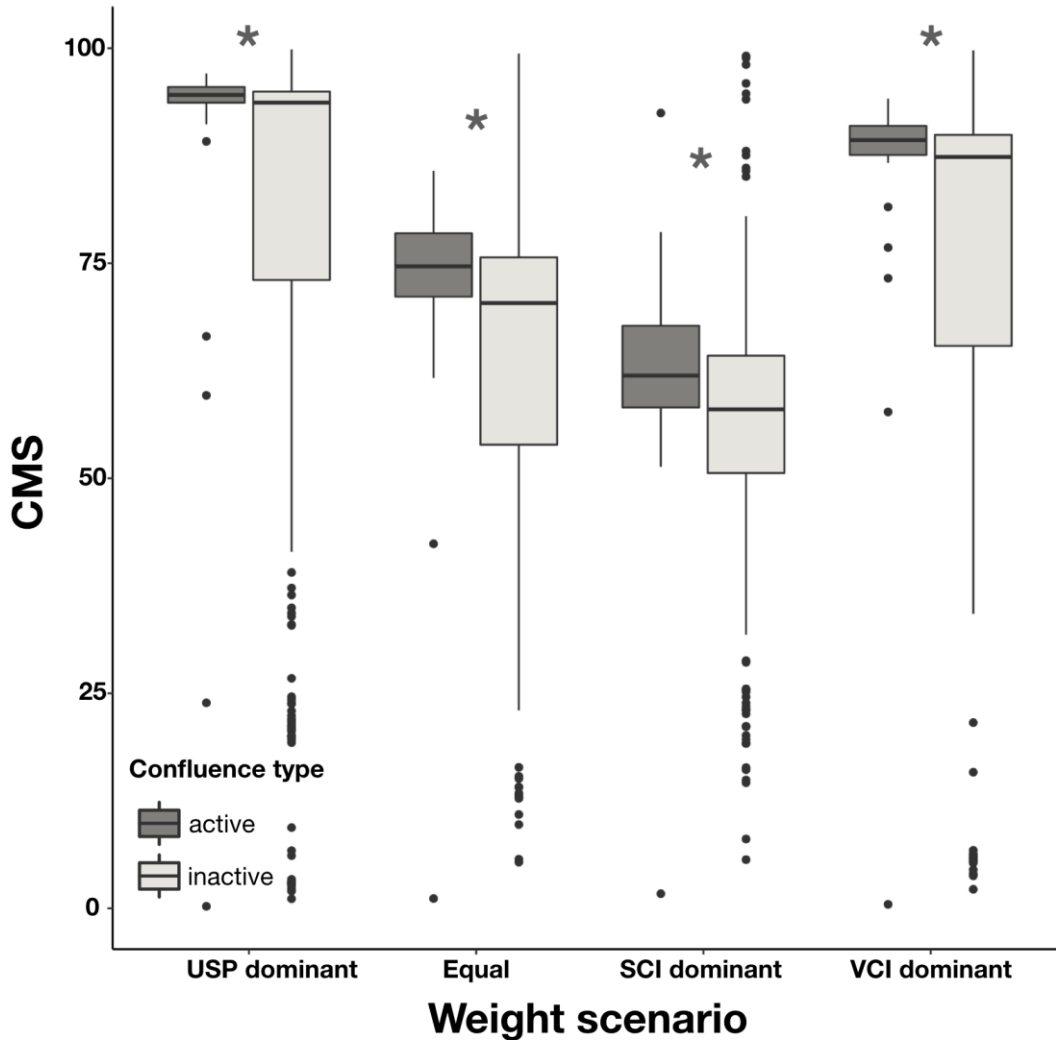


Figure 6.12: Overview of model output using the equal weight scenario (Table 6. 2) for Gaspésie with 10-m DEM data. Active confluences, detected from field and remotely-sensed images, are shown with red triangles, while field study sites are marked by an adjacent purple star and labelled according to confluence type (see Figure 6.14 for the label meaning). (A) Cap Chat watershed; (B) Sainte-Anne watershed; (C) Marsoui watershed; (D) Mont-Saint-Pierre watershed; (E) Mont-Louis watershed.

Surprisingly, the bootstrapping analysis shows that the model can clearly distinguish between active and inactive confluences for the entire Gaspésie dataset. This finding stands in contradiction with the Coaticook result, despite both using 10-m DEMs as inputs to the model. Medians of the active confluences sample are significantly different from those of the bootstrapped, inactive sample, with the greatest differences seen in the equal (2.7) and SCI dominant (2.5) scenarios, followed by the VCI (1.1) and USP dominant (0.5) scenarios.



	USP dominant	Equal	SCI dominant	VCI dominant
median (active)	94.6	74.6	61.9	89.3
95% CI (bootstrapped, inactive)	93.3 - 94.1	68.6 - 71.9	56.8 - 59.4	86.5 - 88.2

Figure 6.13: Boxplots of the CMS score by confluence type in all weight scenarios considered in the sensitivity analysis (Table 6.3) for the Gaspésie study area using 10-m DEM data.

In terms of the field study sites, Figure 6.14 shows that the model was able to correctly distinguish active from inactive confluences: active sites are assigned to higher CMS classes and have higher average CMS scores in all weight scenarios (e.g. 73.52 for active and 43.28 for inactive confluences for the equal scenario). The anthropogenically modified sites are assigned low to medium morphological sensitivity and have an average CMS score of 71.42 in the same weight scenario, which is very close to that of the important sites. By comparison, average modelled CMS for the entire sample of active and inactive confluences for the same weight scenario is 72.01 and 57.77, respectively.

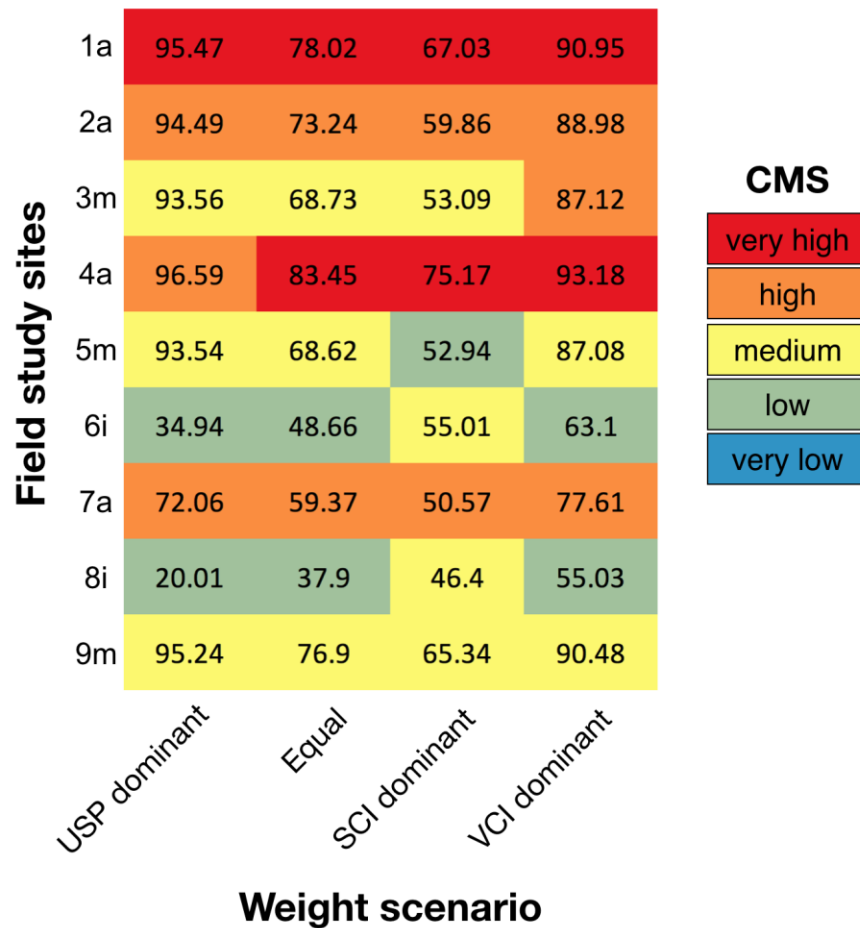


Figure 6.14: CMS score and class of the 9 Gaspésie field study sites. The letters a, i and m stand for active, inactive and modified (anthropogenically) confluence, respectively. For the latter it was hard to distinguish whether the tributaries had and important effect or not, due to their highly modified nature that does not correspond to classic confluence morphologies, such as a tributary bar. Note that the CMS score and class were calculated for each individual watershed so the scores cannot be compared between rows (sites).

Based on field observations (chapter 5) and the results of the bootstrapping analysis, the equal and VCI dominant weighting scenario seem to best describe CMS for the Gaspésie watersheds. Determining which scenario is best is difficult due to the nature of study site #3. In the equal scenario, it is classified as having a medium CMS, while the VCI dominant scenario assigns it a high CMS. The site is characterized by a large compound bar downstream of the confluence, however there is no evidence that would support the assumption that these deposits would be directly related to the tributary. The tributary itself is infilled with sediment as it reaches the valley bottom, which would suggest a high CMS. However, it is then diverted through a culvert, which acts as the connecting link with the main channel. The height of the culvert at the confluence is 2m greater than the bed of the main channel. This would suggest a lower CMS, since the road and the culvert represent both a buffer and a barrier to sediment connectivity.

6.5. Discussion

6.5.1. Advantages of the proposed approach

This study presents a novel approach to detect automatically geomorphologically active confluences through the use of variables not traditionally associated with longitudinal discontinuities induced by tributaries with a high sediment load. The approach is solely based on remotely-sensed raster data and can thus be easily applied at the watershed scale as a preliminary geomorphic assessment tool. Other studies that investigated the possibility of predicting locations of longitudinal disruptions used logistic regression based on data collected from field sites (Rice, 1998; Benda et al. 2004), numerical models (Ferguson et al., 2006; Rice et al., 2006; Czuba and Foufoula Georgiou, 2015) and GIS (Jones and Schmidt, 2017; Rice, 2017; Lisenby and Fryirs, 2017). The major advantage of our approach is that the entire geoprocessing can be carried out within a GIS software, so that field work is not needed in order to obtain initial results. Once the CMS map at the watershed scale is obtained, field work can be targeted to those sites having high CMS scores, thus reducing field work costs and time. Therefore, the model output can be used as a template for further investigations, such as geomorphic mapping of barriers and blankets like reported by Lisenby and Fryirs (2017).

Another advantage of the proposed approach is to use fuzzy logic instead of crisp, Boolean factors (coded as 0 and 1), which we believe is better suited to represent the dynamic nature of tributary-main

channel interactions, in particular the spatial extent of a tributary's effect on the main channel. First, controlling variables identified in Table 6.1, such as the product between tributary area and slope or the discharge ratio (or drainage area ratio) are relatively easy to obtain in a GIS and could be used to predict and prioritize tributaries in terms of their importance. However, these are generally at-a-point measurements, which would miss out the spatial extent of a tributary's effect in the main channel. This is not trivial, as it is known that the effect of an active tributary can persist for a certain distance downstream (Harvey, 1997), as highlighted in Figure 4A with an impact of 14 channel widths (>2 km). Using a model that provides a gradient of values along the main channel thus allows to see the sphere of influence of a tributary. Second, fuzzy logic is better suited at dealing with an imprecise knowledge of parameters. For instance, there is no definite knowledge that a certain unit stream power value always causes deposition; thresholds chosen in this study reflect empirical observations in a range of environments and watershed configurations (Bull, 1979; Baker and Costa, 1987; Magilligan, 1992; Bizzi and Lerner, 2015; Lea and Legleiter, 2016; Magilligan et al., 2015; Parker et al., 2015; Yochum et al., 2017; East et al., 2018), so that it is hard to precisely determine a value that would apply everywhere. Fuzzy variables indicating a membership rather than a crisp statement provides the required flexibility to deal with this uncertainty (Feizizadeh et al. 2014).

6.5.2. Preliminary geomorphic assessment and the choice of the relevant variables

This study considers a unit stream power values less than 86 W/m^2 to be most likely conducive to deposition (Table 6.1), with likelihood decreasing following a sigmoidal fuzzy function until reaching the value of 300 W/m^2 . The upper threshold is based on the work of Yochum et al. (2017), in which instability induced from deposition was observed to result in major geomorphic change even at low unit stream power following an intense flooding event in the Colorado Front Range. The lower threshold is based on the works of Magilligan (1992), who estimated that, for alluvial channels, a minimum of 300 W/m^2 is necessary to produce major geomorphic change. This value was subsequently confirmed by Buraas et al. (2014) and Magilligan et al. (2015). Even though it generally applies that the magnitude of geomorphic change is directly proportional with stream power, studies have found that alluvial rivers experience major geomorphic change even at stream power values of 37 W/m^2 (East et al., 2018), while little geomorphic change was observed at values larger than 1000 W/m^2 (Miller, 1990). Because of this, the model was additionally tested using a modified upper threshold of 35 W/m^2 . This resulted in an overall lower mean CMS score (-3) and higher standard

deviation (+0.6). To observe potential changes, five points were randomly chosen along the Coaticook River and their ranked CMS scores compared between the initial unit stream power threshold and the lowered one. Results showed that the ranks remain consistent. However, when a heterogeneous river section transitioning from a confined to an unconfined valley is chosen instead of the random sampling, some locations appear more sensitive to the unit stream power threshold, namely those located where the valley opens and near some confluences. This suggests that the link between stream power and major geomorphic change is still poorly understood and that it depends on the interplay between driving (e.g. event magnitude and duration, system memory, variations in sediment supply, channel slope and resisting mechanism) and resisting forces (e.g. roughness elements, valley confinement, bank cohesion, vegetation) (Miller, 1990; Buraas et al., 2014; Yochum et al., 2017; East et al., 2018). In other words, perhaps trade-off effects exist between the three factors used in this study, as well as an interdependency of reaches. Thus, the morphological sensitivity of one reach may vary from others as a function of its position relative to the upstream reaches.

Another modification to the model that could better represent connectivity patterns of tributary basins would be the modification of the weighting raster used to calculate the index of connectivity (IC). In its current state, the IC calculation is adapted to alpine environments and so it uses the surface topography to calculate flow paths of sediment routing. Since all watersheds studied herein have a major proportion of agricultural or forested land use, the weighting raster could include the original USLE-RUSLE derived weight (Borselli et al., 2008) or a Manning's n estimate (Persichillo et al., 2018). This would explicitly consider the effects of vegetation on sediment routing. At the same time, these are factors that can change over time, while topography is much more constant. Furthermore, since the IC is calculated based on a DEM, it does not include any measure of the availability of sediment in the watershed. This may lead to areas being depicted as highly connected when, in reality, they are less connected because of a lack of readily available material. Even though tributaries are geomorphic agents that can mobilize sediment masses through entrainment of already deposited material or through bank erosion, this is not considered in the IC.

Despite these caveats, the power of the IC lies in its ease of computation, its minimal number of inputs and the spatially continuous data over the entire watershed that it provides, which was decisive for the purposes of this study. Furthermore, it indirectly considers anthropogenic impacts like infrastructure, since these are most often imprinted on the landscape and thus visible from high-

resolution LiDAR data. These structures act as barriers (sens. strict. Fryirs et al, 2007a) that effectively disconnect tributaries from the main stream. For example, it is well established that roads modify hydro-geomorphological processes and connectivity (Reid and Dunne, 1984; Montgomery, 1994; Croke et al., 2005; Persichillo et al., 2018). Roads break the slope of tributaries, resulting in sudden loss of transport capacity and sediment deposition even before reaching the valley floor and the main channel. The straight and smooth surface of roads creates a new, preferential path for downward movement of water and sediment, such as was documented in several Gaspésie study sites (Mazgareanu, 2019). In the Coaticook watershed, 12 of the 14 active tributaries are dissected by roads (Figure 6.16). To assess the sediment connectivity potential between the tributary and the road and gain a more nuanced understanding about tributary-main channel interactions, the IC could be also computed with respect to the road network.

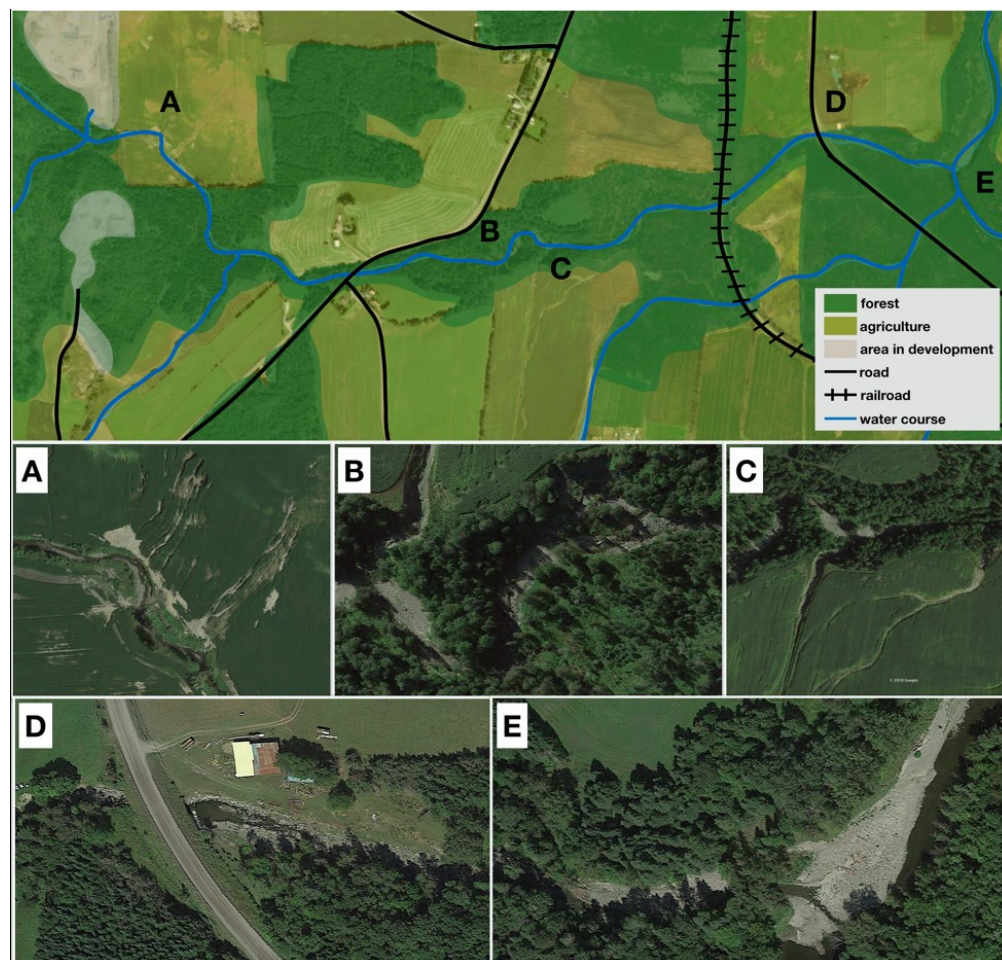


Figure 6.16: Example of a type of tributary-main channel coupling in the Coaticook watershed. Before reaching the main channel, the tributary is dissected by two roads and one railroad. (A) and (C) show gullying due to intensive land use, which serves as an additional source of sediment in the tributary. (B) increased mobility associated with increased sediment load. (D) erosion associated with the presence of the road. (E) tributary mouth bar at the junction with the main channel.

In our fuzzy model, the tributary is represented solely by the sediment connectivity index (SCI). Because of this, we would have expected that a weight scenario where SCI would be dominant would best detect the spatial distribution of sensitivity, with most morphologically sensitive locations corresponding with those tributaries that have the potential of delivering the most sediment. However, our results show that most of the points receiving high CMS scores when SCI is dominant are actually those abutting the valley margin. This may be due to the direct coupling between hillslopes and the main channel, so not directly related to fluvial processes linked to tributary inputs. Furthermore, this finding also supports field observations in Gaspésie, where, according to preliminary DEM analyses, tributaries were expected to produce a big impact on the main channel, yet no visible effect was observed in the confluence zone, likely because the main channel had the necessary energy to transport the delivered sediment downstream. This suggests that it is not solely the sediment delivered at the confluence that dictates whether the tributary has an impact or not, but rather the ability of the main channel to erase that effect, as also pointed out by Ferguson et al. (2006).

6.5.3. Future avenues for application

The result of the model can also be used to investigate relationships between active confluences and the structure of river networks. For instance, basin shape (square root of the basin area/maximum straight-line distance along the basin perimeter) is one of the many elements that may affect the development of active confluence zones. It controls the distribution of tributary basin sizes and thus the number and spacing of confluences within them. Benda et al. (2004a,b) and Benda (2008) postulated a set of hypotheses related to the structure and scaling properties of river networks. In terms of basin shape, they posit that active confluences are more likely to be found in compact basins relative to rectangular basins. This is due to compact basins being formed by dendritic networks, where many small channels merge to form higher order streams and higher symmetry ratios, resulting in a possibly higher occurrence of important confluences in the lower parts of the basin. Conversely, this downstream trend is reversed in rectangular basins, which are formed by trellis or parallel networks. As the symmetry ratio declines with distance downstream, geomorphically active confluences are more likely to be found in the upper parts of the basin.

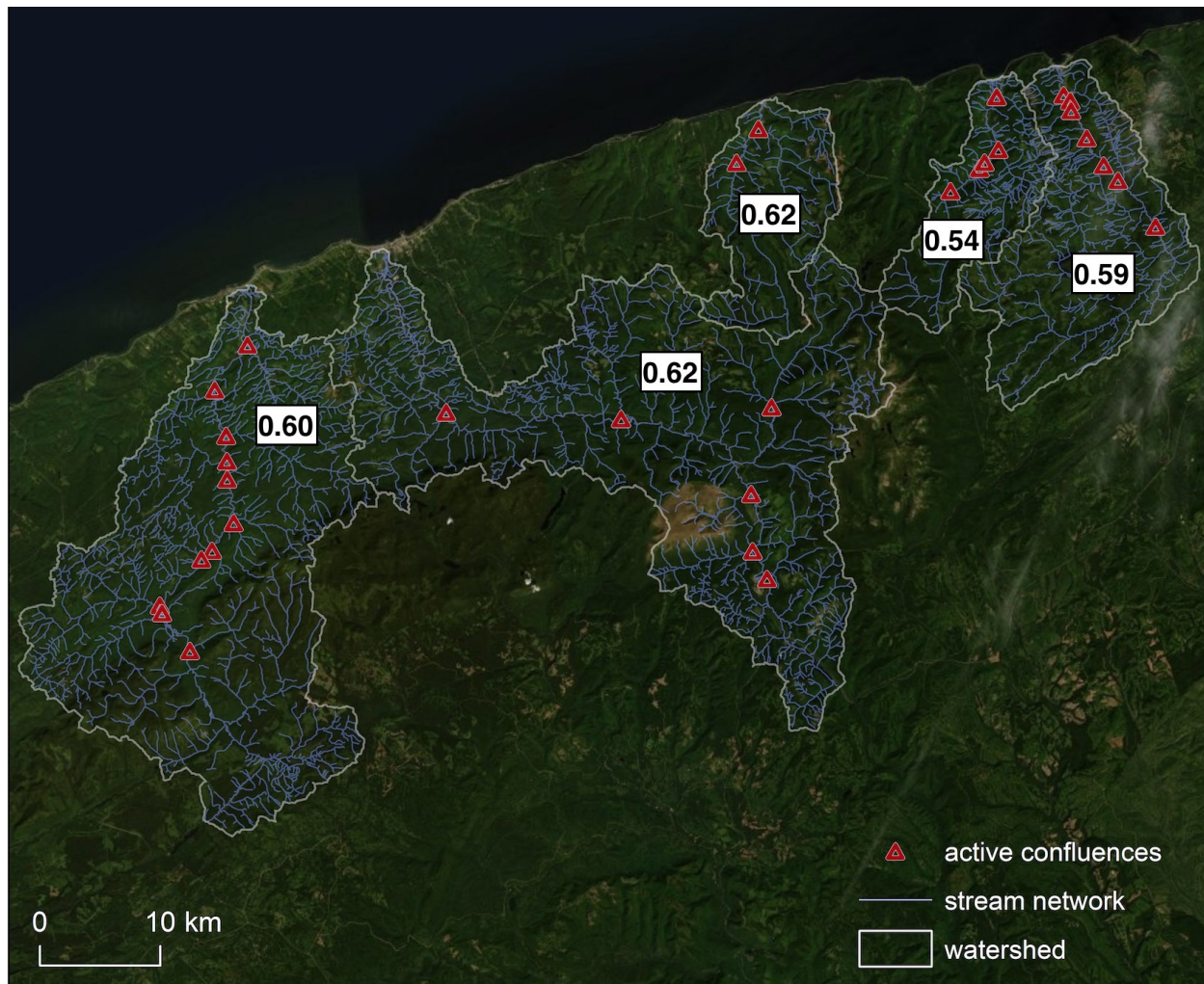


Figure 6.17: Distribution of important confluences (solely along the main river) in the Gaspésie study area and basin shape values for each of the five investigated watersheds. Values closer to 1 indicate more compact basins and small values indicate more rectangular basins.

To test this, we calculated the basin shape for each of the five watersheds in Gaspésie. Figure 6.17 illustrates the distribution of important confluences along the main river in these watersheds, along with the according basin shape values. Values closer to 1 indicate more compact basins and small values indicate more rectangular basins (Rice, 2017). Our study watersheds have values between 0.54-0.62, indicating that their shape is in-between compact and rectangular. By comparison, tributary basins investigated by Rice (2017) had a shape ranging between 0.48-0.70, which were classified by dividing the distribution into three (i.e. compact, mixed, rectangular, with breaking points being 0.63 and 0.55). Figure 6.17 shows that the hypothesis proposed by Benda (2008) cannot be entirely validated, as there is no clear indication that important confluences are concentrated in the lower basin for the compact shape and in the upper basin for the rectangular shape. For example, in the most

rectangular Mont-Saint-Pierre watershed (basin shape = 0.54), the most important confluence in terms of model output is located close to the outlet, similar to the exceptions found by Benda (2008) and Rice (2017). In Gaspésie, the factors that seem to have the greatest control over the distribution of important confluences are geology and anthropogenic modifications (i.e. deforestation and direct intervention). The shape of the networks is determined by the two faults separating two distinctly different rock types (easily erodible sedimentary rocks from resistant igneous and metamorphic rocks). Because of this, the calculation of the basin shape by taking the maximum linear distance anywhere along the basin perimeter may be complicated: for instance, the Sainte-Anne watershed (second from left) has a large basin area and maximum width but is nonetheless getting narrower towards the outlet.

Predictions about the location of expected channel mobility are extremely valuable for informing science-based river management. Confluences are sites susceptible to flooding and bed instability associated with significant tributary inputs and can pose serious hazard to infrastructure. Furthermore, uncertainty associated with climate change, superimposed on equally uncertain outcomes of potential river adjustment, highlights the need to shift towards a more comprehensive and sensible river management (Brierley and Fryirs, 2005). This oftentimes means the river knows best how to “look after itself” (Brierley and Hooke, 2015) and the adoption of a passive approach, where the management action is limited to allowing more space for rivers to migrate, adjust and flood naturally (Kondolf, 2011). The last few years have increasingly seen such approaches, under various names: “room for the river” (Baptist et al., 2004), “erodible corridor” (Piégay et al., 2005), “fluvial territory” (Ollero, 2010), “river corridor” (Kline and Cahoon, 2010), and “freedom space” (Biron et al., 2014; Buffin-Bélanger et al., 2015), the latter integrating the natural river mobility, floodplain areas, as well as riparian wetlands into one single common space.

However, approaches like the freedom space for rivers require hydro-geomorphological knowledge and expertise which is not always available in practice to river managers. The model presented herein therefore helps define these zones in a semi-automated way. Determining geomorphically active confluences with this GIS model can be used to widen the mobility space (used to compute the freedom space) to take into account increased public safety risk in these zones. It can also help planning infrastructure work such as roads and bridges. For example, wider bridge opening may be required to cope with the increased risk of mobility near important confluences.

6.6. Conclusion

A fuzzy GIS model that combines unit stream power, valley confinement and sediment connectivity into an index describing confluence morphological sensitivity (CMS) along the main channel was successfully applied at the watersheds scale in two areas comprising a total of 6 river basins. The model performed equally well with both LiDAR and 10-m DEM data in that it was able to distinguish between geomorphologically active and inactive confluences by assigning significantly higher scores to the first. Weight scenarios were developed to test model sensitivity, whereby each factor received the highest weight, as well as an additional scenario where all factors were weighted equally. Sensitivity analysis, in conjunction with field and orthophoto observations, revealed that the best scenario was that where sediment connectivity had the highest weight (Coaticook), followed by that where all factors have equal weights (Gaspésie). When comparing LiDAR and 10-m DEM data, both are comparable and can be used to model CMS along main channels, however attention must be paid to watershed specific characteristics when interpreting the results, such as valley morphology. Results suggest that even though general patterns of tributary-main channel interactions can be rapidly and reliably identified at a large spatial scale, geomorphic context and contingency can lead to interesting irregularities. This simple GIS model represents a toolkit for river managers, which they can use to better assess and characterize local heterogeneity in their watersheds, as part of the first steps in geomorphic assessments, especially since tributary inputs are not often explicitly considered. Other river management applications, such as the freedom space for rivers, sediment connectivity and hazard reduction may find the results pertinent to their practice.

7. Conclusion

Through a unique dataset of 9 confluence sites, this study investigated tributary-main channel characteristics at the reach scale in mountainous environments in Gaspésie, Québec. Field observations and analysis confirmed that complex morphodynamical interactions exist between high sediment load tributaries and main channels. The main finding of the field component is that there exists high inter-site variability in terms of expected confluence morphology despite the relative homogeneous geological setting of the study area. This reflects a juxtaposition of naturally imposed (i.e. valley setting and bedrock control) and variable (i.e. patterns and rates of sediment fluxes, and history of disturbance events) conditions, as well as direct anthropogenic interventions, such that clear inferences are, at times, difficult to be made.

Field observations demonstrated, however, that tributaries have a substantial role in influencing processes in the main channel and they should therefore be included in hydromorphic characterizations of watersheds, as well as in the ongoing efforts to semi-automate river surveys. To this end, the simple GIS model developed herein proves that geomorphic sensitivity in the main channel to tributary input can be assessed, as the level of accuracy provided by the model is within the error margins needed for preliminary geomorphic assessments at the watershed scale. The use of fuzzy logic provided a suitable means to capture variability related to “unsharp” factor thresholds and to offer a gradation that is inherent in complex natural systems. Despite the difficulty of generating spatially continuous, high resolution datasets to realistically represent variables directly related to tributaries, factors like the ones used in this study have proven to form a sufficiently powerful template, on which more targeted analyses can be added. However, more tests on these factors in a range of geomorphological contexts would be useful. For instance, future work could test whether the stream power gradient is better suited than unit stream power in predicting patterns of erosion or deposition induced by active tributaries.

Although this study predominantly assessed spatial patterns of confluence-specific morphology, integration of the temporal dimension of main channel sensitivity to tributary inputs would bring essential insight into the conditions under which tributaries activate and geomorphic change occurs. Thus, future studies could use repeat surveys to evaluate the impact of various flow stages and floods on confluence morphology and assess whether sensitivity to disturbance has changed over time. This

can be used in conjunction with analysis of historical and contemporary aerial photography, as well as repeat digital elevation models to better understand how tributaries interact with main channels and use this to construct evolutionary trajectories for confluence zones that represent likely adjustment pathways following disturbance. These could also be used to inform the freedom space for rivers approach by widening the mobility space to take into account increased public safety risk associated with active confluence zones.

The results of this research have contributed in the understanding of the role tributaries can play in respect to geomorphic change within a watershed. Hopefully, this work can add to the expertise applied by geomorphologists to environmental issues and, especially, contribute to more resilient river management approaches.

References

- Al Farraj, A. and Harvey, A. (2010): Influence of hillslope-to-channel and tributary-junction coupling on channel morphology and sediments: Bowderdale Beck, Howgill Fells, NW England. *Zeitschrift für Geomorphologie*, 54(2) 203–224.
- Baker, V.R., Costa, J.E. (1987): Flood power. In: Mayer, L., Nash, D. (Eds.), *Catastrophic Flooding*. Allen and Unwin, Boston, pp. 1–21.
- Benda, L., Dunne, T. (1997): Stochastic forcing of sediment routing and storage in channel networks. *Water Resources Research* 33, 2865–2880.
- Benda, L., C. Veldhuisen, and J. Black (2003): Debris flows as agents of morphological heterogeneity at low-order confluences, Olympic Mountains, Washington. *Geological Society of America Bulletin*, 115, 1110–1121.
- Benda, L., Andras, K., Miller, D., Bigelow, P. (2004a): Confluence effects in rivers: Interactions of basin scale, network geometry, and disturbance regimes. *Water Resources Research*, 40, W05402.
- Benda, L., Poff, N.L., Miller, D., Dunne, T., Reeves, G., Pess, G., Pollock, M. (2004b): The Network Dynamics Hypothesis: how channel networks structure riverine habitats. *Bioscience* 54, 413–427.
- Benda, L.E. (2008): Confluence environments at the scale of river networks. In: Rice, S.P., Roy, A.G., Rhoad, B.L. (Eds.), *River Confluences, Tributaries and the Fluvial Network*. John Wiley and Sons, Chichester, pp. 271–300.
- Best, J.L. (1986): The morphology of river channel confluences. *Progress in Physical Geography*, 10, 157–174.
- Best, J.L. (1987): Flow dynamics at river channel confluences: implications for sediment transport and bed morphology. *Recent developments in fluvial sedimentology*. Special Publication Society for Sedimentary Geology (39), 27–35. DOI: <http://dx.doi.org/10.2110/pec.87.39.0027>.
- Best, J.L. (1988): Sediment transport and bed morphology at river channel confluences. *Sedimentology* 35(3), 481–498. DOI: <http://dx.doi.org/10.1111/j.1365-3091.1988.tb00999.x>.

- Best, J.L. and Rhoads, B.L. (2008): Sediment transport, bed morphology and the sedimentology of river channel confluences. Rice, S.P., Roy, A.G., Rhoads, B.L. (Eds.): *River Confluences, Tributaries and the Fluvial Network*. Wiley, Chichester, UK, pp. 45–72 (Ch. 4).
- Biron, P., Roy, A., Best, J.L., Boyer, C.J. (1993): Bed morphology and sedimentology at the confluence of unequal depth channels. *Geomorphology* 8(2–3), 115–129.
- Biron, P.M., Best, J.L., Roy, A.G. (1996): Effects of bed discordance on flow dynamics at open channel confluences. *Journal of Hydraulic Engineering* 122 (12), 676–682.
- Biron, P.M., Buffin-Bélanger, T., Larocque, M., Choné, G., Cloutier, C.A., Ouellet, M.A., Demers, S., Olsen, T., Desjarlais, C., Eyquem, J. (2014): Freedom space for rivers: a sustainable management approach to enhance river resilience. *Environmental Management* 54, 1056–1073.
- Biron, P.M., Choné, G., Buffin-Bélanger, T., Demers, S., Olsen, T. (2013): Improvement of streams hydro-geomorphological assessment using LiDAR DEMs. *Earth Surface Processes and Landforms* 38(15), 1808- 1821.
- Biron, P.M., Richer, A., Kirkbride, A., Roy, A.G., Han, S. (2002): Spatial patterns of water surface topography at a river confluence. *Earth Surface Processes and Landforms* 27, 913–928.
- Blanca, M.J., Alarcon, R., Arnau, J., Bono, R., Bendayan, R. (2017): Non-normal data: Is ANOVA still a valid option? *Psicothema* 29(4): 552-557.
- Borselli, L., Cassi, P., Torri, D. (2008): Prolegomena to sediment and flow connectivity in the landscape: a GIS and field numerical assessment. *Catena* 75, 268–277.
- Boyer, C., Roy, A.G., Best, J.L. (2006): Dynamics of a river channel confluence with discordant beds: flow turbulence, bed load sediment transport, and bed morphology. *Journal of Geophysical Research* 111(F4), F04007. DOI: <http://dx.doi.org/10.1029/2005jf000458>.
- Bracken, L.J., Turnbull, L., Wainwright, J., Bogaart, P. (2015): Sediment connectivity: a framework for understanding sediment transfer at multiple scales. *Earth Surface Processes and Landforms* 40, 177–188.
- Bradbrook, K.F., Lane, S.N., Richards, K.S., (2000a): Numerical simulation of three-dimensional,

- time-averaged flow structure at river channel confluences. *Water Resources Research* 36 (9), 2731–2746.
- Bradbrook, K.F., Lane, S.N., Richards, K.S., Biron, P.M., Roy, A.G. (2000b): Large eddy simulation of periodic flow characteristics at river channel confluences. *Journal of Hydraulic Research* 38(3), 207–215.
- Bradbrook, K.F., Lane, S.N., Richards, K.S., Biron, P.M., Roy, A.G. (2001): Role of bed discordance at symmetrical river confluences. *Journal of Hydraulic Engineering* 127(5), 351–368.
- Bradley, W.C., Fahnestock, R.K., Rowekamp, E.T. (1972): Coarse sediment transport by flood flows on Knik River, Alaska. *Geological Society of America Bulletin* 83, 1261-1284.
- Brierley, G. and Fryirs, K. (1999): Tributary–trunk stream relations in a cut-and- fill landscape: a case study from Wolumla catchment, New South Wales, Australia. *Geomorphology* 28, 61–73.
- Brierley, G. and Fryirs, K. (2005): *Geomorphology and River Management: Applications of the River Styles Framework*. Blackwell Publishing: Victoria, Australia.
- Brierley, G. and J. Hooke (2015): Emerging geomorphic approaches to guide river management practices. *Geomorphology* 251, 1-156.
- Bull, W.B. (1979): Threshold of critical power in streams. *Geological Society of America Bulletin* 90, 453–464.
- Buraas, E. M., Renshaw, C. E., Magilligan, F. J., & Dade, W. B. (2014): Impact of reach geometry on stream channel sensitivity to extreme floods. *Earth Surface Processes and Landforms*, 39, 1778–1789.
- Carbonneau, P.E., Bergeron, N.E., Lane, S.N. (2005): Automated grain size measurements from airborne remote sensing for long profile measurements of fluvial grain sizes. *Water Resources Research* 41, W11426.
- Carbonneau, P.E., Lane, S.N., Bergeron, N.E. (2004): Catchment-scale mapping of surface grain size in gravel bed rivers using airborne digital imagery. *Water Resources Research* 40, W07202.

- Cavalli, M., Trevisani, S., Comiti, F., Marchi, L. (2013): Geomorphometric assessment of spatial sediment connectivity in small Alpine catchments. *Geomorphology* 188, 31–41.
- Church, M. and Ferguson, R.I. (2015): Morphodynamics: Rivers beyond steady state. *Water Resources Research* 51, 1883–1897.
- Church, M. and Kellerhals, R. (1978): On the statistics of grain size variation along a gravel river. *Canadian Journal of Earth Sciences* 15, 1151 – 1160.
- COGESAF (2017): Plan d'adaptation au changement climatique : Phase I Portrait des inondations et du bassin versant de la rivière Coaticook. Document rédigé dans le cadre du projet RésAlliance. Sherbrooke, 54 pages et annexes.
- Cohen, T.J. and Brierley, G.J. (2000): Channel instability in a forested catchment: A case study from Jones creek, East Gippsland, Australia. *Geomorphology* 32, 109–128.
- Constantinescu, G., Miyawaki, S., Rhoads, B., Sukhodolov, A., Kirkil, G. (2011): Structure of turbulent flow at a river confluence with momentum and velocity ratios close to 1: insight provided by an eddy-resolving numerical simulation. *Water Resources Research* 47. DOI: <http://dx.doi.org/10.1029/2010WR010018>.
- Crema, S., Cavalli, M. (2018): SedInConnect: a stand-alone, free and open source tool for the assessment of sediment connectivity. *Computers and Geosciences* 111, 39–45.
- Croke, J., Mockler, S., Fogarty, P., Takken, I. (2005): Sediment concentration changes in run-off pathways from a forest road network and the resultant spatial pattern of catchment connectivity. *Geomorphology* 68, 257–268.
- Czuba, J.A. and Foufoula-Georgiou, E. (2015): Dynamic connectivity in a fluvial network for identifying hotspots of geomorphic change. *Water Resources Research* 51, 1401–1421.
- Demers S., Massé S., Buffin-Bélanger T. 2017. Cartographie des aléas fluviaux de la rivière Coaticook: diagnostic, méthodologie et recommandations. Laboratoire de géomorphologie et dynamique fluviale, Université du Québec à Rimouski. Rapport remis à la MRC de Coaticook et au Ministère de la Sécurité publique du Québec.

- De Serres, B., Roy, A.G., Biron, P.M., Best, J.L. (1999): Three-dimensional structure of flow at a confluence of river channels with discordant beds. *Geomorphology* 26(4), 313–335. DOI: [http://dx.doi.org/10.1016/S0169-555X\(98\)00064-6](http://dx.doi.org/10.1016/S0169-555X(98)00064-6).
- Dixon, S.J., Sambrook Smith, G.H., Best, J.L., Nicholas, A.P., Bull, J.M., Vardy, M.E., Sarker, M.H., Goodbred, S. (2018): The planform mobility of river channel confluences: Insights from analysis of remotely sensed imagery. *Earth Science Reviews* 176, 1–18.
- Duncan, W.W., Poole, G.C., Meyer, J.L. (2009): Large channel confluences influence geomorphic heterogeneity of a southeastern United States river. *Water Resources Research*, 45, W10405, 1-9.
- East, A. E., Logan, J. B., Mastin, M. C., Ritchie, A. C., Bountry, J. A., Magirl, C. S. and Sankey, J. B. (2018): Geomorphic evolution of a gravel-bed river under sediment-starved versus sediment-rich conditions: River response to the world’s largest dam removal. *Journal of Geophysical Research: Earth Surface* 123, 3338–3369.
- Eaton, B.C., Church, M. (2011): A rational sediment transport scaling relation based on dimensionless stream power. *Earth Surface Processes and Landforms* 36, 901–910.
- Ferguson, R. and Hoey, T. (2008): Effects of tributaries on main-channel geomorphology. Rice, S.P., Roy, A.G., Roads, B.L. (Eds.): *River Confluences, Tributaries and the Fluvial Network*. Wiley, Chichester, UK, pp. 183–208 (Ch. 10).
- Ferguson, R.I. (2005): Estimating critical stream power for bedload transport calculations in gravel-bed rivers. *Geomorphology* 70, 33–41.
- Ferguson, R.I., Cudden, J.R., Hoey, T.B., Rice, S.P. (2006): River system discontinuities due to lateral inputs: Generic styles and controls. *Earth Surface Processes and Landforms* 31, 1149–1166.
- Feizizadeh, B., Shadman Roodposhti, M., Jankowski, P., Blaschke, T. (2014): A GIS-based extended fuzzy multi-criteria evaluation for landslide susceptibility mapping. *Computers & Geosciences*, 73, 208-221.
- Florsheim, J.L., Mount, J.F., Rutten, L.T. (2001): Effect of base level change on floodplain and fan sediment storage and ephemeral tributary channel morphology, Navarro River, California. *Earth Surface Processes and Landforms* 26, 219–232.

- Florsheim, J.L. (2004): Side-valley tributary fans in high-energy river floodplain environments: Sediment sources and depositional processes, Navarro River basin, California. *Geological Society of America Bulletin* 116: 923–937.
- Fonstad, M.A. and Marcus, W.A. (2010): High resolution, basin extent observations and implications for understanding river form and process. *Earth Surface Processes and Landforms* 35, 680–698.
- Fryirs, K. (2017): River sensitivity: a lost foundation concept in fluvial geomorphology. *Earth Surface Processes and Landforms* 42, 55–70.
- Fryirs, K. and Gore, D.B. (2014): Geochemical insights to the formation of “sedimentary buffers”: Considering the role of tributary–trunk stream interactions on catchment-scale sediment flux and drainage network dynamics. *Geomorphology* 219, 1-9.
- Fryirs, K., Brierley, G.J., Preston, N.J., Kasai, M. (2007a): Buffers, barriers and blankets: the (dis)connectivity of catchment-scale sediment cascades. *Catena* 70, 49–67.
- Fryirs, K., Brierley, G.J., Preston, N.J., Spencer, J. (2007b): Catchment-scale (dis)connectivity in sediment flux in the upper Hunter catchment, New South Wales, Australia. *Geomorphology* 84, 297–316.
- Gartner, J.D., Dade, W.B., Renshaw, C.E., Magilligan, F.J., Buraas, E.M. (2015): Gradients in stream power influence lateral and downstream sediment flux in floods. *Geology*.
- Gilbert, J. T., Macfarlane, W. W. and Wheaton, J. M. (2016): The valley bottom extraction tool (V-BET): A GIS tool for delineating valley bottoms across entire drainage networks. *Computers and Geosciences*, 97, 1-14.
- Graf, W.L. (1983): Downstream changes in stream power in the Henry Mountains, Utah. *Annals of the Association of American Geographers* 73, 373–387.
- Guillén Ludeña, S., Cheng, Z., Constantinescu, G., Franca, M. J. (2017a): Hydrodynamics of mountain- river confluences and its relationship to sediment transport. *Geophysical Research: Earth Surface* 122, 901–924.
- Guillén-Ludeña, S., Franca, M.J., Alegria, F., Schleiss, A.J., Cardoso, A.H. (2017b):

- Hydromorphodynamic effects of the width ratio and local tributary widening on discordant confluences. *Geomorphology* 293, 289-304.
- Guillén-Ludeña, S., Franca, M.J., Cardoso, A.H., Schleiss, A.J. (2015): Hydro-morphodynamic evolution in a 90° movable bed discordant confluence with low discharge ratio. *Earth Surface Processes and Landforms* 40(14), 1927–1938.
- Guillén-Ludeña, S., Franca, M.J., Cardoso, A.H., Schleiss, A.J., (2016): Evolution of the hydromorphodynamics of mountain river confluences for varying discharge ratios and junction angles. *Geomorphology* 255, 1–15.
- Hanks, T.C. and Webb, R.H. (2006): Effects of tributary debris on the longitudinal profile of the Colorado River in Grand Canyon. *Geophysical Research: Earth Surface* 111, F02020.
- Harvey, A.M. (1997): Coupling between hillslope gully systems and stream channels in the Howgill Fells, northwest England: temporal implications. *Geomorphologie: Relief, Processus, Environnement* 1, 3–20.
- Harvey, A.M. (2001): Coupling between hillslopes and channels in upland fluvial systems: implications for landscape sensitivity, illustrated from the Howgill Fells, northwest England. *Catena* 42, 225–250.
- Harvey, A.M. (2002): Effective timescales of coupling within fluvial systems. *Geomorphology* 44, 175–201.
- Hugue, F., Lapointe, M., Eaton, B.C., Lepoutre, A. (2016): Satellite-based remote sensing of running water habitats at large riverscape scales: tools to analyze habitat heterogeneity for river ecosystem management. *Geomorphology* 253, 353–369.
- Jones, N.E. and Schmidt, B.J. (2017): Tributary effects in rivers: interactions of spatial scale, network structure, and landscape characteristics. *Canadian Journal of Fisheries and Aquatic Sciences* 74, 503–510.
- Kline, M. and Cahoon, B. (2010): Protecting river corridors in Vermont. *Journal of the American Water Resources Association* 46(2), 227–236.

- Knighton, A.D. (1980): Longitudinal changes in size and sorting of stream-bed material in four English rivers. *Geological Society of America Bulletin* 91, 55–62.
- Knighton, D. (1998): *Fluvial forms and processes*. Arnold, New York.
- Kondolf, M.G. (2011): Setting goals in river restoration: when and where can the river “Heal itself”? Simon A, Bennett SJ, Castro JM (eds): *Stream restoration in dynamic fluvial systems: scientific approaches, analyses, and tools*, vol 194. American Geophysical Union, Washington, DC, 29–43.
- Lapointe, M.F., Secretan, Y., Driscoll, S.N., Bergeron, N., Leclerc, M. (1998): Response of the Ha!Ha! River to the flood of July 1996 in the Saguenay Region of Quebec: large-scale avulsion in a glaciated valley. *Water Resources Research* 34, 2383–2392.
- Lea, D.M. and Legleiter, C.J. (2016): Mapping the spatial patterns of stream power and channel change along a gravel-bed river in northern Yellowstone. *Geomorphology* 252, 66–79.
- Lecce, S.A. (1997): Nonlinear downstream changes in stream power on Wisconsin’s Blue River. *Annals of the Association of American Geographers* 87, 471–486.
- Leite Ribeiro, M., Blanckaert, K., Roy, A. G., Schleiss, A. J. (2012): Flow and sediment dynamics in channel confluences. *Journal of Geophysical Research* 117, F01035. DOI: 10.1029/2011JF002171.
- Lewis, S., and Maslin, M. (2015): Defining the Anthropocene. *Nature* 519, 171–180.
- Lisenby, P.E. and Fryirs, K. (2016): Catchment- and reach-scale controls on the distribution and expectation of geomorphic channel adjustment. *Water Resources and Research* 52, 3408–3427.
- Lisenby, P.E. and Fryirs, K.A. (2017): Sedimentologically significant tributaries: catchment-scale controls on sediment (dis)connectivity in the Lockyer Valley, SEQ, Australia. *Earth Surfaces Processes and Landforms* (2017).
- Magilligan, F.J. (1992): Thresholds and the spatial variability of flood power during extreme floods. *Geomorphology* 5, 373–390.
- Magilligan, F.J., Buraas, E.M., Renshaw, C.E. (2015): The efficacy of stream power and flow duration on geomorphic responses to catastrophic flooding. *Geomorphology* 228: 175–188.

- Malczewski, J. (1999): GIS and Multicriteria Decision Analysis. Wiley New York. ISBN 0-471-32944-4.
- Malczewski, J. (2006): GIS-based multicriteria decision analysis: A survey of the literature. *International Journal of Geographical Information Science* 20(7), 703–726.
- Malczewski, J. and Rinner, C. (2015): *Multicriteria Decision Analysis in Geographic Information Science*. Springer-Verlag Berlin Heidelberg. eISBN 978-3-540-74757-4.
- Marcus, W.A. and Fonstad, M.A. (2008): Optical remote mapping of rivers at sub-meter resolutions and watershed extents. *Earth Surface Processes and Landforms* 33, 4–24.
- Martín-Vide, J.P., Plana-Casado, A., Sambola, A., Capapé, S. (2015): Bedload transport in a river confluence. *Geomorphology* 250, 15–28.
- Massé, S., Demers, S., Besnard, C., Buffin-Bélanger, T., Biron, P.M., Choné, G., Massey, W. Development of a mapping approach encompassing most fluvial processes: Lessons learned from the freedom space for rivers concept in Quebec (Canada). *River Research and Applications*. Accepted with minor revisions May 6, 2019.
- Miller, A. J. (1990): Flood hydrology and geomorphic effectiveness in the central Appalachians. *Earth Surface Processes and Landforms* 15, 119–134.
- Montgomery, D. R. (1994): Road surface drainage, channel initiation, and slope instability. *Water Resources Research*, 30(6), 1925–1932.
- Mosley, M.P. (1976): An experimental study of channel confluences. *Journal of Geology* 84, 535–562.
- MRNF (2006): *Portrait territorial de la Gaspésie-Îles-de-la-Madeleine*. Charlesbourg (Québec). 112pp. ISBN-10 : 2-550-48679-X.
- MRNFP (2004): *Portrait forestier de la région de la Gaspésie-Îles-de-la-Madeleine*. 68pp.
- Ollero, A. (2010): Channel changes and floodplain management in the meandering middle Ebro River, Spain. *Geomorphology* 117(3–4), 247–260.
- Parker, C., Thorne, C.R., Clifford, N.J. (2015): Development of ST:REAM: a reach-based stream

- power balance approach for predicting alluvial river channel adjustment. *Earth Surface Processes and Landforms* 40, 403–413.
- Parsons, D.R., Best, J.L., Lane, S.N., Orfeo, O., Hardy, R.J., Kostaschuck, R. (2007): Form roughness and the absence of secondary flow in a large confluence–difffluence, Rio Parana, Argentina. *Earth Surface Processes and Landforms* 32, 155–162.
- Persichillo, M., Bordoni, M., Cavalli, M., Crema, S., Meisina, C. (2018): The role of human activities on sediment connectivity of shallow landslides. *Catena* 160, 261–274.
- Piégay, H., Darby, S.E., Mosselman, E., Surian, N. (2005): A review of techniques available for delimiting the erodible river corridor: a sustainable approach to managing bank erosion. *River Research Applications* 21(7), 773–789.
- Reid, L. and Dunne, T. (1984): Sediment production from forest road surfaces. *Water Resources Research* 2 (11), 1753–1761.
- Rengers, F., Wohl, E. (2007): Trends of grain sizes on gravel bars in the Rio Chagres, Panama. *Geomorphology* 83, 282–293.
- Rhoads, B.L. (1987): Changes in stream channel characteristics at tributary junctions. *Physical Geography* 8, 346–361.
- Rhoads, B.L., Riley, J.D., Mayer, D.R. (2009): Response of bed morphology and bed material texture to hydrological conditions at an asymmetrical stream confluence. *Geomorphology* 109, 161–173.
- Rice, S.P. (1998): Which tributaries disrupt downstream fining along gravel-bed rivers? *Geomorphology* 22, 39–56.
- Rice, S.P. (2017): Tributary connectivity, confluence aggradation and network biodiversity. *Geomorphology* 277, 6–16.
- Rice, S.P., Church, M. (1998): Grain size along two gravel-bed rivers: Statistical variation, spatial pattern and sedimentary links. *Earth Surface Processes and Landforms* 23, 345–363.
- Rice, S.P., Church, M. (2001): Longitudinal profiles in simple alluvial systems. *Water Resources*

- Research 37, 417–426.
- Rice, S.P., Ferguson, R.I., Hoey, T.B. (2006): Tributary control of physical heterogeneity and biological diversity at river confluences. *Canadian Journal of Fisheries and Aquatic Sciences* 63(11), 2553–2566.
- Richards, K.S. (1980): A note on changes in channel geometry at tributary junctions. *Water Resources Research* 16, 241–244.
- Rinaldi M., Surian N., Comiti F., Bussettini M. (2012): Guidebook for the evaluation of stream morphological conditions by the Morphological Quality Index (MQI), Istituto Superiore per la Protezione e la Ricerca Ambientale, Roma, 90 pp.
- Roca, M., Martin-Vide, J., Moreta, P. (2009): Modelling a torrential event in a river confluence. *Journal of Hydrology* 364, 207–215.
- RStudio Team (2016): RStudio: Integrated Development for R. RStudio, Inc., Boston, MA. <http://www.rstudio.com/>.
- Saaty, T. L. (1980): The analytic hierarchy process. Planning, Priority Setting, Resource Allocation. McGraw-Hill, New York. ISBN 978-0-070-54371-3.
- Schmider, E., Ziegler, M., Danay, E., Beyer, L., & Bühner, M. (2010): Is It Really Robust? *Methodology*, 6(4), 147–151.
- Scorpio, V., Crema, S., Marra, F., Righini, M., Ciccacese, G., Borga, M., Cavalli, M., Corsini, A., Marchi, L., Surian, N., Comiti, F. (2018): Basin-scale analysis of the geomorphic effectiveness of flash floods: A study in the northern Apennines (Italy). *Science of the Total Environment* 640–641, 337–351.
- Singer, M.B. (2008): Downstream patterns of bed material grain size in a large, lowland alluvial river subject to low sediment supply. *Water Resources Research* 44, W12202. DOI: 10.1029/2008WR007183.
- Sternberg, H. (1875): Untersuchungen über Längen und Querprofil geschiebeführender Flüsse. *Zeitschrift für Bauwesen* 25, 483–506.

- Surian, N., Righini, M., Lucia, A., Nardi, L., Amponsah, W., Benvenuti, M., Borga, M., Cavalli, M., Comiti, F., Marchi, L., Rinaldi, M., Viero, A. (2016): Channel response to extreme floods: insights on controlling factors from six mountain rivers in northern Apennines, Italy. *Geomorphology, Floods in Mountain Environments* 272, 78–91.
- Swanson, B.J. and Meyer, G. (2014): Tributary confluences and discontinuities in channel form and sediment texture: Rio Chama, NM. *Earth Surface Processes and Landforms* 39, 1927–1943.
- Thorne, C.R., Wallerstein, N.P., Soar, P.J., Brookes, A., Wishart, D., Biedenharn, D.S., Gibson, S.A., Little, C.D., Mooney, D.M., Watson, C.C., Green, A.P.E., Coulthard, T.J., Van de Wiel, M.J. (2011): Accounting for sediment in flood risk management. Pender, G., Faulkner, H. (eds): *Flood Risk Science and Management*. Wiley-Blackwell, Chichester, 87–113.
- Vocal Ferencevic, M. and Ashmore, P. (2012): Creating and evaluating digital elevation model-based stream-power map as a stream assessment tool. *River Research and Applications* 28, 1394–1416.
- Voogd, H., 1983. *Multicriteria Evaluation for Urban and Regional Planning*. Pion, Ltd., London. 367pp. ISBN-13: 978-0850861068
- Waters, C. N., Zalasiewicz, J., Summerhayes, C., Barnosky, A. D., Poirier, C., Galuszka, A., Cearreta, A., Edgeworth, M., Ellis, E.C., Ellis, M., Jeandel, C., Leinfelder, R., McNeill, J.R., Richter, DdeB, Steffen, W., Syvitski, J., Vidas, D., Wagreich, M., Williams, M., Zhisheng, A., Grinevald, J., Odada, E., Oreskes, N., Wolfe, A.P. (2016): The Anthropocene is functionally and stratigraphically distinct from the Holocene. *Science*, 351(6269), aad2622-1- aad2622-10.
- Wheaton, J. M., Fryirs, K. A., Brierley, G., Bangen, S. G., Bouwes, N., O'Brien, G. (2015): Geomorphic mapping and taxonomy of fluvial landforms. *Geomorphology* 248, 273-295.
- Willet, S.D. (1999): Orography and orography: the effects of erosion on the structure of mountain belts. *Journal of Geophysical Research* 104, 28957–28981.
- Wohl, E., Lane, S.N., Wilcox, A.C. (2015): The science and practice of river restoration. *Water Resources Research* 51, 5974–5997.
- Wolman, M.G. (1954): A method of sampling coarse river-bed material. *Eos, Transactions American Geophysical Union* 35, 951–956.

Yochum, S.E., Sholtes, J.S., Scott, J.A., Bledsoe, B.P. (2017): Stream power framework for predicting geomorphic change: The 2013 Colorado Front Range flood. *Geomorphology* 292, 178–192.